

Hydrodynamic modelling of tsunami inundation in Whitianga

Prepared by:
Gegar Prasetya
Prof. Terry R. Healy
Dr. Willem de Lange
Coastal Marine Group
Department of Earth and Ocean Sciences
University of Waikato

For:
Waikato Regional Council
Private Bag 3038
Waikato Mail Centre
HAMILTON 3240

July 2011

Document #: 2323083

Approved for release by:
Adam Munro

Date January 2015

Disclaimer

This technical report has been prepared for the use of Waikato Regional Council as a reference document and as such does not constitute Council's policy.

Council requests that if excerpts or inferences are drawn from this document for further use by individuals or organisations, due care should be taken to ensure that the appropriate context has been preserved, and is accurately reflected and referenced in any subsequent spoken or written communication.

While Waikato Regional Council has exercised all reasonable skill and care in controlling the contents of this report, Council accepts no liability in contract, tort or otherwise, for any loss, damage, injury or expense (whether direct, indirect or consequential) arising out of the provision of this information or its use by you or any other party.

Hydrodynamic modelling of tsunami inundation in Whitianga

Prepared for:

Waikato Regional Council

By

Gegar Prasetya

Prof. Terry R. Healy

Dr. Willem de Lange

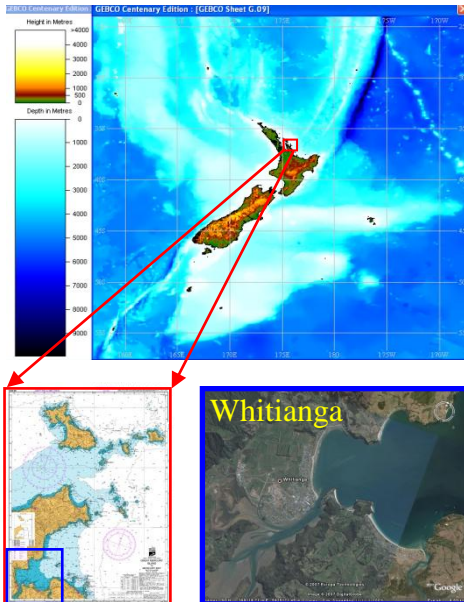
Coastal Marine Group

Department of Earth and Ocean Sciences

University of Waikato

Private Bag 3105

Hamilton, New Zealand.



January 2008

Revised Version July 2011

Table of Contents

Executive Summary.....	iii
Introduction.....	1
Background	2
Historical and potential tsunami sources	3
Distant tsunami sources	4
Regional/local tsunami sources	4
Hydrodynamic Modelling of Tsunami	6
Numerical model	6
Model grids	8
Wide area model grid	8
Regional and local nested grid models	9
Modelling Results	11
Potential sources - wide area model	12
Initial conditions	12
Mt Healy eruption.....	12
Kermadec Trench earthquake	15
The 1960 Chilean tsunami	21
Regional model 50 m grid.....	23
Mt Healy eruption.....	23
Kermadec Trench earthquake	25
The 1960 Chilean tsunami	34
Summary of wide area and regional model results.....	37
Local grid model.....	38
Kermadec Trench subduction normal fault event (Mw 9.0).	40
1960 Chilean Tsunami.....	43
Tsunami hazards and risks – flow depths, flow speeds and hazard zones.	45
Tsunami flow depths.....	45
Tsunami flow speeds.....	50
Tsunami hazard zones	51
High risk zone.....	53
Moderate risk zone.....	53
Low risk zone	54
High risk estuarine zone	54
Discussion.....	54
Summary of results	54
Evacuation routes and shelter sites	55
Buffalo Beach Scenic Reserve	58
Airfield area (corner of Racecourse Road and Whitianga Bypass)	59
Marina parking area.....	59
Vertical evacuation	59
Overland flow velocities and the Building Code	61

Coastal defence structures	63
Safety planning for ships and boats	65
Location of critical facilities	66
Information and education programmes	66
Bibliography	70
Appendix 1: Kermadec trench normal fault event scenario (Mw 9.0) inundation sequence and extent. Local model	74
Appendix 2: 1960 Chilean-type scenario inundation sequence and extent. Local model	87
Appendix 3: animations of tsunami simulation results.....	96

Executive Summary

In 2006, Waikato Regional Council (WRC) provided research funding for the Coastal Marine Group, Department of Earth and Ocean Sciences, University of Waikato, to undertake research on the impacts of tsunami inundation on Whitianga town and harbour.

The main aims of the study are to:

- Identify potential tsunami sources;
- Establish an understanding of tsunami inundation impacts in Whitianga township and harbour – including the hydrodynamic processes and responses of Mercury Bay, Buffalo Bay, Whitianga Harbour and adjacent land to tsunami wave action;
- Develop tsunami inundation maps, showing depth and velocity (speed) of tsunami waves; and
- Provide sound evidence upon which to base community risk mitigation measures – including recommendations for evacuation planning, public education and awareness, protection of infrastructure, management of impacts to marine vessels and future land use planning.

The numerical model used in this study is the 3DD Suite-Computational Marine and Freshwater Laboratory model (Black, 2001). The model has demonstrated the ability to accurately reproduce tsunami hydrodynamics during propagation and run up on both laboratory and real-world scales.

There are three primary tsunami sources that could potentially affect Whitianga from the Kermadec Trench, and beyond the New Zealand continental shelf, being:

1. Mt Healy undersea volcano eruptions (15th Century event);
2. Large earthquakes along segments 1 and 2 of the Kermadec Trench subduction zone; and
3. A 1960 Chilean-type earthquake event.

Each source is modelled, and the results that show the greatest risk and impacts to Whitianga are used as the basis for the hazard maps and hazard zones.

Modelling results indicate that:

- The Mt Healy type of eruption produced a minimal impact on Whitianga. The tsunami waves generated from this event did not inundate Whitianga. Despite this, strong currents of up to 2.5 m/s were generated inside Buffalo Bay and at the Whitianga Harbour inlet.
- The Kermadec Trench earthquake scenarios with both positive and negative leading waves, as a result of a subduction fault dislocation along segments 1 and 2, have a significant impact on Whitianga. The waves inundate the coastal area up to 2.5 and 3 km inland for the subduction thrust fault and normal fault events respectively, and affect the entire area of Whitianga Harbour. The normal fault event that produces positive leading waves has more impact than the thrust fault event that produces negative leading waves.
- The 1960 Chilean-type earthquake event produced tsunami waves that inundated Buffalo Beach Road and houses in Whitianga, as observed by eyewitnesses. Strong currents of up to 5 m/s are generated inside Buffalo Bay and the Whitianga Harbour inlet.

The modelling indicates that:

- Whitianga would be inundated five times by a Kermadec Trench earthquake scenario, and three times by a 1960 Chilean-type of tsunami
- For the Kermadec Trench scenario (normal fault), the first waves penetrate Mercury Bay within 75–98 minutes after the fault rupture
- Regardless of the tsunami source, it takes 11–18 minutes for waves to arrive at the Whitianga foreshore once they have entered Mercury Bay.

The modelling indicates that the period between waves is 40 – 60 minutes, which is consistent with the 1960 Chilean event. The geometry of Buffalo Bay and Mercury Bay amplify the incoming tsunami waves, and the sea level inside the bay continues to oscillate, even after the sea level outside of Mercury Bay returns to normal. This situation is consistent with eyewitness accounts of the 1960 Chilean tsunami.

Modelling also shows that strong currents are produced within Buffalo Bay and Whitianga Harbour, as well as during the overland flows - especially in areas adjacent to the Taputapuatea Stream and in the foreshore area between Albert Street and the wharf. The flow speed ranged from 1.5 m/s to 8 m/s for overland flows, and above 8 m/s within the entrance of Whitianga Harbour and in the middle of Buffalo Bay.

For the first time in New Zealand, a combination of non-ground striking and ground striking LIDAR data was used in modelling tsunami inundation, which increased the accuracy of the modelling results considerably. Inundation flow behaviour and the effect of topography, as well as land use, can be analysed more accurately, and a more precise hazard map can be produced accordingly.

Mitigation measures suggested to protect the Whitianga waterfront include a combination of enhanced coastal sand dunes and planted forest belts, which could be done along both sides of the Taputapuatea Stream. A stop gate could also be constructed at the entrance of the Taputapuatea Stream to minimise the impact of the tsunami flows upstream.

With respect to evacuation, it is concluded that due to the lag time between a local event from the Kermadec Trench and wave arrival at the Whitianga foreshore, there is enough time for residents to be evacuated to shelter sites using major roads. Three locations are identified as evacuation shelter sites. These are the marina parking area and Buffalo Beach scenic reserve (both of which are located on high ground adjacent to the high-risk zone), and further inland at the airfield. Vertical evacuation sites are needed inside the high-risk zone, and recommendations on potential locations are provided. It is important that vertical evacuation measures are integrated into community response plans, and that they be reviewed and revised regularly.

Overland flow information derived from modelling using the ground-striking and non-ground striking LIDAR data provides a basis to influence new development that occurs within tsunami hazard risk zones. Overland flow information also indicates the areas of existing development that need protection from future tsunami events. Risk mitigation may be accomplished through redevelopment, retrofit, coastal defence measures, safety planning for ships and boats, land reuse plans, and also via public education and awareness programmes.

A major challenge of risk mitigation is to maintain emergency preparedness programmes and procedures when the threat of tsunami is perceived as remote. Periodic exercises are essential to maintain awareness, and regular information should be provided for those occupying tsunami hazard areas.

Tsunami are rare events, but their impacts on coastal communities can be devastating. It is quite dangerous to believe that the impacts of a tsunami can be completely prevented by man-made

structures (Horikawa and Shuto, 1983). However, possible impacts may be minimised through careful design of solutions based on systematic research. An important consideration for risk mitigation works is that they may affect the quality of daily life, and risk mitigation involves choices and trade-offs between risk management and other uses.

Video animations of each scenario are provided at regional, intermediate and local scales. The animations cover tsunami wave behaviour during generation, propagation, run up, and overland flows, and may be used to inform land use planning and public education and awareness programmes.

Introduction

In 2006, Waikato Regional Council (WRC) provided research funding for the Coastal Marine Group, Department of Earth and Ocean Sciences, University of Waikato, to undertake research on the impacts of tsunami¹ inundation on Whitianga town and harbour.

The main aims of the study were to:

- Establish an understanding of tsunami inundation impacts in Whitianga township and harbour;
- Develop tsunami inundation maps, showing depth and velocity (speed) of tsunami waves; and
- Provide sound evidence upon which to base community risk mitigation measures – including recommendations for evacuation planning, public education and awareness, protection of infrastructure, management of impacts to marine vessels and future land use planning.

The model utilised high-resolution digital terrain data (LIDAR² data set on land), as well as a high-resolution, multi-beam bathymetric (ocean depth) data.

The study area is illustrated in Figure 1.

This report addresses the following issues:

- Potential tsunami sources likely to significantly affect Whitianga township and lowland coastal areas;
- The hydrodynamic (forces exerted by tsunami waves) processes and response of the bays, inlets, and adjacent coastal land areas to tsunami wave action;
- The interaction of tsunami run up and overland flows on coastal land areas with existing infrastructure and possible future development areas; and
- Mitigation measures for the community, including, but not limited to:
 - i. Evacuation routes
 - ii. Shelter sites
 - iii. Public infrastructure (such as power and rest homes)
 - iv. Protection of the marina, harbour, Whitianga Waterways and other coastal developments; and

¹ Within this report, the word “tsunami” is used to denote both the singular and plural – the same as the original usage of the word in Japanese.

² Light Imaging Detection and Range – a method for obtaining highly accurate land elevations.

- v. Educational outreach material for the community and visitors to the area.

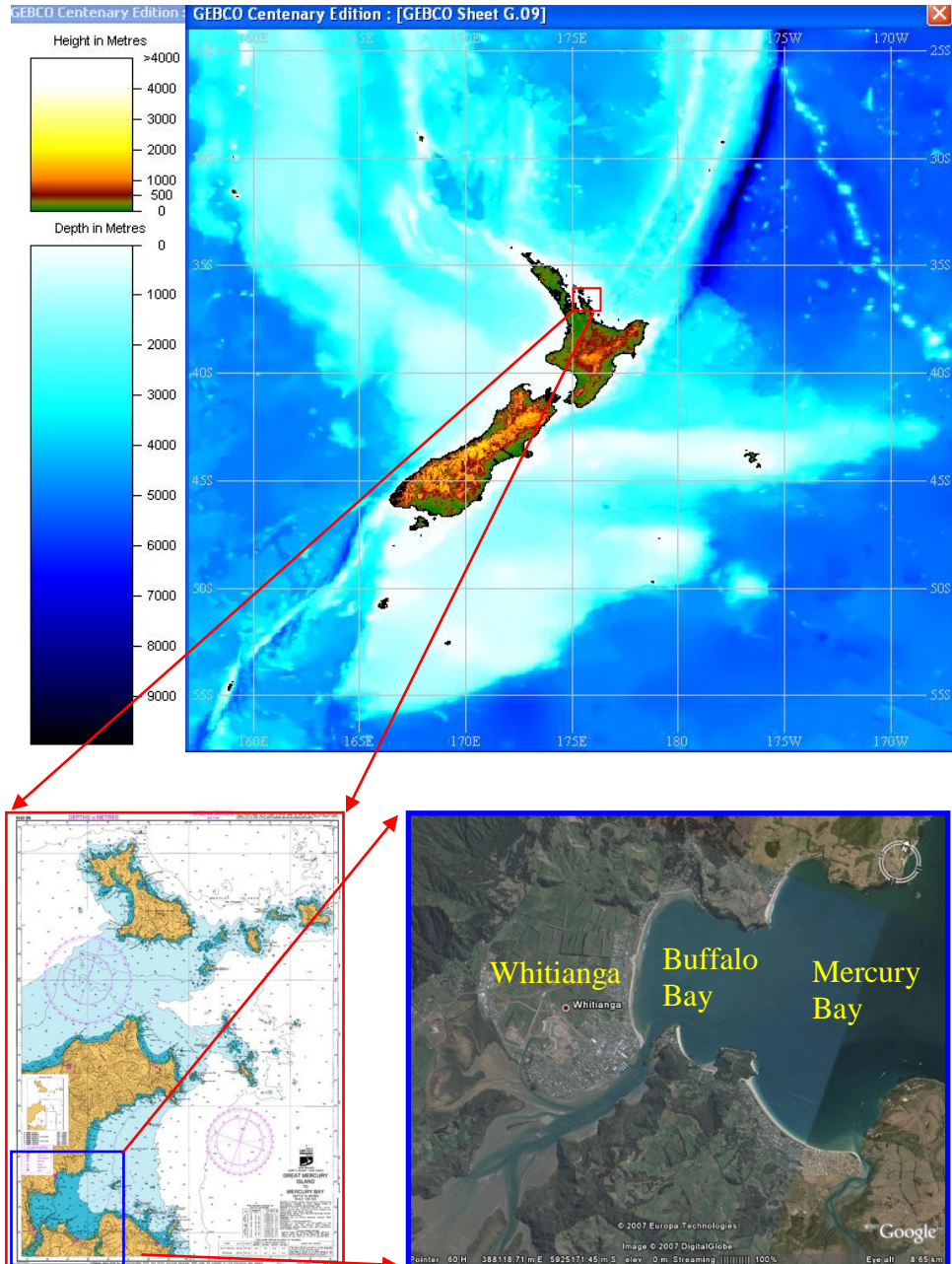


Figure 1. The study area – Whitianga, located within Buffalo Bay, Mercury Bay, North Island, New Zealand. (Map source: GEBCO/Centennial Edition 2003, NZ 5318 – LINZ, Google Image Satellite).

Background

Mercury Bay has been shown to be susceptible to historical distantly generated tsunami impacts (de Lange and Healy, 1988). The May 1960 Chilean event is one example where tsunami waves were observed and inundated the Esplanade/Buffalo Beach Road, several houses, and swept many boats from their moorings. Recent work by GNS Science (GNS) (Berryman, 2005), the national

Institute of Water and Atmosphere (NIWA) (Goff et al., 2006) and de Lange and Moon (2007), identified that in addition to distant sources, the east coast of the North Island of New Zealand is also susceptible to local source tsunami generated along the Kermadec Trench, such as the 15th century eruptions of the undersea volcano Mt Healy.

A lesson learned from the May 1960 event shows that the response of each location along the coast to the incoming tsunami wave trains was distinct, as recorded on tide gauges and the eyewitness accounts. The response of each location depends on the

- coastal shelf and seabed bathymetry;
- beach topography;
- shore margin; and
- shape of the coastal bay or harbour.

In many cases, the records within the coastal bay also showed the arrival of the tsunami wave was emergent at all stations – it took several wave cycles over several hours for larger waves to develop. This is comparable to the phenomena when a coastal bay has incident waves similar to the natural resonance period of the bay. In these cases (such as Mercury Bay), large amplification of the tsunami waves may occur within the bay.

A detailed study of the hydrodynamics of the tsunami waves on land, the level of inundation and the impacts that may occur within the coastal bay is needed. In order to undertake a detailed modelling study, high-resolution topographic data, such as LIDAR (on land), as well as bathymetric data is required. Both types of data are available for Whitianga and Buffalo Bay.

Historical and potential tsunami sources

Tsunami sources for the Waikato region can be classified as either distant or regional/local sources. Distant tsunami sources are those located beyond the New Zealand continental shelf, and have the potential to affect not only Mercury Bay, but also most of the New Zealand coast (de Lange and Fraser, 1999). It takes more than 10 hours for the first tsunami waves to arrive on the New Zealand coast from North and South American distant sources (refer to Figure 2). Regional/locally generated tsunami comprise all sources within close proximity to Mercury Bay. The first tsunami waves from these sources will arrive at the coastline within 1-3 hours after fault rupture and/or submarine landslide if it is due to earthquake, or eruption of a submarine volcano (refer to Figure 3).

Distant tsunami sources

Historically, most distant source tsunami that significantly affect the New Zealand coast originate from the South American subduction zone – such as the 22 May 1960 Chilean earthquake and tsunami. This tsunami arrived at Whitianga 12.5 hours after the earthquake, and produced an initial drawdown (lowering of water in Mercury Bay) of approximately 2m, followed by a run-up of approximately 5m in Whitianga. At the lowest drawdown, the wreck of the Buffalo was exposed, meaning that the maximum tsunami wave height (peak-to-trough) was nearly 7m. Another two large distant tsunami events on the historical record - namely the 1868 Peru and 1877 Chile events (de Lange and Fraser, 1999, Power et al., 2007) - entered Mercury Bay, since the waves are known to have affected Mercury Island and most of the east coast³. Recent studies by Atwater et al. (2005) showed another possible distant source of tsunami for the New Zealand coast is from the Cascadia Subduction Zone of North America.

Regional/local tsunami sources

The most significant potential regional/local sources of tsunami impacting upon Mercury Bay is from the subduction zone earthquakes that occur along the Kermadec Trench, and undersea volcanism in the Kermadec-Tonga system. Even though it is not yet certain if the entire subduction zone can generate potentially hazardous tsunami, the 26 December 2004 South East Asian Tsunami event showed that rupture lengths of nearly 1,200km along subduction zones can occur, contrary to expectations. Hence, an assessment of all submarine subduction zones is necessary to ascertain whether they could produce a major tsunami hazard, and has become a high priority in many countries facing a subduction zone.

³ The impact is not specifically mentioned however, due to a probable lack of human observation.

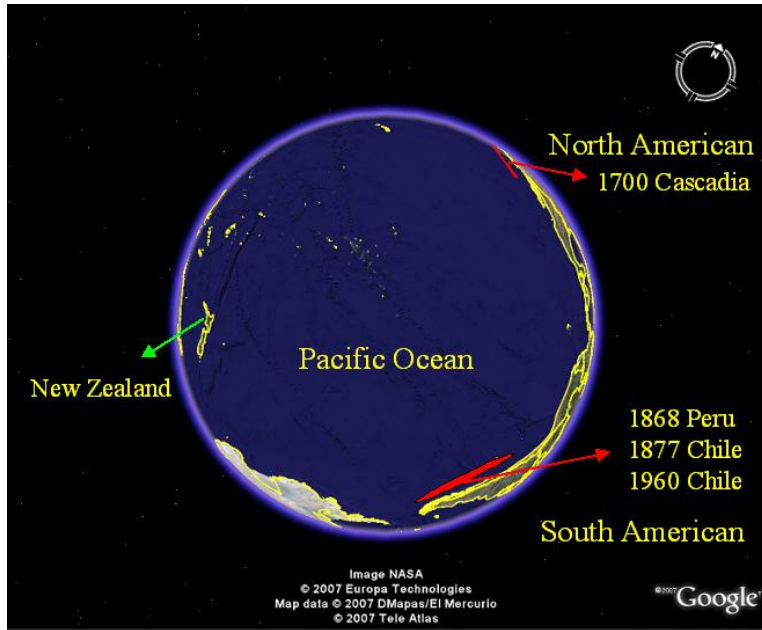


Figure 2. Distant source tsunami for New Zealand mostly originate from North and South American fault rupture along the subduction zones (Image source: Google earth).

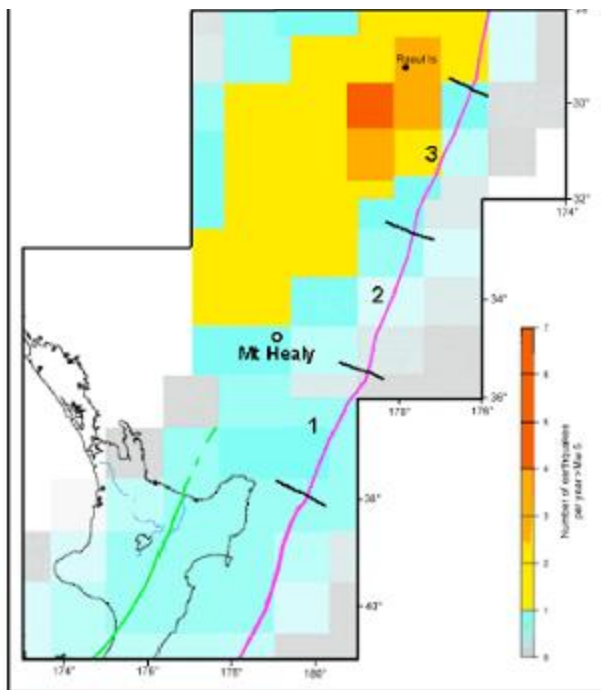


Figure 3. The Kermadec Trench - a regional/local tsunami source that potentially affects Whitianga. The majority of tsunami capable of affecting the east coast of the North Island coast originate from segments 1 and 2 of the Kermadec Trench, and the volcanic arc at the southern end of the Kermadec Trench. (Source: de Lange et al., 2007)

From historical records since 1840, no regional/local tsunami sources are known to have affected Whitianga. However, this does not indicate that there is no major threat for the region from regional/local sources. Generally, tsunami-generating earthquakes tend to have a return period of 200-800 years (Zachariassen et al. 1999; Walters et al. 2006; Okal et al. 2006), and tsunami-generating volcanic eruptions more than 1,000 years. In comparison, the New Zealand historical record is relatively short - only covering events of the last 150 years.

The historical record shows that earthquakes with M_w^4 8.0 to 8.3 have previously occurred along the Kermadec Ridge (ITDB/PAC 2004) and the paleotsunami (ancient tsunami) record suggests the eruptions of the undersea volcano Mt Healy in the 15th century generated a significant tsunami that affected the entire east coast (de Lange and Moon, 2007). There are at least 23 submarine volcanoes of the active southern Kermadec arc, three of which (Rumble II, Brothers and Healy) are silicic⁵ calderas. Seafloor multi-beam mapping reveals that many of these volcanoes undergo cycles of sector collapse, but it is still unknown how these sectors collapse and their likelihood of generating tsunami (Bell et al. 2004).

In this study, the impact of distant tsunami (such as the 1960 Chilean-type), regional/local sources from the Kermadec Trench, and Mt Healy eruptions were assessed to ascertain which sources could potentially affect the Whitianga coastal lowland. The “worst-case⁶” scenarios were chosen to model the impacts of tsunami on Whitianga Township and harbour.

Hydrodynamic Modelling of Tsunami

Numerical model

Following the Sumatra Tsunami of 2004, interest in the numerical modelling of tsunami has grown substantially. There are many models that have been developed ranging from simple one-dimensional models to complex three-dimensional, and from linear to nonlinear theory. A major challenge in modelling tsunami is how to accurately model the inundation and run up of tsunami waves, since it involves highly nonlinear phenomena, moving boundaries, and fast moving flows on dry bed (Synolakis and Bernard, 2006).

⁴ M_w refers to the Moment Magnitude Scale – a scale used by seismologists to measure the size of earthquakes in terms of the energy released.

⁵ Rich in silica, and typically regarded as highly explosive.

⁶ The maximum size events that are considered possible at this time.

One modelling approach has been the “dam break mechanism” – inundation from a sudden release of large fluid volumes. However, this approach is too simplistic, and hardly replicates the real situation, since tsunami waves arriving at the shore consist of three to seven separate wave trains. Tsunami waves create not only high speed flows in the near-shore zone and on land for the duration of inundation flows, but also during the return/backwash flows, as happened in the 2004 Sumatran event. In this event, receding water was one of the most serious threats, as it dragged people and considerable amounts of both natural material and man-made debris into the sea.

The numerical model used in this study is the 3DD Suite-Computational Marine and Freshwater Laboratory model (Black, 2001). The model was initially developed and applied for simulating the physical processes from micro-scale circulation over sand beds (Black and Vincent, 2001) to continental shelf scale circulation (Middleton and Black, 1994). However, the model can also be used to study tsunami dynamics, with purpose-designed schemes to allow the seabed to move in response to earthquakes or volcanic eruptions. The model is based on nonlinear shallow water equations with a Boussinesq term⁷, and can be set into ‘2 dimensional’ (2D) and ‘3 dimensional’ (3D) mode with capabilities of simulating the flooding and drying of large intertidal zones (Black, 2001).

3DD uses a fully explicit time stepping solution, and its’ flooding and drying scheme is designed to allow smooth transition and reduced instabilities by avoiding a sudden jump of the current velocity during the drying and wetting processes while simulating large intertidal zones. This feature allows the model to simulate the inundation dynamics of tsunami accurately. The model was used to replicate benchmark problem #2 developed by the third workshop on Long Wave Runup Models (held on June 17-18 2004 on Catalina Island, California), and has been applied to real world scales for the 2004 Sumatra Tsunami (Borrero et al., 2007). The model has demonstrated the ability to accurately reproduce tsunami hydrodynamics during propagation and run up at both laboratory and real-world scales.

⁷ An approximation method used in the modelling of fluid dynamics.

Model grids

Three model grids were developed for simulating tsunami generation, propagation, and inundation with respect to Whitianga, in order to provide the maximum resolution while minimizing the processing requirements. These grids were:

1. Wide area model 500/1000 m grid
2. Regional model – 50 m grid
3. Local model – 5m/10m grid.

Used in combination, the three grids define the model boundaries. The nested grid system allows for representation of all scenarios at an appropriate scale – from relatively coarse resolution at the regional scale to finer resolution for determining inundation onto land in Whitianga.

For this study, the following datasets were used:

- Topographic: ETOPO⁸; Shuttle Radar Topography Mission (SRTM); and LIDAR data (Environment Waikato, 2004)
- Bathymetric: General Bathymetric Chart of the Oceans (GEBCO); digitized navigational charts (NZ 531; NZ 5318); and high resolution shallow multi-beam data (University of Waikato)

Both the shallow multi-beam and LIDAR data sets have not been previously used in tsunami model studies for Whitianga, and allow fine resolution model grids to be made.

Wide area model grid

The wide area model grid was developed to represent the various source scenarios that may potentially impact Mercury Bay and Whitianga. This grid spans from 172°E to 179°E and 31°S to 39°S, and covers all potential sources from the Kermadec Trench - including undersea volcanoes. The grid size for this wide area model varies between 1000 m (Figure 4) and 500 m. Results from this model were used as the initial conditions for the finer 50m regional and 5m/10m local nested model grids.

⁸ Also contains bathymetric data

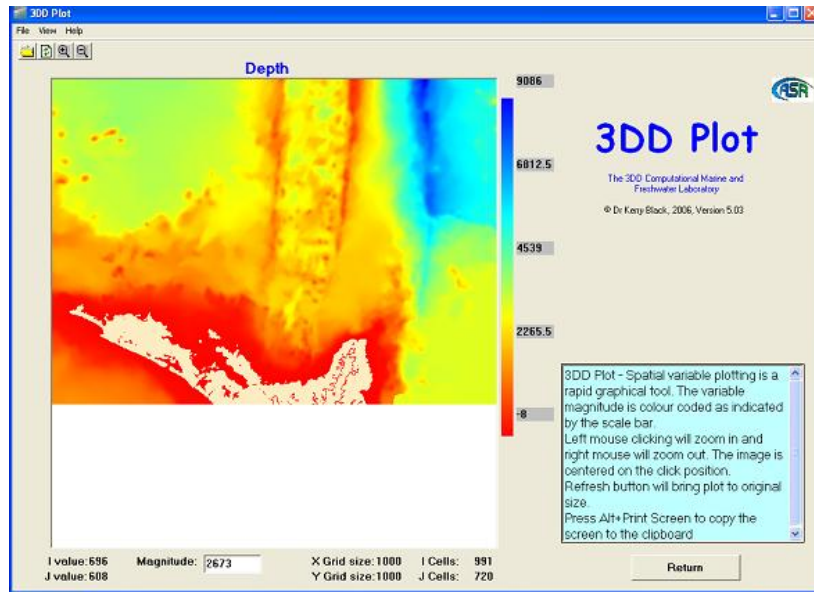


Figure 4. The wide area model with 500-1000 m grid size.

Regional and local nested grid models

The 50m regional nested grid model (Figure 5) was generated to investigate tsunami behaviour during propagation into Mercury Bay and Buffalo Bay. The finer resolution 5m/10m local model grids were generated to investigate fine-scale tsunami inundation. The nested local grid models were derived from a highly accurate LIDAR data set (2004) provided by Environment Waikato (Figures 6 and 7), as well as recent hydrographic multi-beam survey data sets. The LIDAR data consists of two types:

1. Ground striking - a pure digital terrain data set where all structures, houses and trees have been removed; and
2. Non-ground striking - digital terrain data where all houses, structures and trees remain.

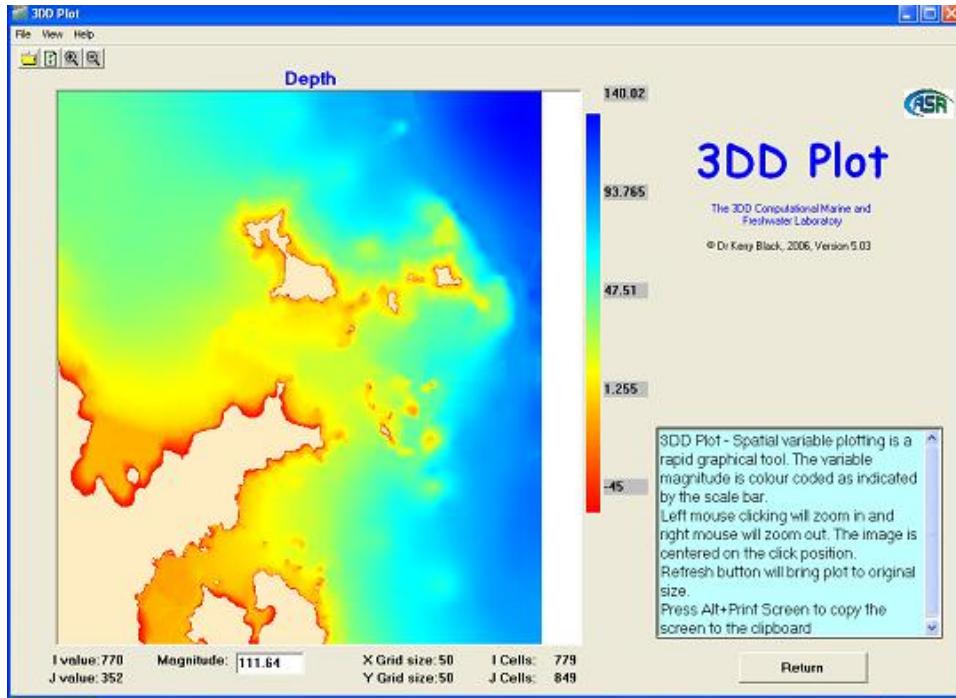


Figure 5. The regional model with 50m grid size

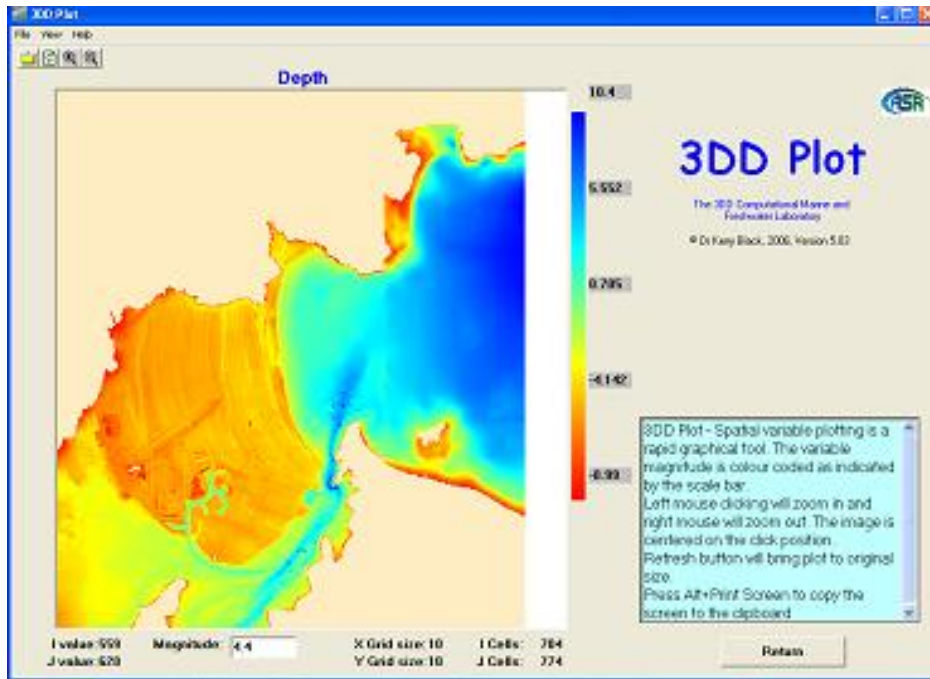


Figure 6. The local model with 5-10m grid size generated with ground striking LIDAR data.

The bathymetric data set was digitized from NZ 531 and 5318 hydrographic charts, and verified with recent sounding (multi-beam and single beam) carried out by the Coastal Marine Group at the University of Waikato.

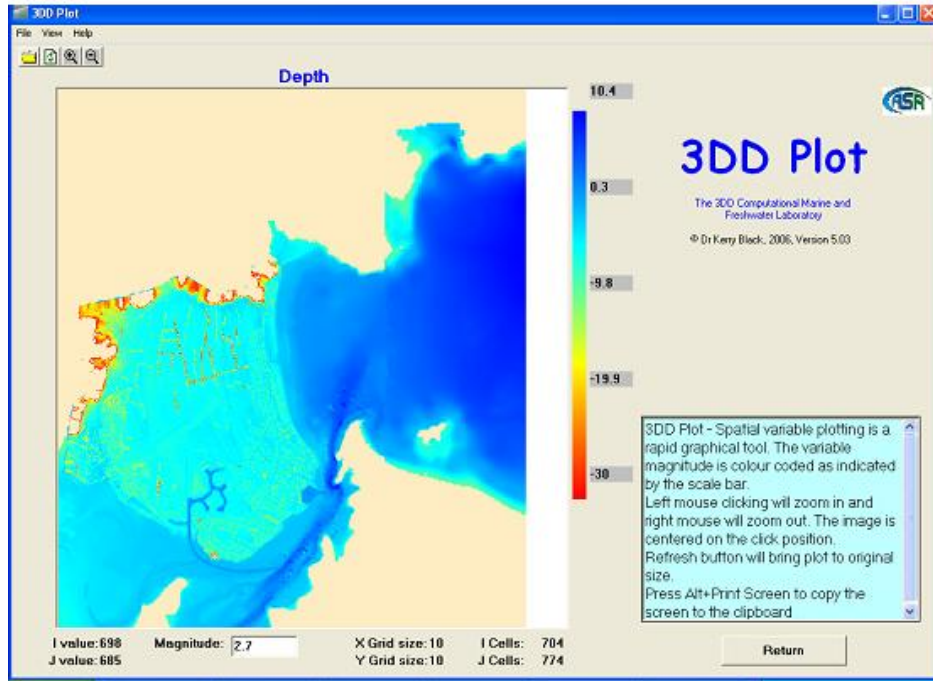


Figure 7. The local model with 5-10m grid size, generated with non-ground striking LIDAR data

Modelling Results

An assessment was made of the tsunami sources that could potentially affect Whitianga from the Kermadec Trench, and beyond the New Zealand continental shelf. There are three primary potential tsunami sources considered:

1. Mt Healy eruptions (15th Century event);
2. Segments 1 and 2 of the Kermadec subduction zone; and
3. The 1960 Chilean events.

Based on this assessment, the worst-case scenario was selected to produce an inundation map, and community mitigation measures. The modelling results are discussed below.

Potential sources - wide area model

Initial conditions

The initial conditions for the Mt Healy eruption follows the method described by de Lange et al. (2001), where the source is located under the sea.

Initial conditions for the earthquake faulting mechanism for an event along the Kermadec Trench followed the Manshina and Smylie (1971) and Okada (1985) method. Using this fault dislocation method, the calculation of the tsunami initial conditions for “thrust” and “normal” faulting are as follows:

- Thrust faulting will produce positive leading waves for the near field, and generally positive leading waves for the far field; and
- Normal faulting will produce negative⁹ (or ‘depression’) leading waves.

The 1960 Chilean tsunami produced a negative leading wave upon arrival in Whitianga.

The regional (wide area) model was run for the following scenarios:

- The Mt Healy eruption
- Kermadec Trench subduction thrust and normal fault events; and
- The 1960 Chilean tsunami.

The results of each of these are shown below.

Mt Healy eruption

The submarine Mt Healy caldera is located in the southern Kermadec volcanic arc, and was formed by a pyroclastic eruption and subsequent collapse in water depths of 550–1,000 m (Goff et al., 2006). Pyroclastic eruption and collapse processes could generate tsunami, and have been considered as the main cause of a large sand wash-over lobe deposit found in a back-beach wetland of Tawharanui Peninsula, north of Auckland (de Lange and Moon, 2006). The initial condition of the tsunami generated by this eruption replicates a Krakatau type eruption as described by de Lange et al. (2001).

⁹ A negative or depression leading wave means that the initial effect of tsunami arrival will be a drawdown or lowering of water levels.

Taking into account the volume erupted, and radial pyroclastic flow distribution and subsequent cone collapse, this event generated circular tsunami waves that propagated outwards from the generating area with a maximum initial wave height of 10 m. These waves are illustrated in Figures 8 and 9¹⁰. The leading waves with a height of 2-4m penetrated Mercury Bay 57 minutes after generation. The leading positive wave was followed by another five smaller waves (Figure 10). The maximum wave height distribution resulting from the source to the shore is illustrated in Figure 11.

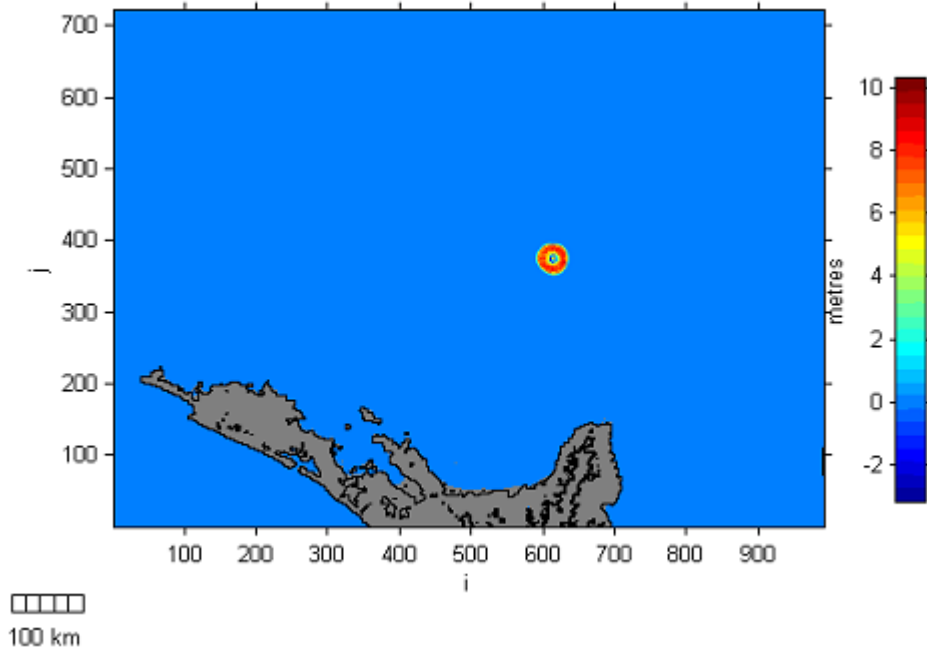


Figure 8. Wide-area model, Mt Healy eruption: initial wave conditions.

¹⁰ Scale bar unit for all figures is in metres.

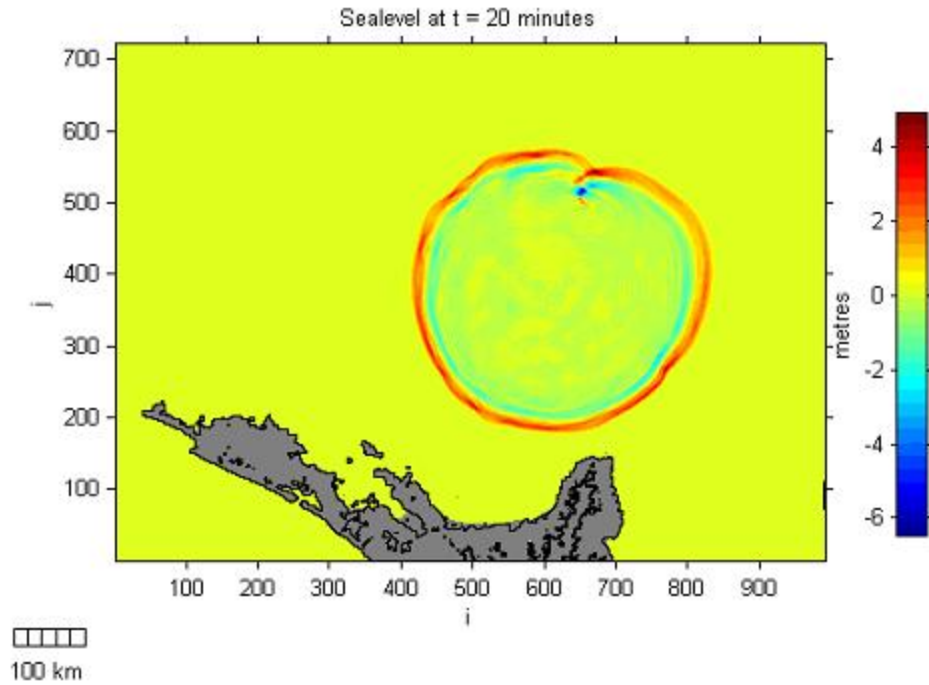


Figure 9. Wide-area model, Mt Healy eruption: radial propagation of waves outwards from Mt Healy, 20 minutes after the eruption.

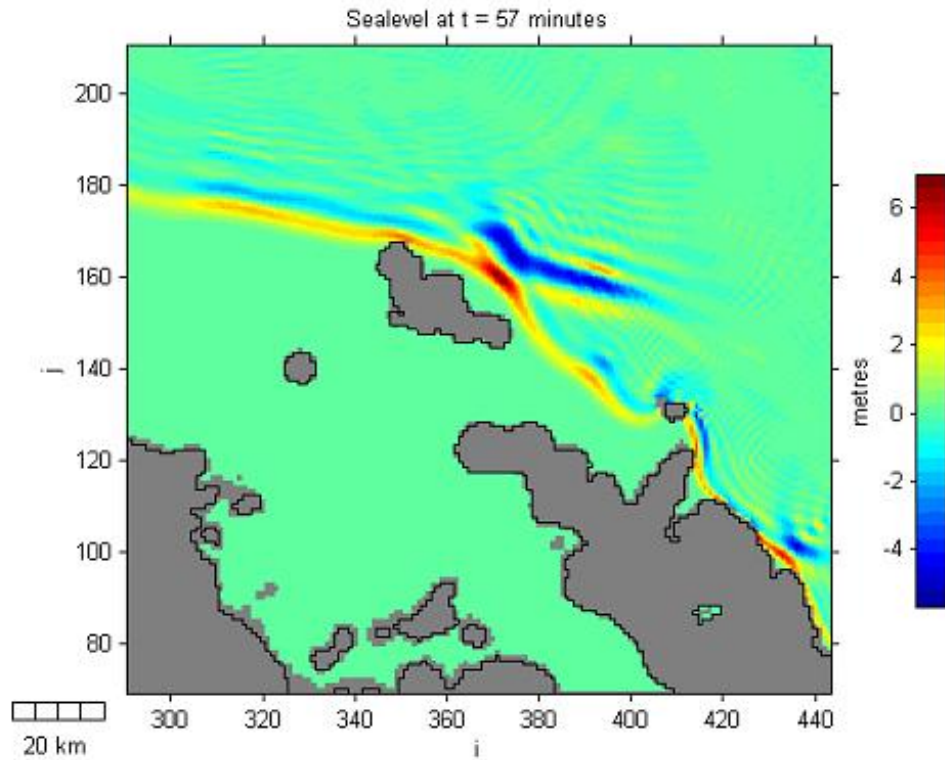


Figure 10. Wide-area model, Mt Healy eruption: the first positive leading waves from Mt Healy penetrate Mercury Bay 57 minutes after generation.

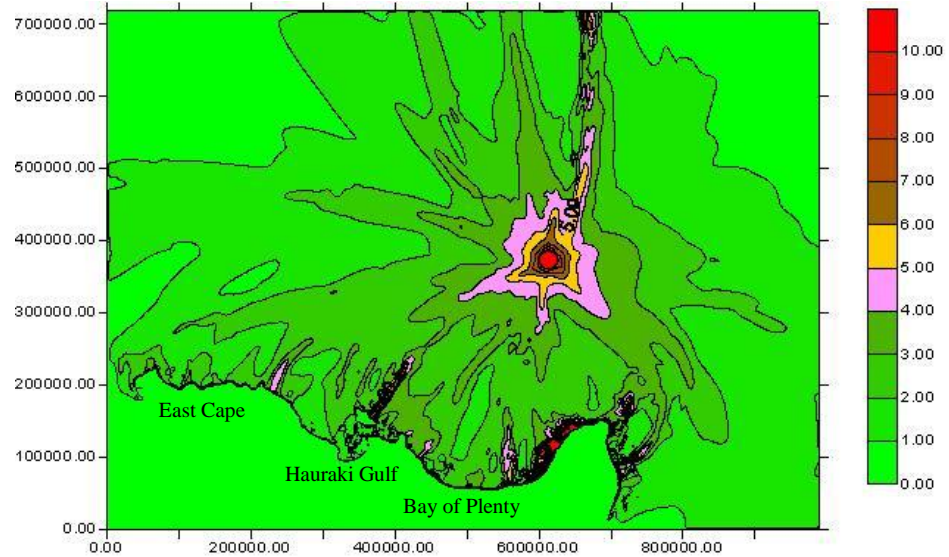


Figure 11. Wide-area model, Mt Healy eruption: distribution of maximum tsunami wave heights from Mt Healy. The diagram shows the variation of maximum wave height along the coast.

Kermadec Trench earthquake

Historical data from the Integrated Tsunami Database for the Pacific 2004 (ITDB/PAC) show that events with Mw 8.0 and 8.3 have occurred in the northern Kermadec Trench. Lessons learned from the 2004 and 2005 Sumatra tsunami events suggest that the maximum credible event would be around a magnitude Mw 8.5 – 9.0 along this subduction zone system. A ‘*worst-case scenario*’ (Mw 9.0) was modelled, with both negative and positive leading waves, as a result of fault ruptures along segments 1 and 2 of the Kermadec subduction zone (refer to Figure 3).

The initial tsunami conditions for a fault rupture of segments 1 and 2 was calculated as follows:

- Vertical displacement was assumed to be between 8 m (Mw 8.7) and 15 m (Mw 9.0);
- Width and length of displacement was:
 - Segment 1: width of 100 km (2 x 50km), and length of 201 km;
 - Segment 2: width of 100 km (2 x 50km) and length of 249 km;
- Both segments assumed dip and slip angles of 10° and 110° respectively; and
- Total fault rupture length (segment 1 + 2) is 450 km.

By comparison, the 2004 Sumatra tsunami event was magnitude Mw 9.3, had a rupture length of 1,200 km, width of 100 km, and vertical displacement between 10 m and 21 m.

Subduction thrust fault event (Mw 9.0)

The initial negative (depression) leading waves as a result of the thrust fault mechanism are illustrated in Figure 12. The negative leading wave propagates onshore towards the New Zealand coast, while a positive wave propagates offshore to the Pacific Ocean (Figure 13). The first wave reaches Mercury Bay 66 minutes after the fault rupture as a negative leading wave of -5m, as illustrated in Figure 14.

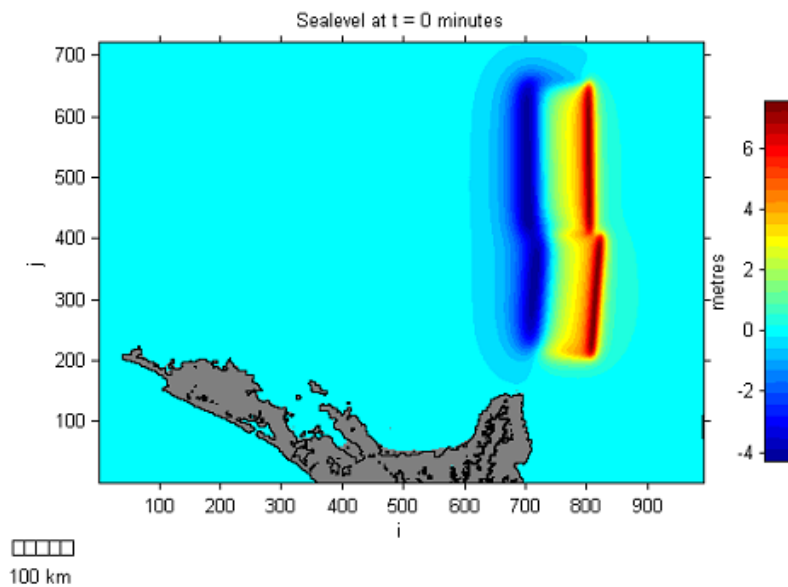


Figure 12. Wide-area model, Kermadec Trench subduction thrust fault event: initial wave conditions.

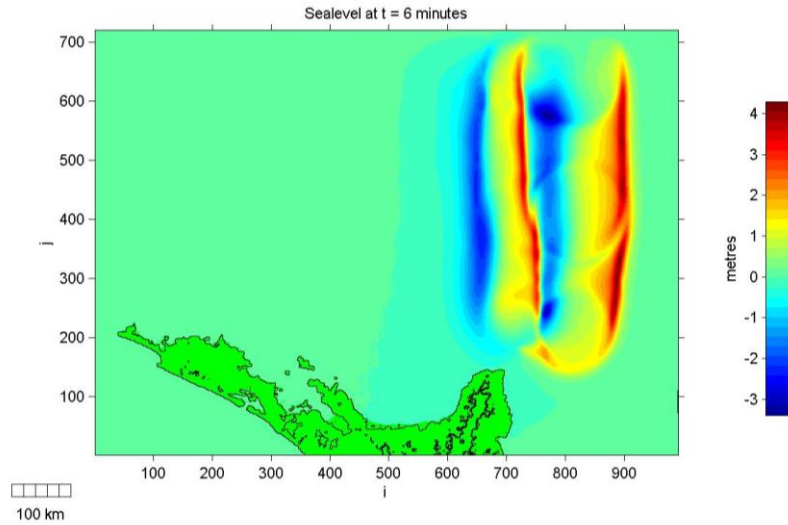


Figure 13. Wide-area model, Kermadec Trench subduction thrust fault event: wave propagation six minutes after the event. The negative leading wave propagates north-westward towards the New Zealand east coast, and the positive leading waves propagate south-eastward into the Pacific Ocean.

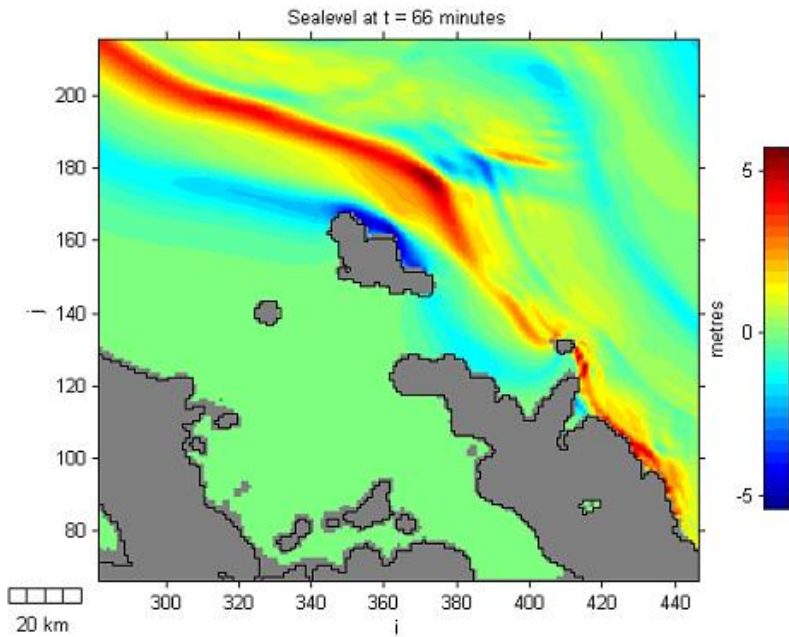


Figure 14. Regional (wide-area) model, Kermadec Trench subduction thrust fault event: 66 minutes after the initial wave was formed, the waves penetrate Mercury Bay.

The model shows that the waves propagating onshore and affecting Whitianga originated from segment 1, while most of the waves from segment 2 affected the coast further north (Figure 15). Hence, Whitianga is more vulnerable to large earthquakes at the southern end of the Kermadec Trench. This result shows the importance of recognising the fault rupture origin, direction and length in relation to early warning and emergency response, since not all fault ruptures along the Kermadec Trench will affect Mercury Bay and Whitianga.

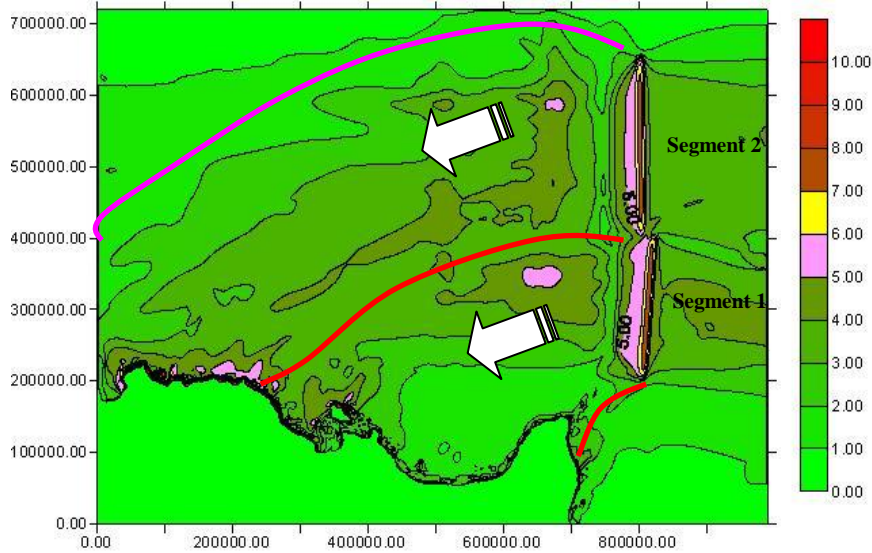


Figure 15. Wide-area model, Kermadec Trench subduction thrust fault event: distribution of maximum tsunami wave heights. Mercury Bay is primarily affected by waves generated in section 1, while waves from section 2 affect the coast further north (Northland).

Subduction normal fault event (Mw 9.0)

The initial positive leading wave produced as a result of a normal fault mechanism is illustrated in Figure 16. The positive leading wave propagates towards the New Zealand coast, while the negative leading wave propagates into the Pacific Ocean (Figure 17).

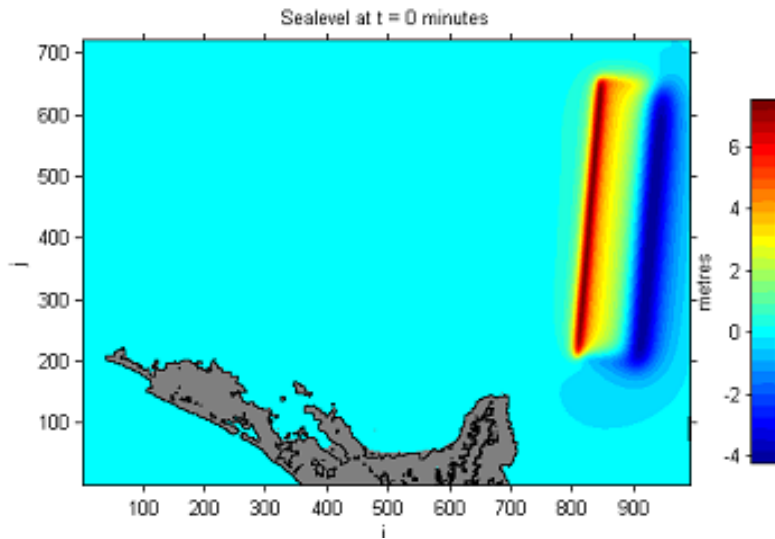


Figure 16. Regional (wide-area) model, Kermadec Trench subduction normal fault event: initial wave condition with a positive leading wave.

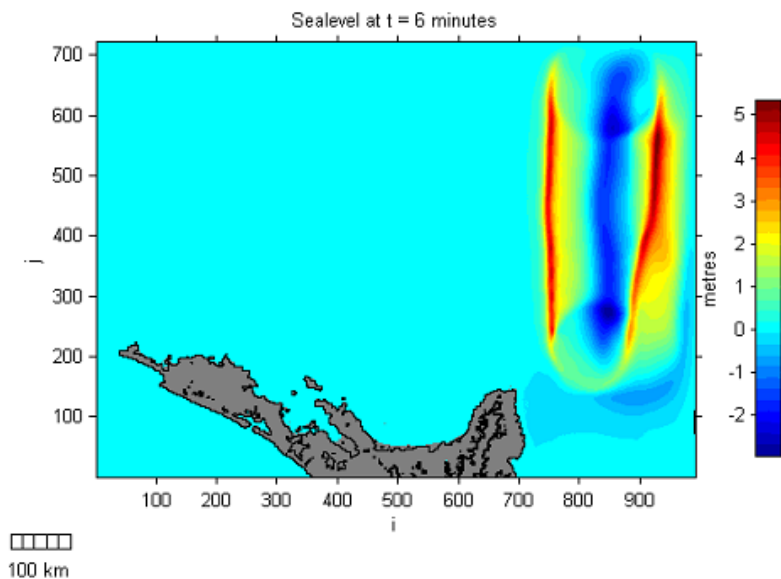


Figure 17. Wide-area model, Kermadec Trench subduction normal fault event: wave propagation six minutes after the event. Positive leading waves propagate towards the New Zealand east coast and negative leading waves propagate into the Pacific Ocean.

The leading tsunami wave reaches Mercury Bay 68 minutes after the fault rupture, with a height of ~5m, as seen in Figure 18. Similar to negative leading waves, the model shows that the waves

affecting Whitianga originated predominantly from segment 1, while most of the waves from segment 2 affected the coast further north (Figure 19).

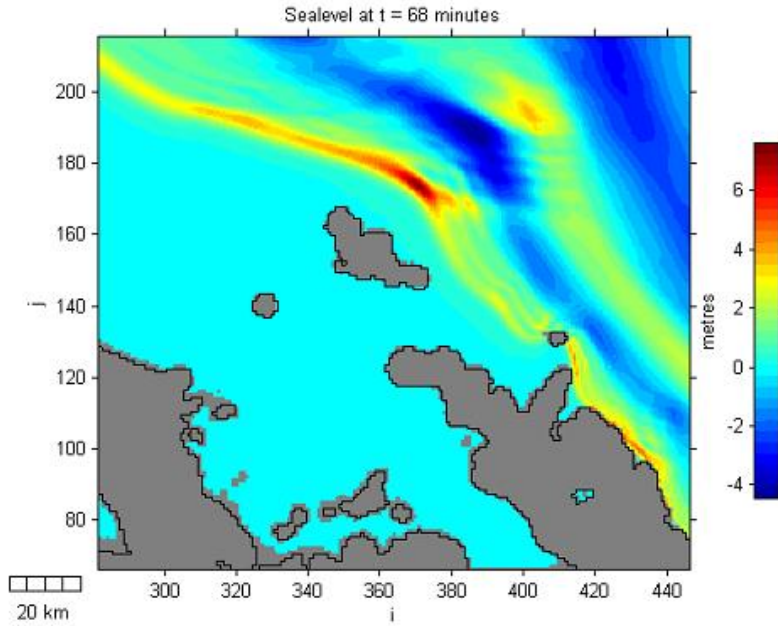


Figure 18. Wide-area) model, Kermadec Trench subduction normal fault event: 68 minutes after the earthquake, the wave penetrated Mercury Bay.

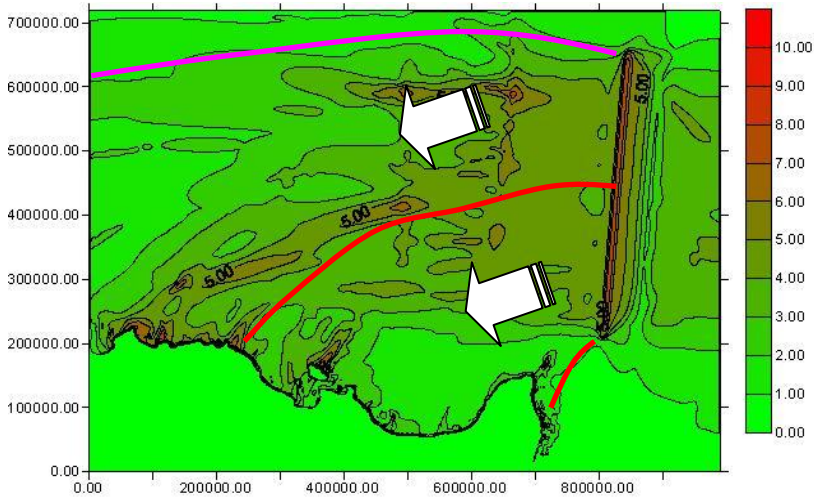
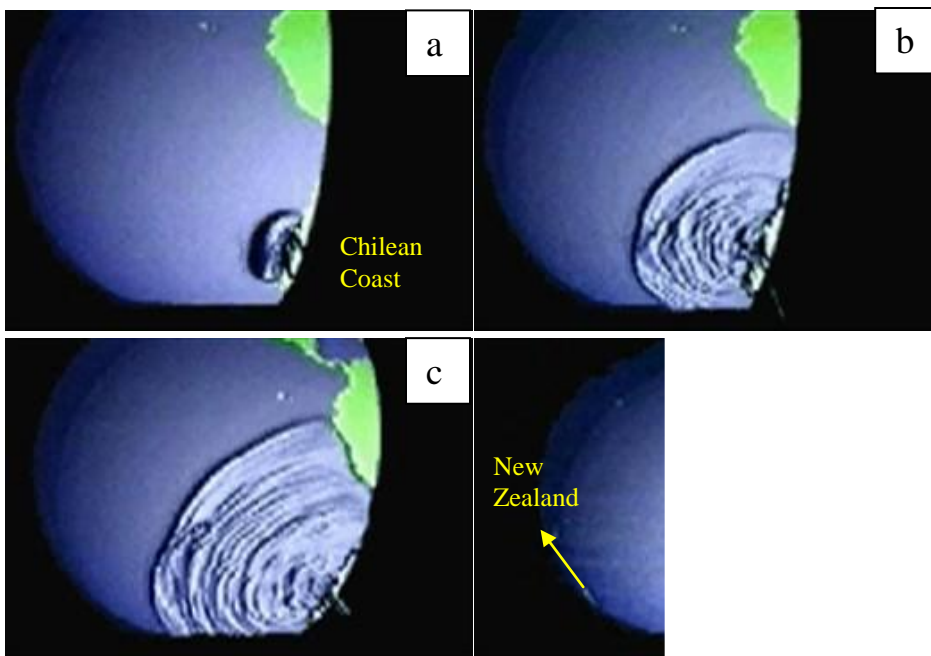


Figure 19. Wide-area model, Kermadec Trench subduction normal fault event: distribution of maximum tsunami wave heights. The positive leading waves illustrate similar patterns to the leading negative waves.

The 1960 Chilean tsunami

Professor Shuto from the Disaster Control Research Centre, Tohoku University, Japan, previously simulated the 1960 Chilean tsunami (Shuto, 1991). His model simulated the transoceanic propagation of this tsunami within the Pacific Ocean, and a sequence showing the tsunami propagation from Chile to the New Zealand coast is illustrated in Figure 20 a-k.

In this case, the leading wave was negative, and the New Zealand coast initially experienced drawdown (or lowering) of sea level at the coast. The tsunami wave-to-wave interaction in the middle of the Pacific Ocean (as seen in Figure 20 g-k), generated new waves with different heights and wavelengths that oscillated within the Pacific Ocean for some considerable time. Eyewitness accounts from Mercury Bay indicate that the Chilean Tsunami was marked by an initial withdrawal of water, and continued for several days¹¹.



Continued.

¹¹ Pascoe, H. (1960): "Recollections of a tidal wave".

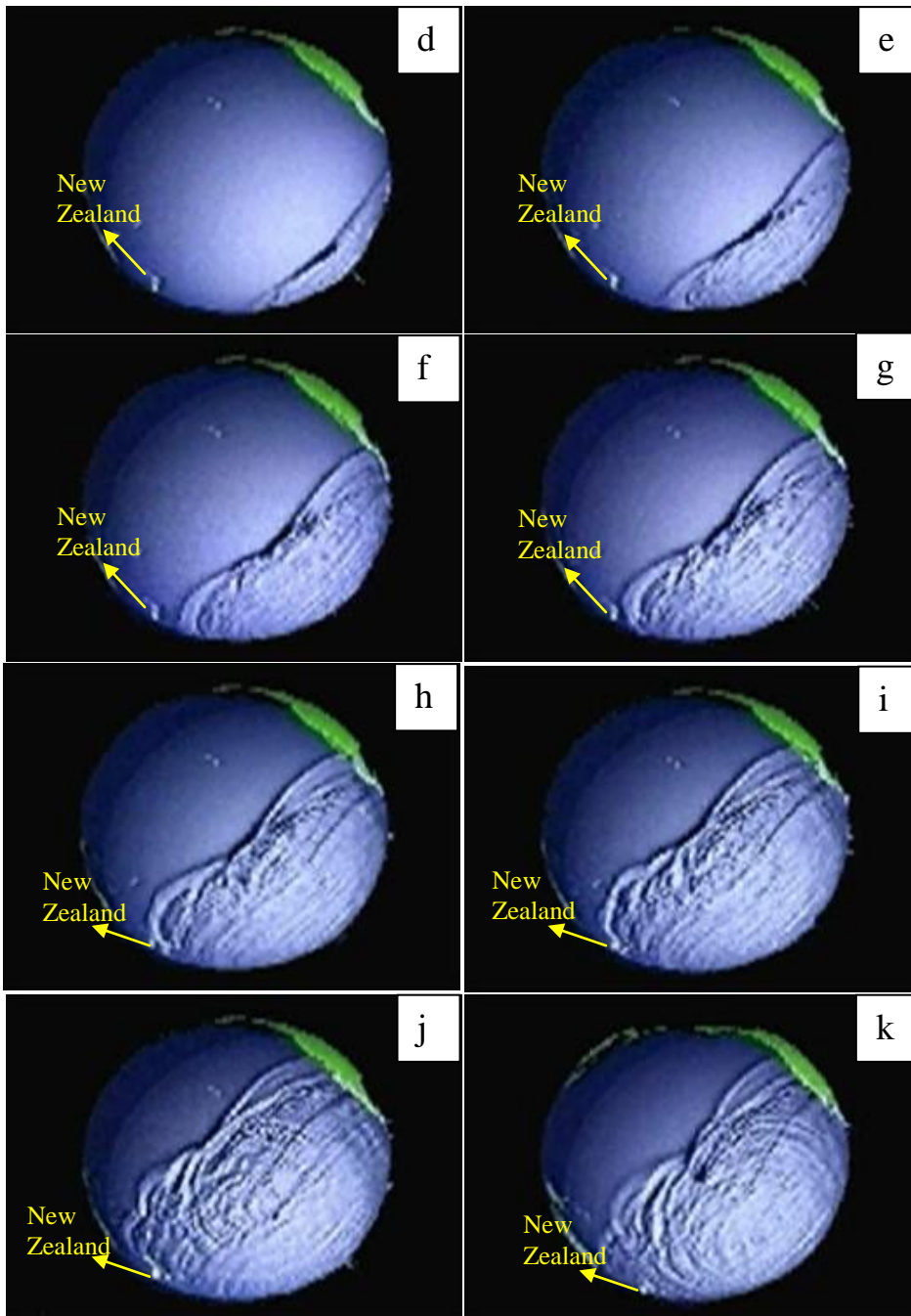


Figure 20 (a-k). Sequence of the propagation of the 1960 Chilean tsunami across the Pacific Ocean (Source: Prof. N. Shuto. Disaster Control Research Center. Tohoku University).

Regional model 50 m grid

Results from the wide area models were used as the initial boundary conditions for a regional model of Mercury Bay with 50 m grid resolution. With this grid size, more detailed analysis was performed to:

- Better understand the dynamics of a tsunami once it has entered Mercury Bay; and
- Identify sources that provide the most significant tsunami impact upon the Whitianga coastal area.

The regional model 50m grid was run for the same scenarios as the wide area model:

- A Mt Healy eruption
- Kermadec Trench subduction thrust and normal fault events; and
- The 1960 Chilean tsunami.

The results of each of these are summarised below.

Mt Healy eruption

The sequences of tsunami waves propagating into Mercury Bay are illustrated in Figures 21-24. The direction of incoming waves is perpendicular to Mercury Bay, with positive leading waves. The leading waves have a height of ~ 5m and a wave length of ~5,500m as they begin to enter Mercury Bay. This is followed by smaller wave trains that consist of three waves with heights less than 3m, and wavelengths greater than 5,000m. Within 10 minutes of entering Mercury Bay, the first tsunami waves hit Buffalo Beach (77 minutes after the eruption).

However, there is no significant inundation at the Whitianga waterfront or further inland. Strong currents are generated at the inlet to Whitianga Harbour and within Buffalo Bay, ranging from 1 m/s to 3.5 m/s.

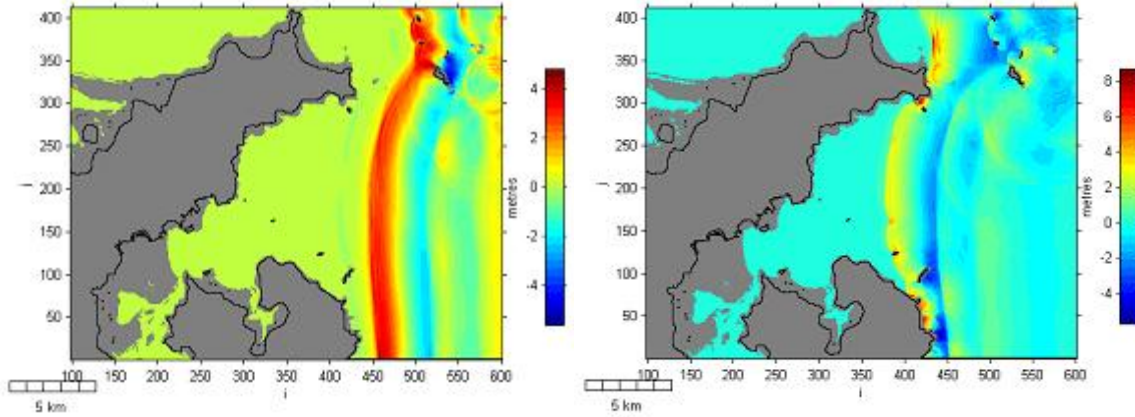


Figure 21. Regional model, Mt Healy eruption: propagation of tsunami waves entering Mercury Bay 57 minutes (left) and 62 minutes (right) following an eruption.

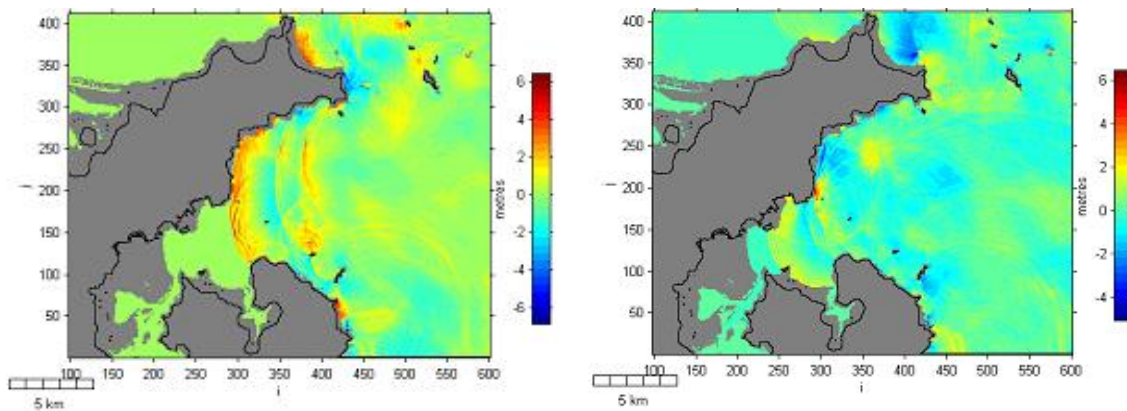


Figure 22. Regional model, Mt Healy eruption: the wave trains consist of three main waves entering Mercury Bay 67 minutes (left) and 72 minutes (right) following an eruption.

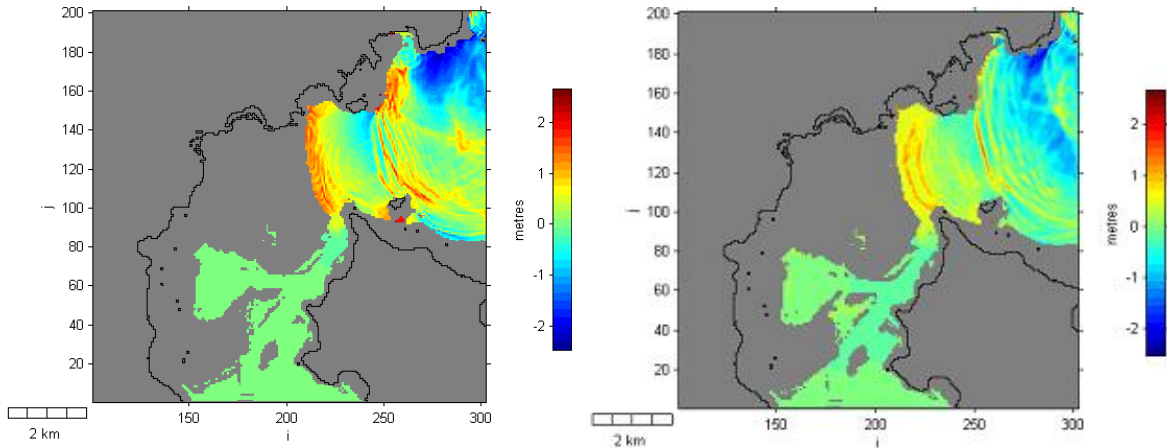


Figure 23. Regional model, Mt Healy eruption: tsunami waves hit the Whitianga coastline 77 minutes (left) following an eruption, but do not inundate the town. Sea level continues to oscillate in Buffalo Bay for some time (right).

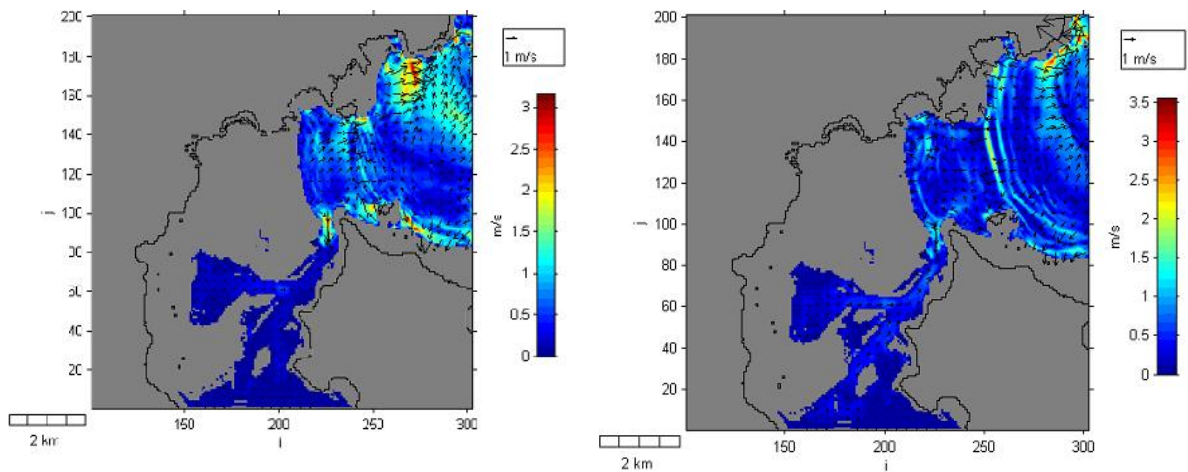


Figure 24. Regional model, Mt Healy eruption: strong currents are generated in Whitianga Harbour during incoming (left) and outgoing (right) tsunami waves.

Kermadec Trench earthquake

Subduction thrust event (Mw 9.0)

The initial waves for the regional model 50m grid were extracted from the corresponding wide area model. Figure 25 shows the first negative displacement tsunami waves penetrating Mercury Bay 98 minutes after the fault rupture. An initial drawdown of 3m is created by this wave in the middle of Mercury Bay, producing a relatively strong seawards directed current towards the outside of Buffalo Bay (Figure 26).

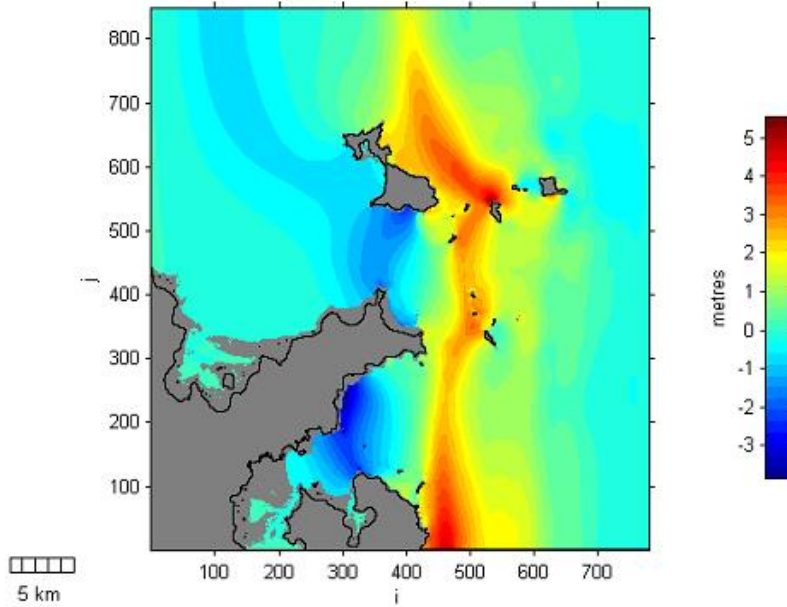


Figure 25. Regional model, Kermadec Trench subduction thrust fault event: propagation of leading negative wave 98 minutes after fault rupture.

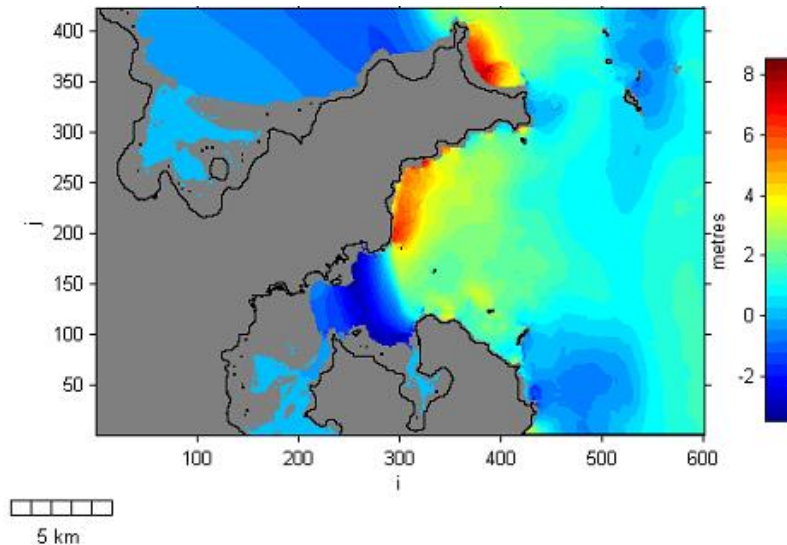


Figure 26. Regional model, Kermadec Trench subduction thrust fault event: initial drawdown in Mercury Bay. The leading depression waves continue to Buffalo Bay causing the sea to recede at the coast. Most of the current at this stage flows out of Buffalo Bay in an offshore direction.

Within 12 minutes, the sea has withdrawn at Buffalo Bay to an elevation of -3.5m (Figure 27), and 6 minutes later, long crested waves of ~6m height start to inundate the Whitianga waterfront (Figure 28). It takes 22 minutes to inundate Whitianga Township up to 2.5 km inland after the arrival of the wave at Buffalo Beach (Figure 29). Strong currents of between 5 m/s and 6.5 m/s

are created during tsunami inundation, both within the Whitianga Harbour inlet, and inside Buffalo Bay (Figures 30 and 31).

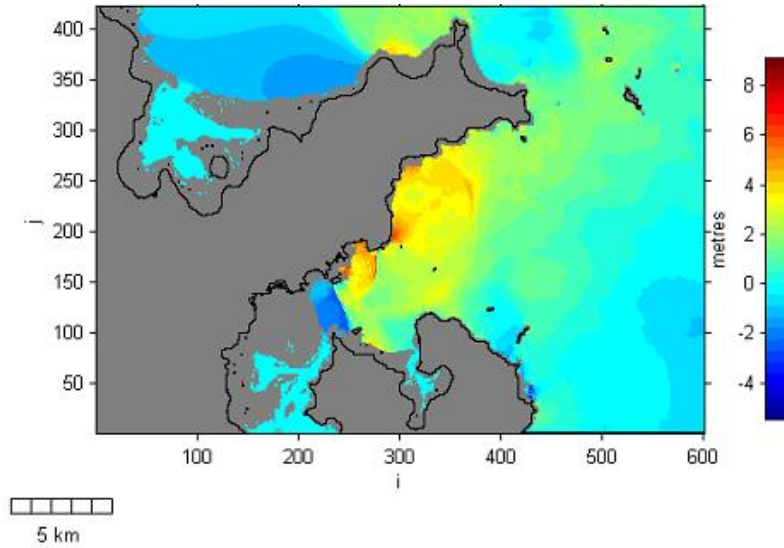


Figure 27. Regional model, Kermadec Trench subduction thrust fault event: wave reflection is amplifying tsunami waves towards Buffalo Bay.

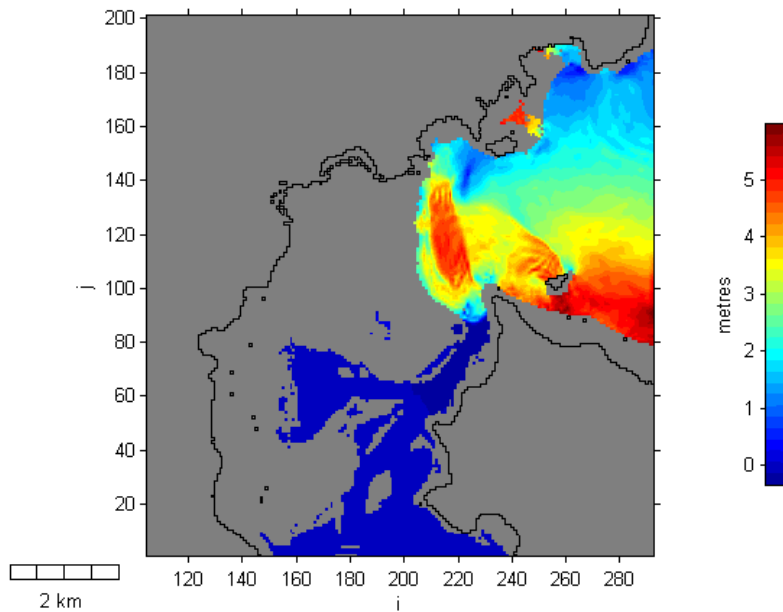


Figure 28. Regional model, Kermadec Trench subduction thrust fault event: inundation of Whitianga begins 1 hour and 58 minutes after the event. Reflection from the southern shore of Mercury Bay has intensified the tsunami.

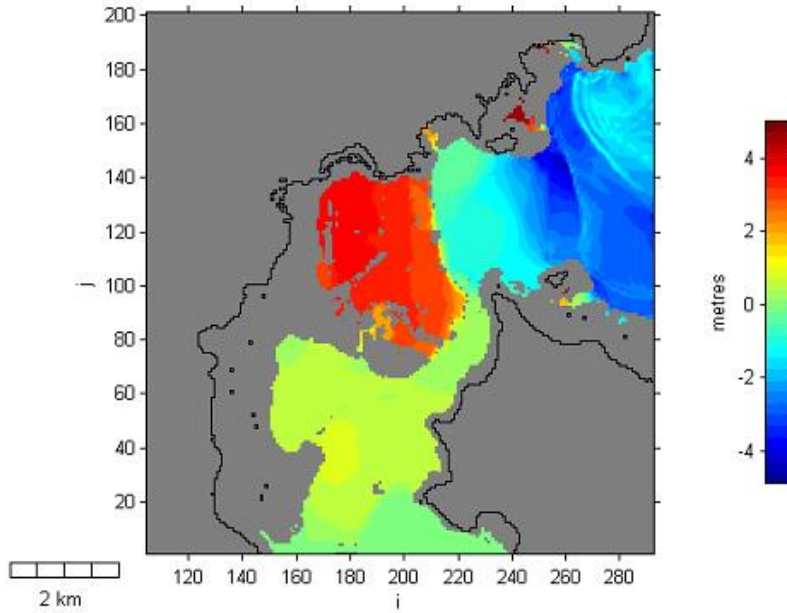


Figure 29. Regional model, Kermadec Trench subduction thrust fault event: inundation of Whitianga from first tsunami wave arrival. It takes ~ 22 minutes to inundate Whitianga Township up to 2.5 km inland. The tsunami flows up to 5 km upstream through the Whitianga Harbour.

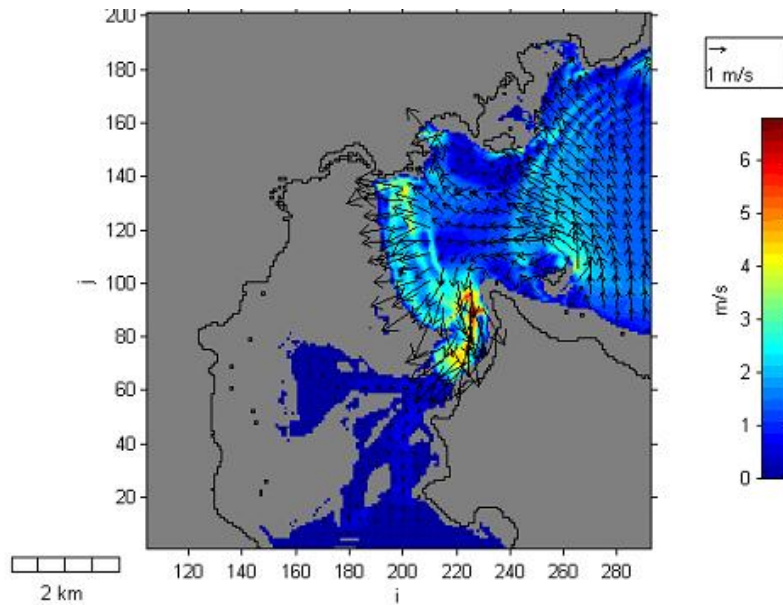


Figure 30. Regional model, Kermadec Trench subduction thrust fault event: current patterns during Whitianga waterfront inundation. Strong currents of up to 5 m/s have been generated at the Whitianga Harbour inlet, and up to 3.5 m/s overland.

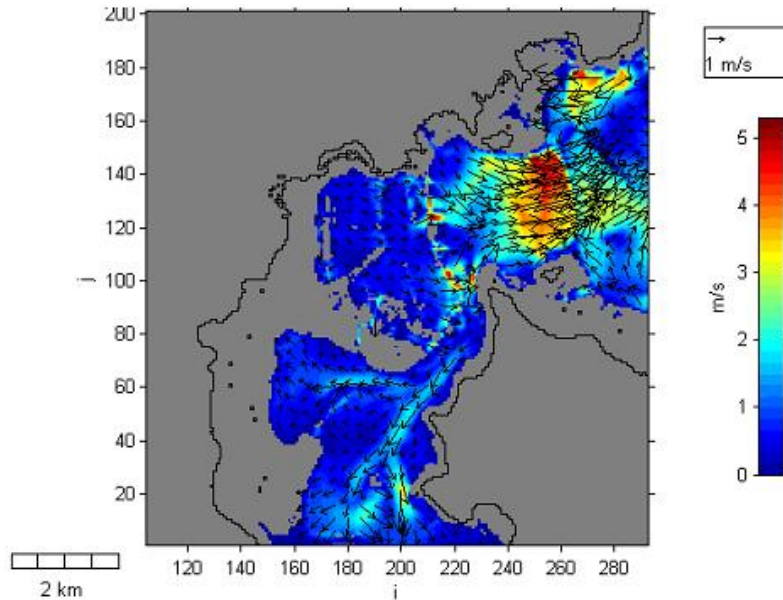


Figure 31. Regional model, Kermadec Trench subduction thrust fault event: current pattern during return flows after maximum inundation. At this time, there was still an upstream flow within Whitianga Harbour, and strong offshore currents had been generated in the middle of Buffalo Bay.

Normal fault event (Mw 9.0)

This scenario considers the result of a normal fault event along segments 1 and 2 of the Kermadec trench. The initial waves were extracted from the corresponding wide area model. The first tsunami waves penetrated Mercury Bay 75 minutes after the event (Figure 32) and propagated into Buffalo Bay (Figures 33 and 34). It took 11 minutes after the tsunami entered Mercury Bay to inundate the Whitianga waterfront (Figure 35), and 24 minutes to inundate the Whitianga coastal area up to 2.4 km inland (Figure 36).

Strong currents of 5-7 m/s are created during inundation - both in the Whitianga Harbour inlet, and within Buffalo Bay (Figures 37 and 38). The maximum inundation areas reached almost 3 km inland (Figure 39).

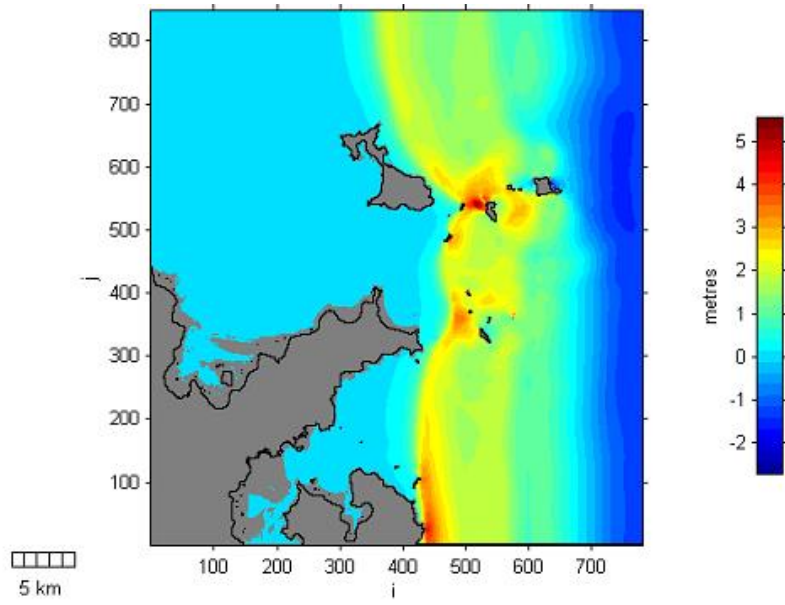


Figure 32. Regional model, Kermadec Trench normal fault event: propagation of leading positive wave entering Mercury Bay 75 minutes after fault rupture.

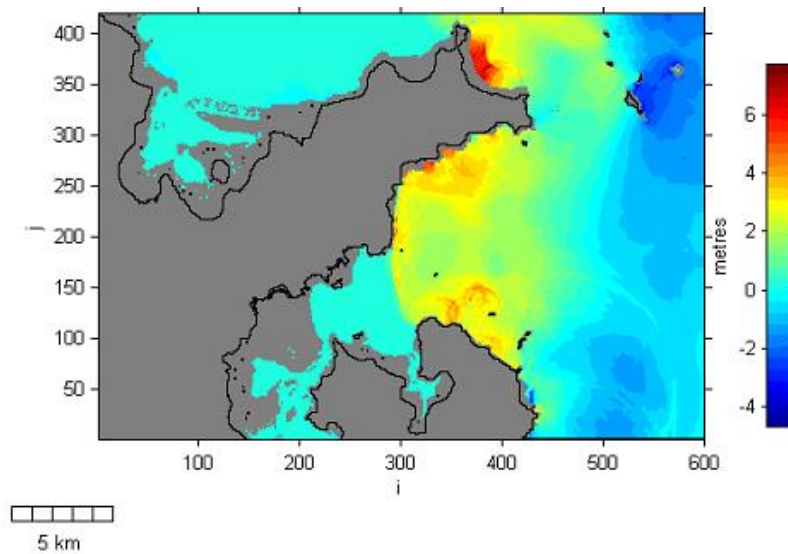


Figure 33. Regional model, Kermadec Trench normal fault event: leading positive waves continue, and interact with reflected waves from both sides of outer Mercury Bay. The resultant waves propagate towards Buffalo Bay.

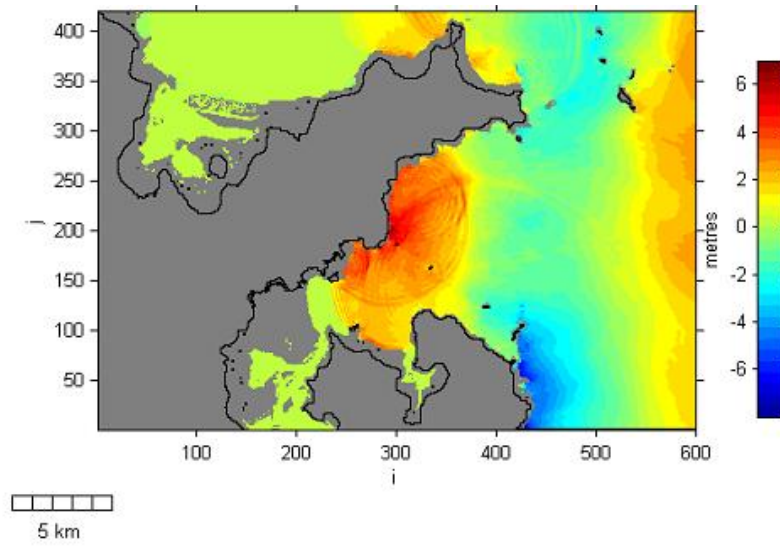


Figure 34. Regional model, Kermadec Trench normal fault event: oscillations along the northern shore of Mercury Bay become more intense and amplify the incoming waves towards Buffalo Bay.

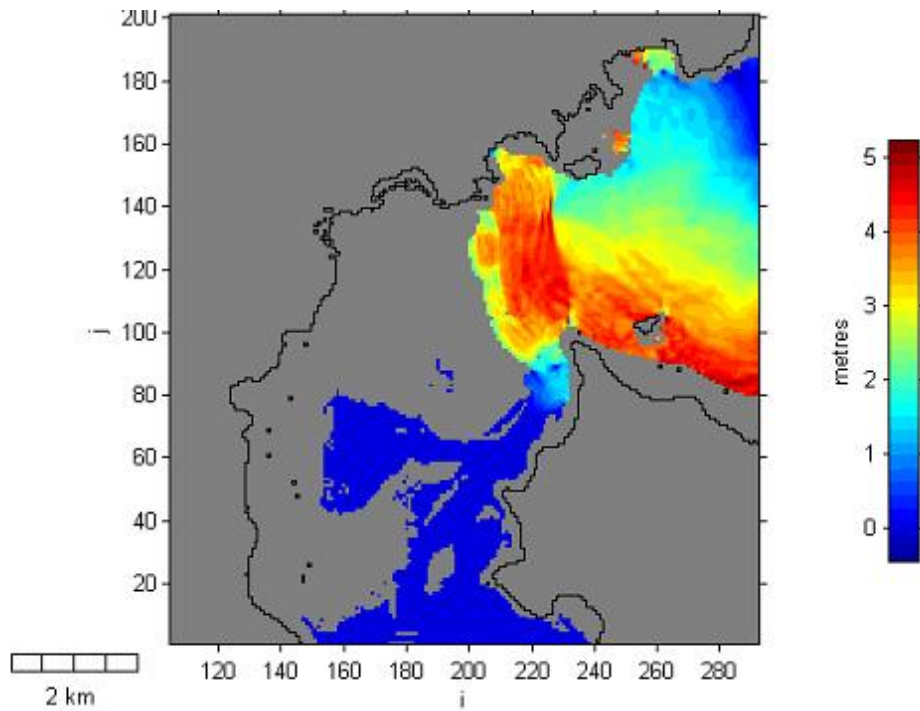


Figure 35. Regional model, Kermadec Trench normal fault event: inundation of the Whitianga waterfront 11 minutes after the first waves penetrate Mercury Bay (1 hour 28 minutes after the event). At this stage, sea levels are elevated in Buffalo Bay, and at the southern shore of Mercury Bay.

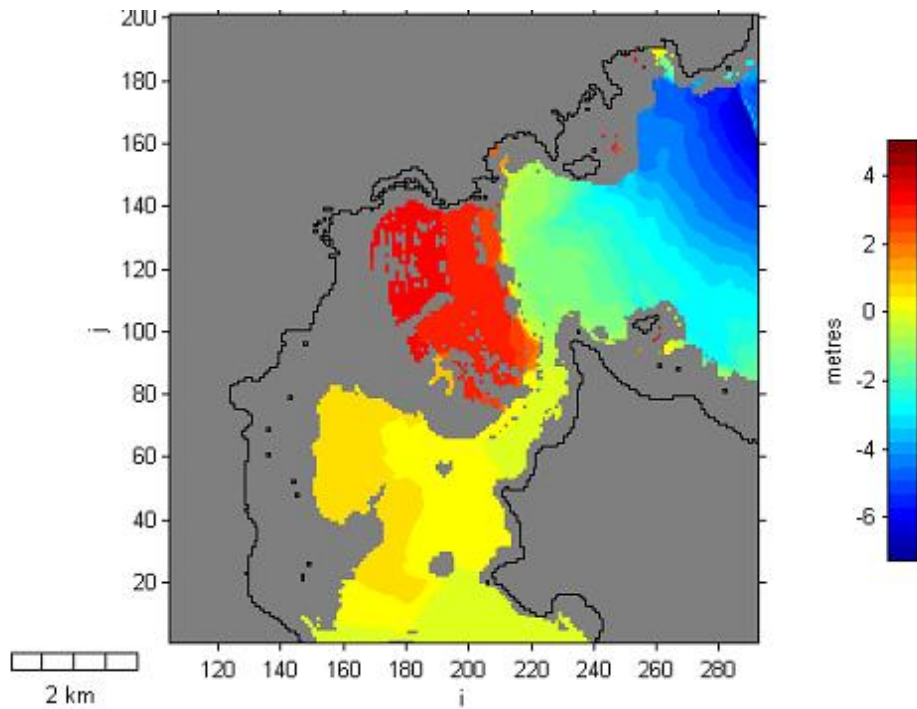


Figure 36. Regional model, Kermadec Trench normal fault event: inundation of Whitianga from first wave arrival onshore. It takes 24 minutes to inundate Whitianga up to 2.4 km inland, and affects Whitianga Harbour up to 5 km upstream.

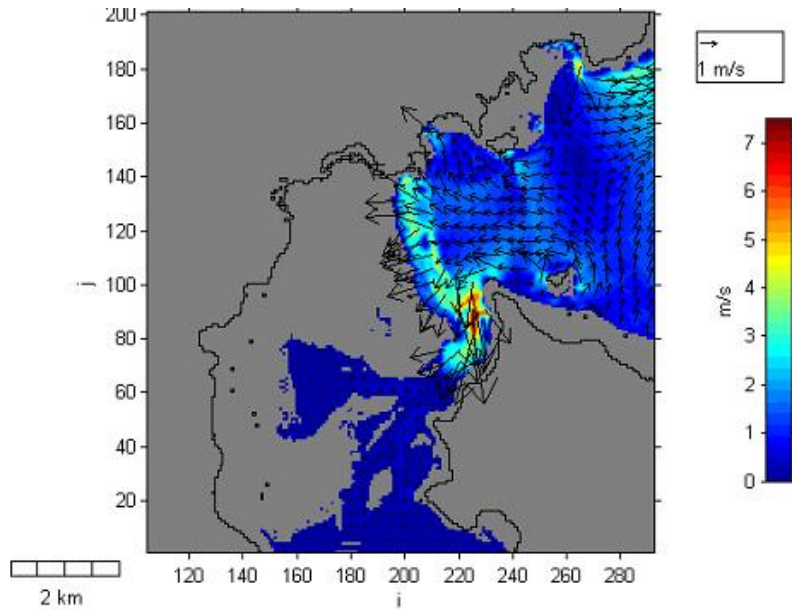


Figure 37. Regional model, Kermadec Trench normal fault event: current patterns during Whitianga waterfront inundation. Strong currents of up to 6 m/s were generated within the Whitianga Harbour inlet, and up to 4 m/s overland.

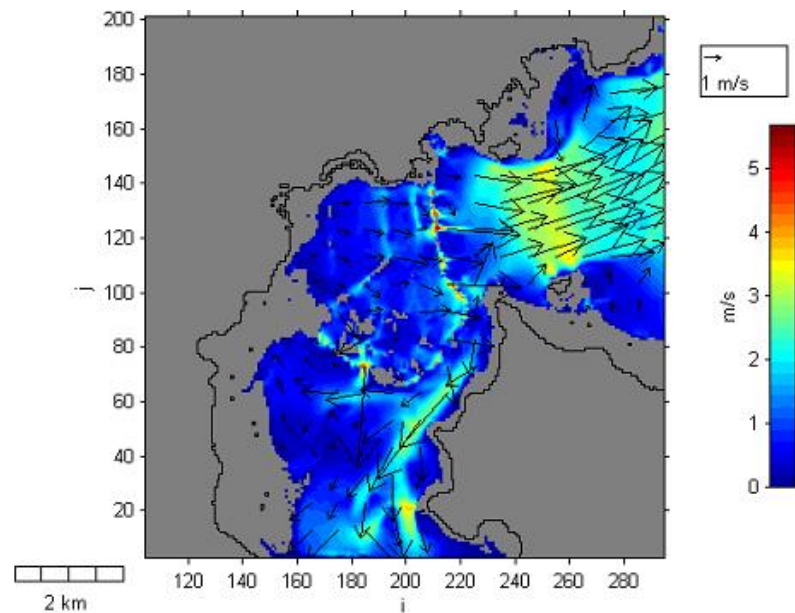


Figure 38. Regional model, Kermadec Trench normal fault event: current pattern during returning flows following maximum inundation. Strong return flows on land can be seen at several places along the coast, such as on stream outlets, and in the middle of Buffalo Bay.

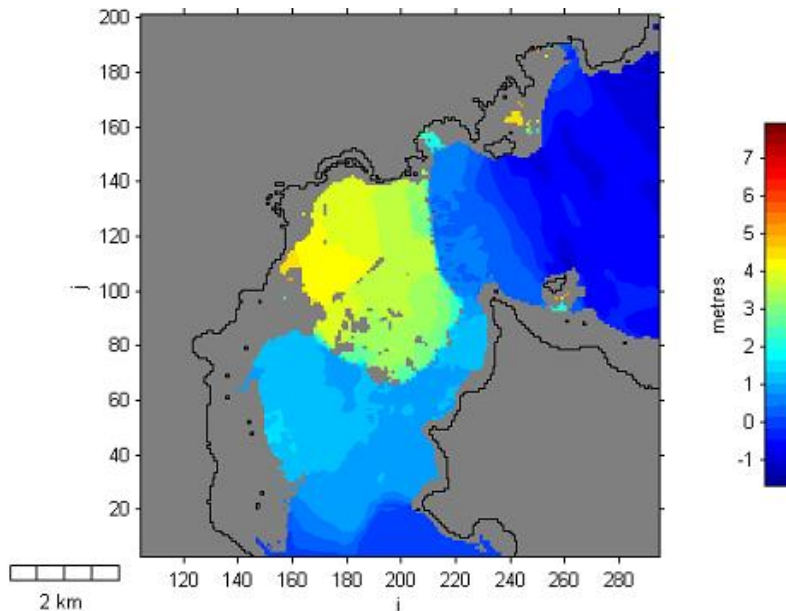


Figure 39. Regional model, Kermadec Trench normal fault event: maximum inundation (four hours after the event) covers most of the Whitianga low lying areas - around 3 km inland.

The 1960 Chilean tsunami

The global model of the 1960 Chilean tsunami (Shuto, 1991) shows that the first waves that arrived at the New Zealand east coast were leading negative waves. This agrees with the eyewitness accounts from Whitianga for this event.

Therefore, the initial condition for the boundaries of this model used the leading negative waves as shown in Figure 40. The leading negative wave caused the sea level to drop within Mercury Bay, before the sea rushed up and inundated the Whitianga waterfront up to Buffalo Road (Figures 41 and 42).

Strong currents of up to 5 m/s were generated within the Whitianga Harbour inlet and at Buffalo Bay (Figures 43 and 44). The geometry of Mercury Bay had a major role in amplifying the incoming tsunami waves. Interaction between the incoming waves and reflected waves within Mercury Bay produced considerably higher waves that propagated into Buffalo Bay, and inundated Whitianga.

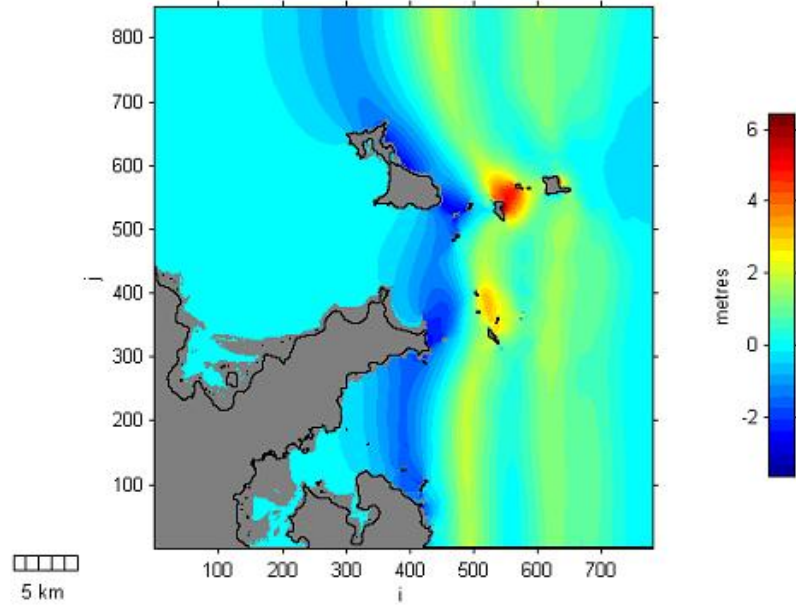


Figure 40. Regional model, 1960 Chilean-type tsunami: propagation of leading negative waves entering Mercury Bay.

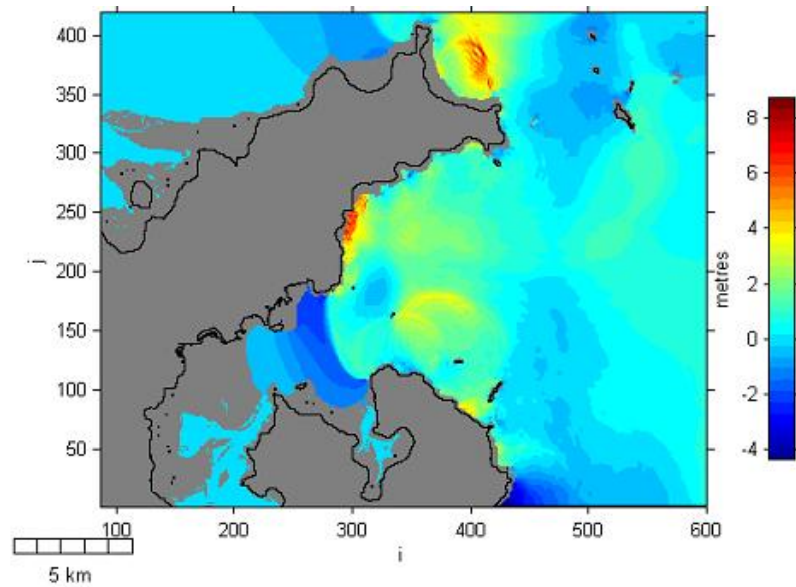


Figure 41. Regional model, 1960 Chilean-type tsunami: leading negative waves caused an initial recession of sea level in Buffalo Bay and Mercury Bay, and generated offshore currents.

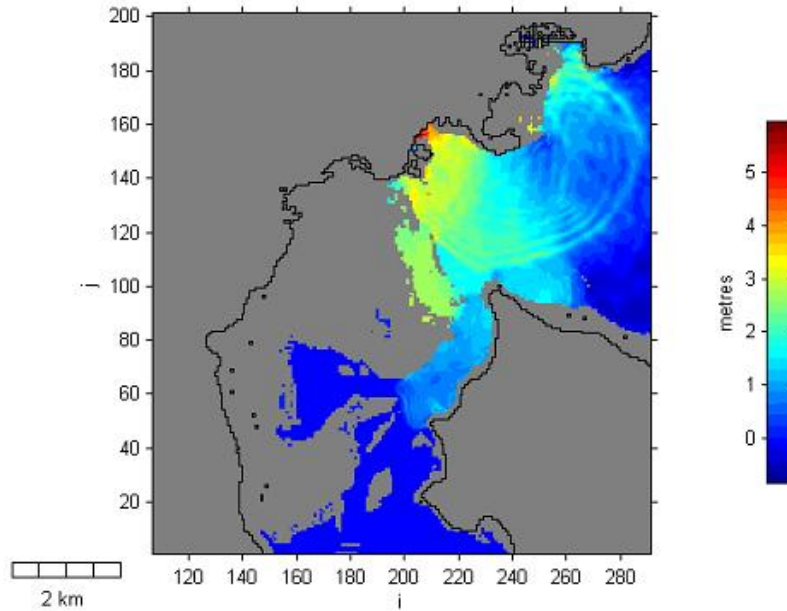


Figure 42. Regional model, 1960 Chilean-type tsunami: inundation of Whitianga. Inundation was due to the interaction of reflected waves and the incoming tsunami waves inside Mercury Bay and Buffalo Bay. The geometry of the bay plays a significant role in amplifying the incoming tsunami waves.

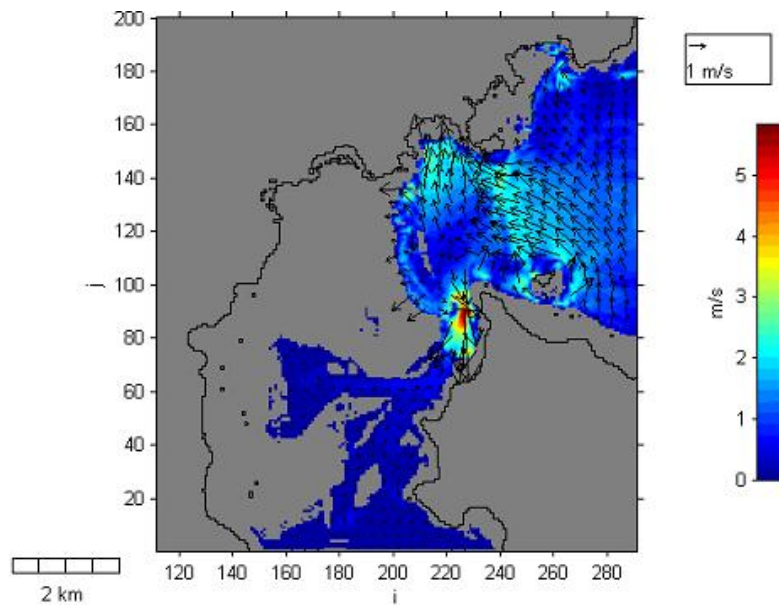


Figure 43. Regional model, 1960 Chilean-type tsunami: strong currents were generated within the Whitianga Harbour inlet during inundation. Eyewitnesses of the event reported these.

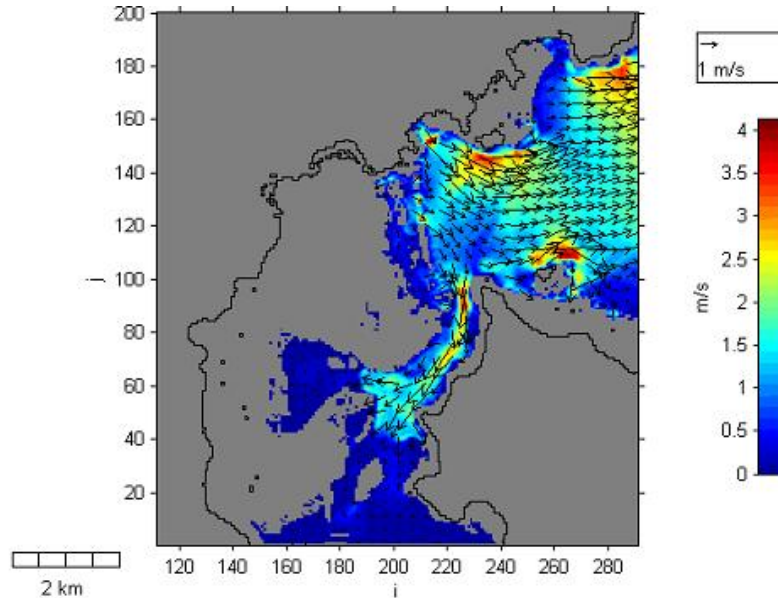


Figure 44. Regional model, 1960 Chilean-type tsunami: current patterns during returning flows following maximum inundation. The model shows the high-speed current flow of the tsunami propagating inside the Whitianga Harbour simultaneous with backflows in Mercury Bay. At this stage, maximum inundation had been reached on land, but the high-speed flow was still propagating upstream inside the harbour.

Summary of wide area and regional model results.

The results of these models show that:

- The Mt Healy eruption event produced a minimal impact at Whitianga. The tsunami generated by this event did not inundate Whitianga. Despite this, strong currents of up to 2.5 m/s were generated inside Buffalo Bay and within the Whitianga Harbour inlet.
- The Kermadec Trench earthquake scenarios with both positive and negative leading waves, as a result of a subduction fault dislocation along segments 1 and 2, have a significant impact on Whitianga. The waves inundate the coastal area up to 2.5 and 3 km inland for the subduction thrust fault and normal fault events respectively, and affect the entire area of Whitianga Harbour. The normal fault event with positive leading waves has more impact than the thrust fault event that produces negative leading waves.
- The 1960 Chilean event produced tsunami waves that inundated Buffalo Beach Road and houses in Whitianga, as observed by eyewitnesses. Strong currents of up to 5 m/s are generated inside Buffalo Bay and the Whitianga Harbour inlet.

Local grid model.

The extent of inundation on land of using the regional model was based on a model that used a uniform bed roughness coefficient. Further investigations were made using a finer local model grid that used different bed roughness coefficients through the model domain, and that considered the features of the terrain within the LIDAR data set provided.

Based on the regional model assessments, the Kermadec Trench earthquake “worst case” scenario (Mw 9.0 with normal faulting) and the 1960 Chilean-type tsunami were used as initial conditions for the fine scale local model to better simulate inundation of Whitianga. The characteristics of tsunami waves determined by the regional model in deep water (off the continental shelf), inside Mercury Bay and near-shore to Whitianga before inundation can be seen in Figures 45 and 46. After 7 hours, sea level was still oscillating inside Mercury Bay with considerable amplitude – around 2 m. Meanwhile, outside Mercury Bay, the sea levels returned back to normal.

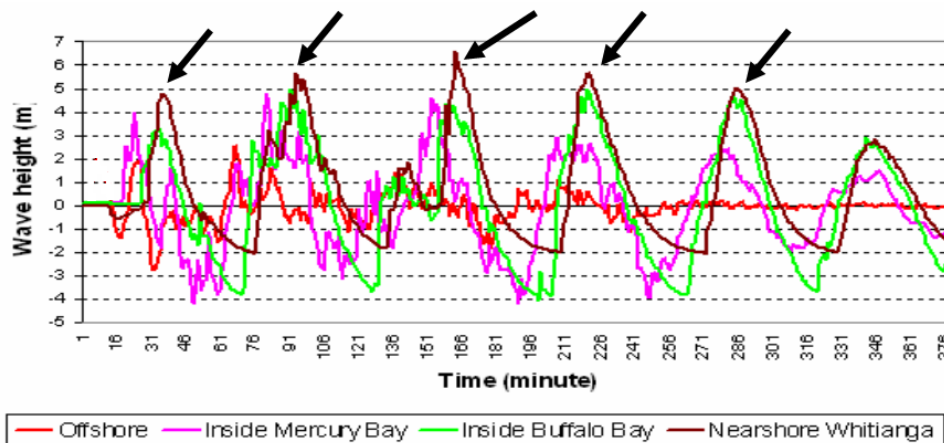


Figure 45. Time series of the Kermadec Trench subduction reverse fault event (Mw 9.0). The graph shows waves from offshore to near-shore, and shows wave amplification inside Buffalo Bay. After 7 hours, the waves outside Mercury Bay disappear, but inside Mercury Bay, sea level oscillates with considerable amplitude. Whitianga Township is inundated five times, as indicated by arrows on the graph.

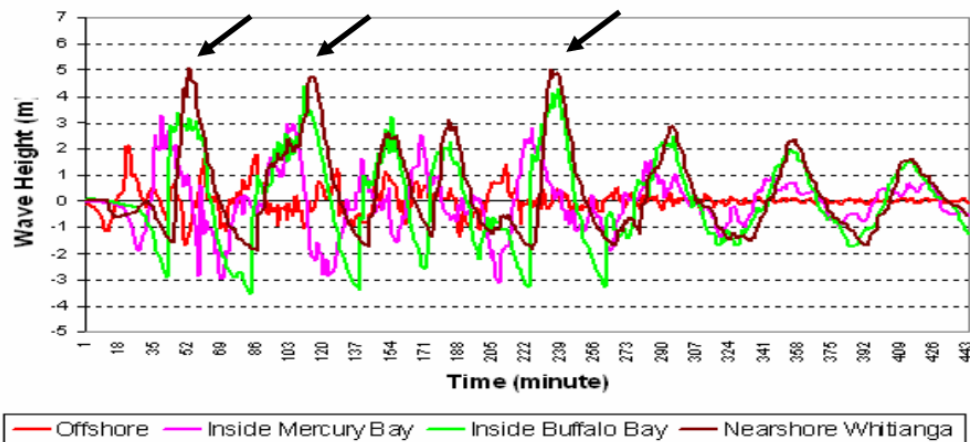


Figure 46. Time series of the Kermadec Trench subduction normal fault event (Mw 9.0). The graph shows waves from offshore to near-shore, and shows wave amplification inside Buffalo Bay. After 7 hours, the sea level outside Mercury Bay levels off, but inside Mercury Bay, sea level still oscillates with considerable amplitude. Whitianga Township is inundated three times, as indicated by arrows on the graph.

The local grids were generated at 5m and 10m grid resolutions using the Waikato Regional Council LIDAR data set, comprising both ground striking (without any vegetation, buildings or other structural influences) and non-ground striking data (with vegetation, buildings or other structural influences).

The ground-striking model grid produced the maximum tsunami inundation inland at Whitianga due to the reduced number of obstructions to the flow. Bed roughness coefficients were applied to the ground-striking model, with values varying from 0.001 to 0.01 based on the terrain features.

Local model assessments were made for both the Kermadec Trench subduction normal fault event (Mw 9.0) and the 1960 Chilean-type tsunami, using both ground striking and non-ground striking model grids. The scenarios were run during high tide, low tide and at Mean Sea Level (MSL) conditions. However, the tide levels were kept constant during the simulations, and did not vary as tides would normally do.

In general, a tsunami arriving during high tide would produce a much greater effect than a tsunami arriving during low tide. However, the regional model showed that the impact of sea level position on inundation distance was not as great as would usually be expected during tsunami inundation.

Kermadec Trench subduction normal fault event (Mw 9.0).

Inundation model results for ground striking LIDAR data

As shown in Figures 45 and 46, the Kermadec Trench subduction normal fault event has a greater impact on Whitianga than the reverse fault scenario. Both also have a greater impact than observed during the 1960 Chilean tsunami. The Kermadec Trench event inundates Whitianga five times within six hours, and the waves continue to oscillate within Mercury Bay with considerable amplitude for some time - even though the offshore sea level has already returned to normal. This is due to resonance inside Mercury and Buffalo Bays that amplifies the waves. Historical observations during the 1960 Chilean event confirm that Mercury Bay experienced oscillations for several days following the event.

The maximum tsunami inundation for this model is shown in Figure 47. At 11 minutes after the first waves penetrate Mercury Bay, Whitianga is inundated some 800m from the coastline. A further 61 minutes later, the second wave strikes, and inundates up to 1 km inland over most of the town, and up to 1.3 km inland along the Taputapuatea Stream.

The third and fourth inundations are the largest, and occur 130 and 187 minutes after the first inundation. The waves inundate Whitianga up to 1.8 km inland, and affect most of the Whitianga Harbour. The last inundation occurs 90 minutes later, but is minor, and does not penetrate further inland. Strong currents of up to 6 m/s are generated during run-up and run-down on land, within the harbour, and within Buffalo Bay. These strong currents are dangerous to people, buildings, vessels in the marina and harbour, and to other infrastructure.

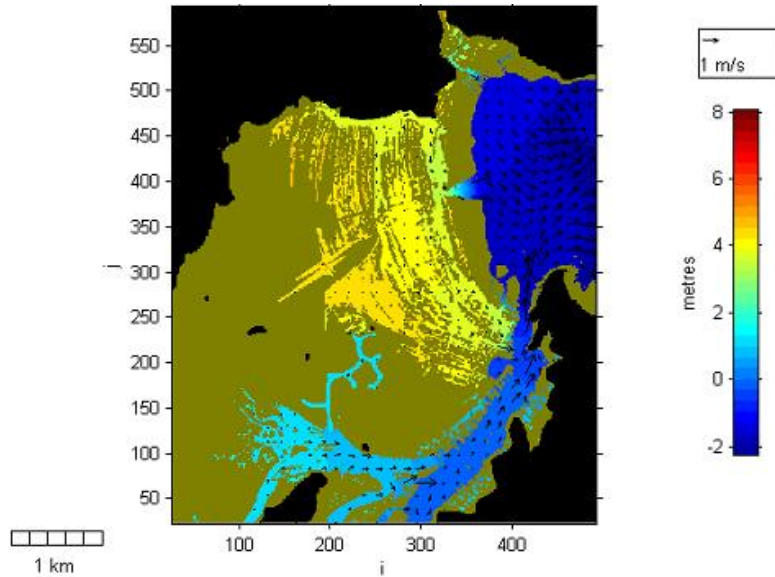


Figure 47. Local model, Kermadec Trench subduction normal fault event: maximum inundation for ground-striking LIDAR data. Inundation occurs up to 1.8 km inland, when five tsunami waves of considerable height inundate the town within six hours. The scale shows the tsunami elevation above mean sea level in metres.

When the waves first arrive at the foreshore¹², inundation of land begins at the Taputapuatea Stream entrance in the middle of Buffalo Beach, and at low-lying areas to the south that are close to the marina and Whitianga Harbour inlet. The coastal sand dunes located in between these areas apparently have sufficient height to prevent inundation from the first tsunami waves.

Despite their height, the coastal dune system was overtopped by the third and fourth waves, and blocked and diverted most of the current flows during the run-down process. The run-down currents mainly flow from the land back to the sea through the streams and low-lying coastal areas to the south.

It is important to understand the flow direction and processes during run-up and run-down, as this helps in formulating risk mitigation plans. The sequence of inundation and its extent can be seen in detail in Appendix 1.

¹² Applies to both Kermadec Trench Subduction and 1960 Chilean-type events.

Inundation model results for non-ground striking LIDAR data

The overall effects within Mercury Bay are the same as for the ground-striking LIDAR model (Figure 48). However, the increased flow resistance due to buildings and vegetation resulted in the following differences:

- The second wave does not reach as far up the Taputapuatea Stream as with the ground striking LIDAR data (1 km for non-ground striking versus 1.3 km for ground striking);

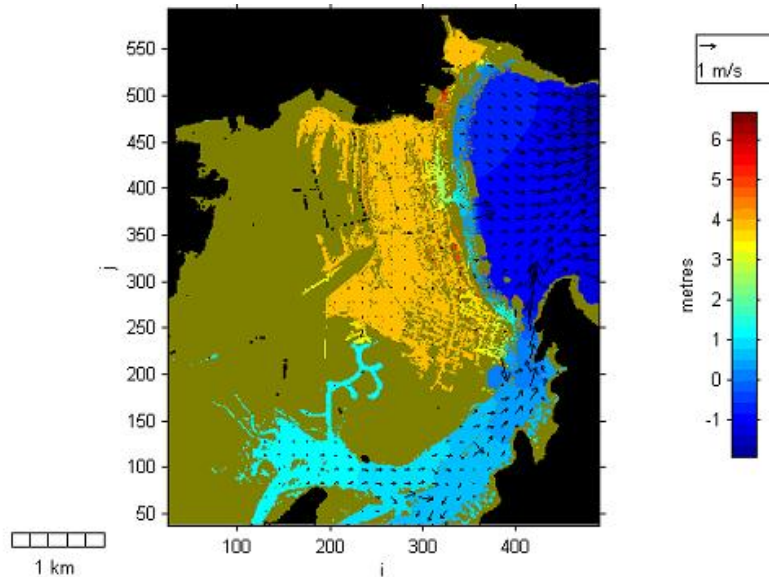


Figure 48. Local model, Kermadec Trench subduction normal fault event: maximum inundation for non-ground striking LIDAR data. Five waves inundate Whitianga within six hours of the first wave entering Mercury Bay. The flows are clearly seen passing through residential areas, and through roads and streams. Inundation also occurs on lowland areas parallel with the dune ridges and swales system further inland in farmland areas. The scale shows maximum tsunami elevation measured above mean sea level in metres.

- During run-up of the second wave, most of the northern residential areas become flooded from the Taputapuatea Stream, while to the south, inundation passes the residential areas 300 m inland via roads; and
- During the third and fourth waves, most of the residential land within 300m of the shoreline becomes completely inundated. Further inland to the north, the farm area floods through the Taputapuatea Stream and swales that parallel the dune system.

The Whitianga airfield was not affected by the tsunami, and is therefore a location place for an evacuation centre.

The sequence of inundation and the extent for this scenario can be seen in Appendix 1.

1960 Chilean Tsunami

Inundation model results for ground-striking LIDAR data

Simulation of the historic 1960 Chilean Tsunami allows some validation of the numerical models by comparing the simulations with eyewitness observations. After seven hours of simulation, eight waves of 3-7 m height penetrated Mercury Bay and Buffalo Bay, with three waves inundating Whitianga. The first inundation occurred 18 minutes after the first wave entered Mercury Bay, and inundated Whitianga up to 800 m inland. Sixty-two minutes after the first wave, the second inundation takes place, and floods a similar area with the same magnitude and extent.

The third and fourth waves do not inundate the town, while the fifth wave inundates Whitianga as far as 800m inland, and up to 1.3 km along the Taputapuatea Stream. The fifth wave is the biggest wave, and is the last to inundate the town. The sixth, seventh and eighth waves are too small to inundate the town, but still have a substantial height of ~2-3.5 m, with periods of 40-60 minutes. Due to resonance within Mercury Bay, the waves oscillate for some time even though the sea outside Mercury Bay is already back to normal levels.

The tsunami flows affected the Whitianga Harbour up to 6 km upstream. The model shows that the area up to 300m inland from the coastline was inundated by high-speed flows. The flow becomes slower as the inundation goes further inland, where the topography controls its' direction and speed. Strong currents of >5 m/s are generated during run-up and run-down on land, as well as within the harbour and inside Buffalo Bay. The negative leading waves cause strong currents to flow seaward from Buffalo Bay before the first waves arrived.

The maximum tsunami inundation for this model is shown in Figure 49, and the sequence of inundation and its' extent can be seen in Appendix 2.

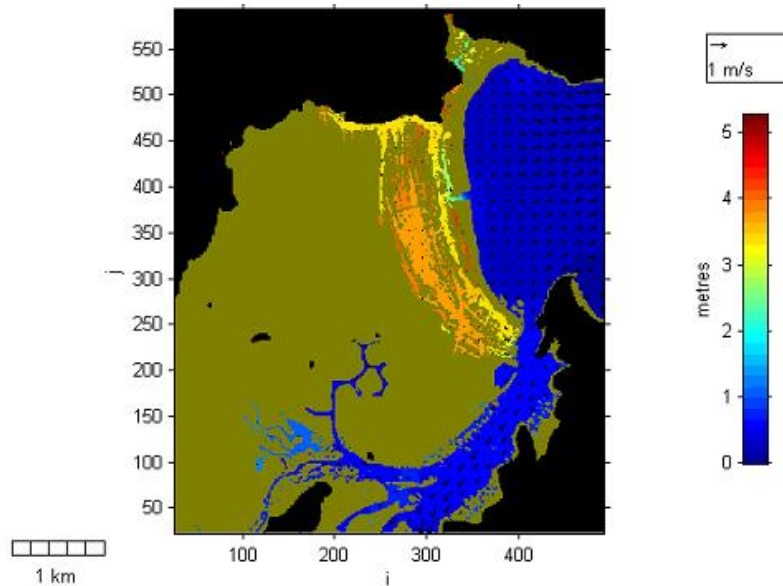


Figure 49. Local model, 1960 Chilean Tsunami: maximum inundation for ground-striking LIDAR. Three waves inundate Whitianga up to 800 m inland within 6 hours of the first wave entering Mercury Bay. The scale shows maximum tsunami elevation measured above mean sea level in metres.

Inundation model results for non-ground striking LIDAR data.

The overall effects within Mercury Bay are the same as for the ground striking LIDAR model (Figure 50), with the following differences:

- The first wave inundates Whitianga up to 1 km inland to the north, and up to 800 m inland in the south;
- Most of the overland flows pass through roads and between buildings¹³. During inundation from the second wave, flows continue to inundate the lowland areas through streams and major roads, such as Racecourse Road to the north, and Cook Drive to the south;
- Inundation is characterized by high-speed flows within 300m of the foreshore – particularly between buildings; and
- Strong currents of >6m/s are generated during run-up and run-down on land, as well as within Buffalo Bay.

The sequence of inundation and its' extent can be seen in Appendix 1.

¹³ It is assumed that buildings remain standing during inundation.

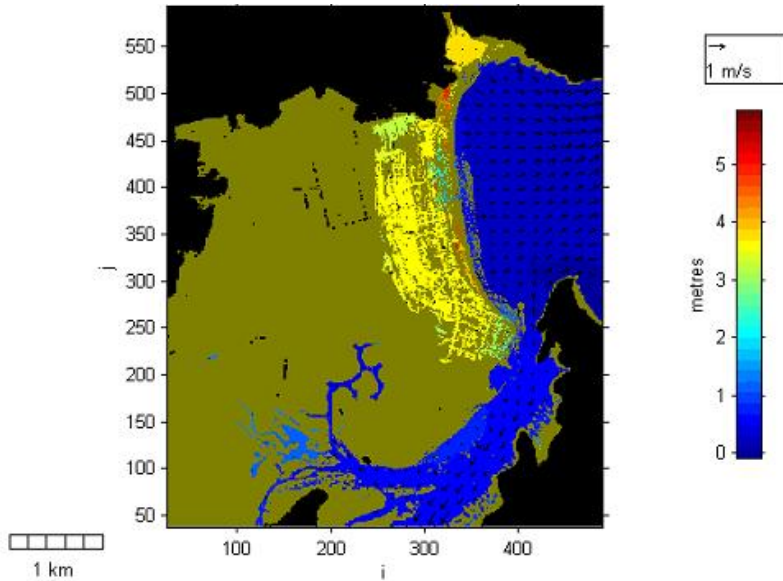


Figure 50. Local model, 1960 Chilean Tsunami: maximum inundation for non-ground striking LIDAR. Three waves inundate Whitianga up to 1 km inland within six hours of the first wave entering Mercury Bay. The inundation distance to the north is less than that using ground-striking LIDAR data. Inundation flows are seen passing residential areas, and along roads as inundation progresses inland. The scale shows maximum tsunami elevation measured above mean sea level in metres.

Tsunami hazards and risks – flow depths, flow speeds and hazard zones.

Tsunami hazard maps for Whitianga were developed using the model results, assuming that flow depths and flow speeds are the main contributors to hazard

Tsunami flow depths

The distribution of maximum inundation depths determined for the Kermadec normal faulting and 1960 Chilean Tsunami¹⁴ can be seen in Figures 51-54.

¹⁴ All scenarios being the Kermadec Trench and 1960 Chilean-type events, using both ground-striking and non-ground striking LIDAR data.

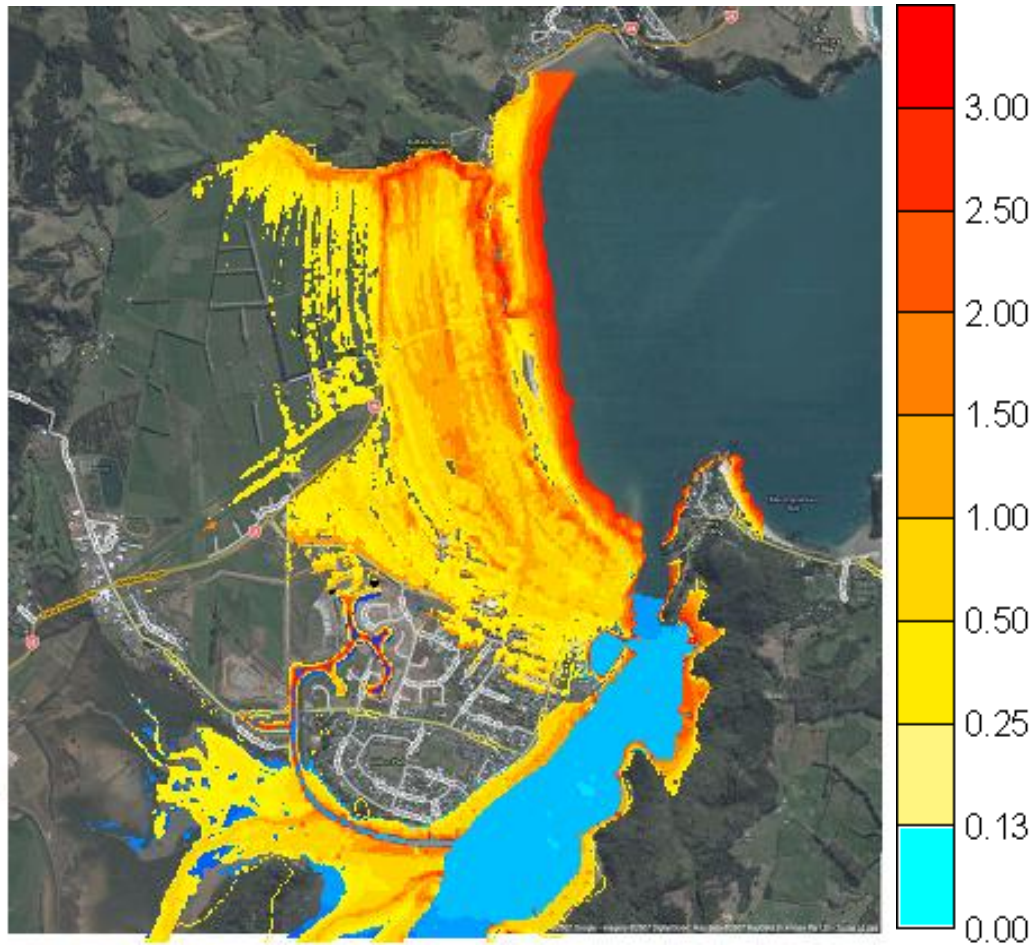


Figure 51. Kermadec Trench (Mw 9.0) tsunami inundation depth (in metres) for ground-striking LIDAR data. The diagram shows inundation levels above the ground within Whitianga, and levels above MHWS within Whitianga Harbour. Inundation is controlled only by topographic features (without buildings, roads and other infrastructure). The Taputapuatea Stream at the center of Buffalo Beach becomes dangerous during wave run-up and run-down due to strong currents and high flow depths, and floods most of the low-lying land to the north. The tsunami flow that enters the Whitianga Harbour does not inundate the town, but generates strong currents that affect the marina and nearby intertidal zone. The flow that overtops the sand dunes along the foreshore is lower, but passes over the dunes at a high speed - up to 8 m/s.

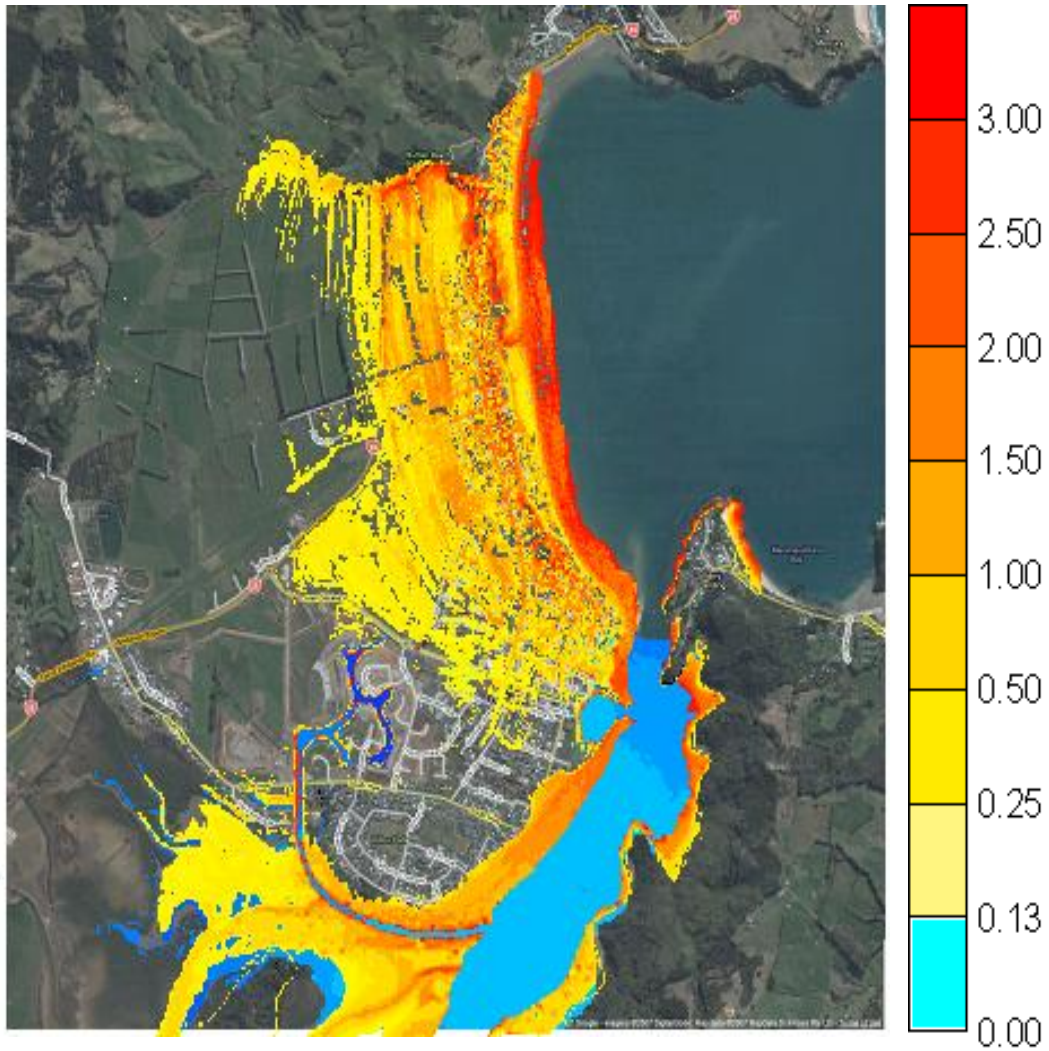


Figure 52. Kermadec Trench (Mw 9.0) tsunami inundation depth distribution (in metres) for the non-ground striking LIDAR data. This model shows impacts similar in nature to Figure 51; however in this case, the extent of inundation and flow depths are controlled by buildings, roads and other infrastructure.

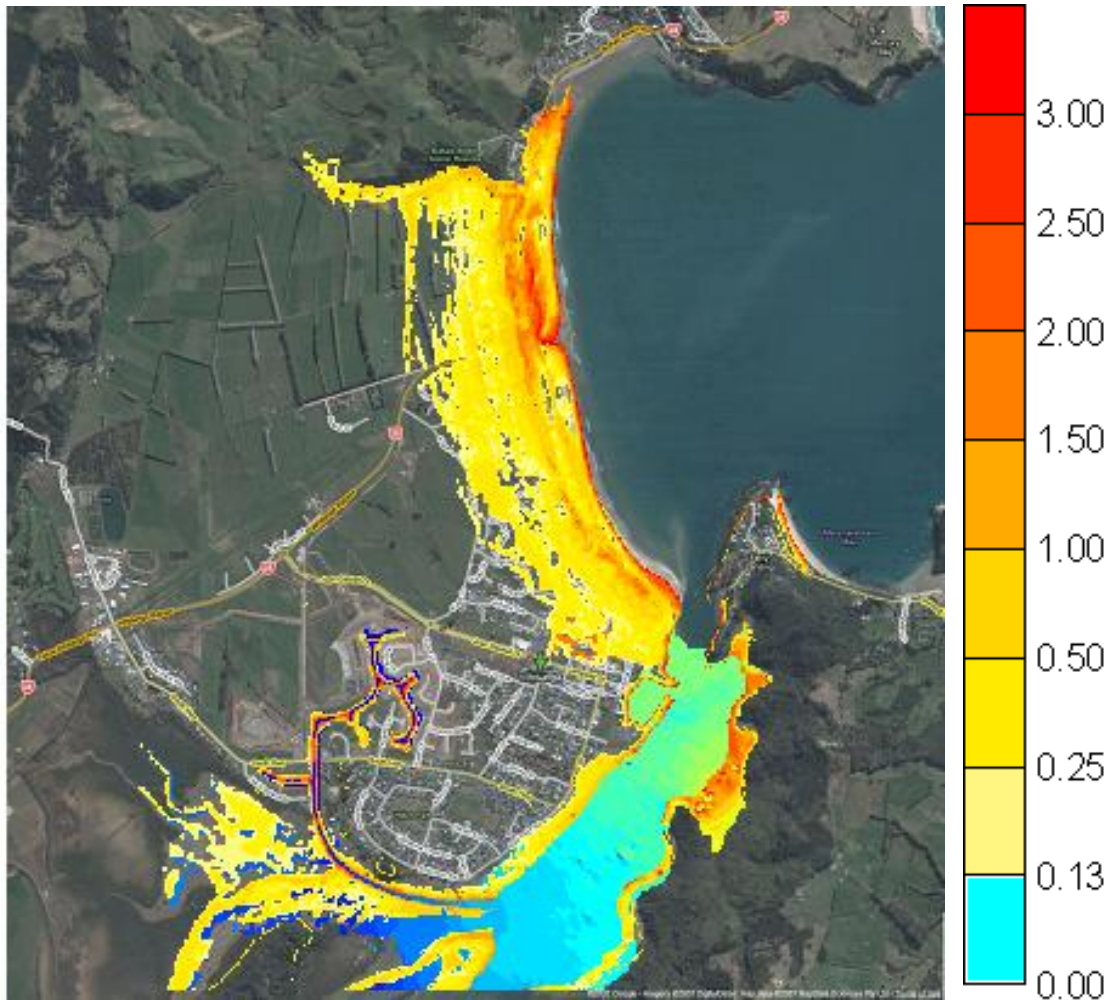


Figure 53. 1960 Chilean Tsunami inundation depth distribution (in metres) for ground-striking LIDAR data. Like the Kermadec Trench event, the diagram shows inundation levels above the ground within Whitianga, and levels above MHWs within Whitianga Harbour. Tsunami flows entering the harbour do not inundate the town, but create strong currents that affect the marina and the adjacent intertidal zone. The sand dunes at the Taputapuatea Stream entrance along Buffalo Beach have low flow depths, but experience strong currents of up to 8 m/s. The Taputapuatea Stream becomes dangerous during wave run-up and run-down, due to strong currents and high flow depths.

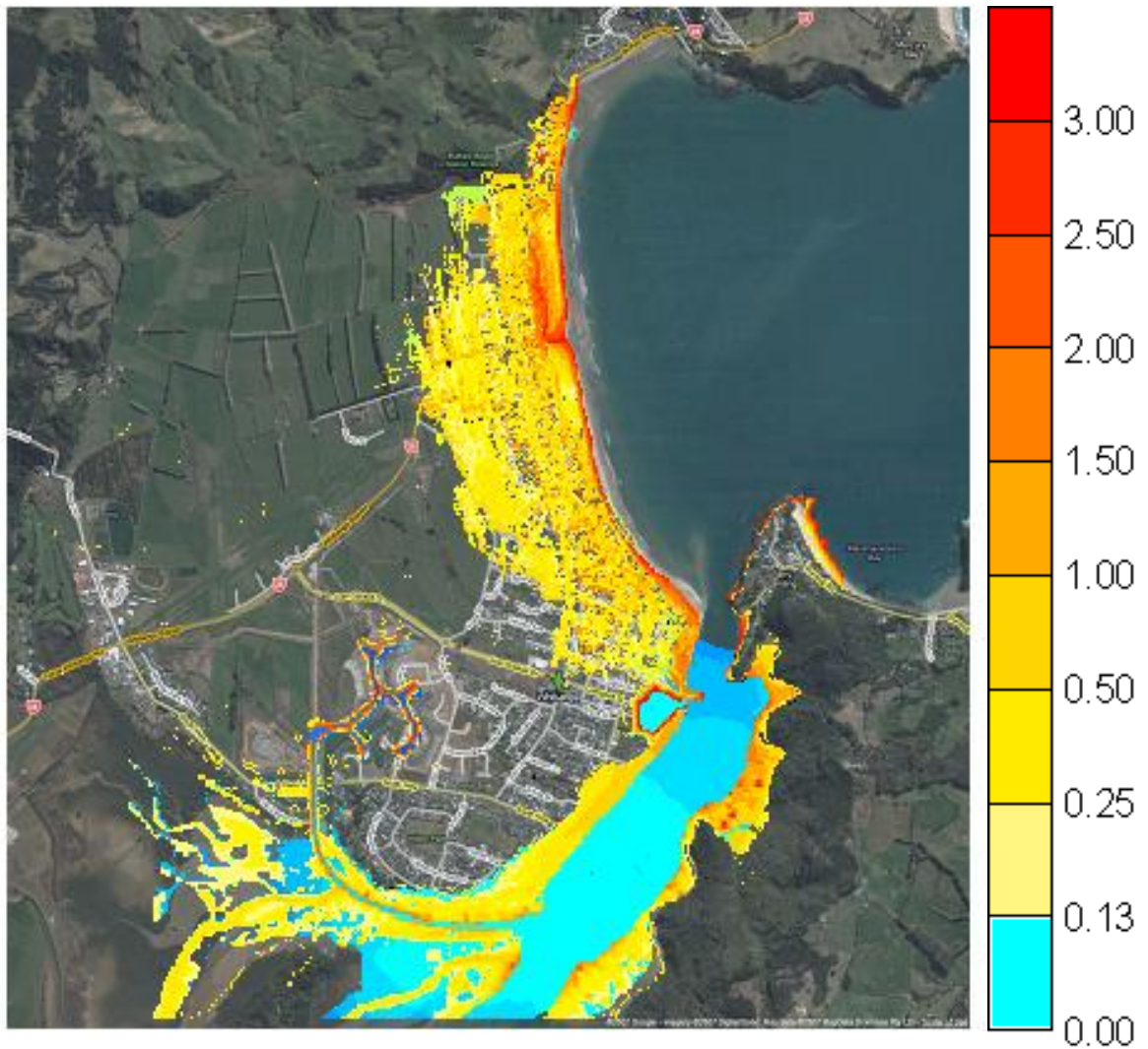


Figure 54. 1960 Chilean Tsunami inundation depth distribution (in metres) for non-ground striking LIDAR data. This model shows impacts similar in nature to Figure 53; however in this case, the extent of inundation and flow depths are controlled by buildings, roads and other infrastructure.

Tsunami flow speeds

The maximum overland flow velocities and maximum current speeds for offshore areas for all scenarios are summarised as Figures 55 and 56 respectively.

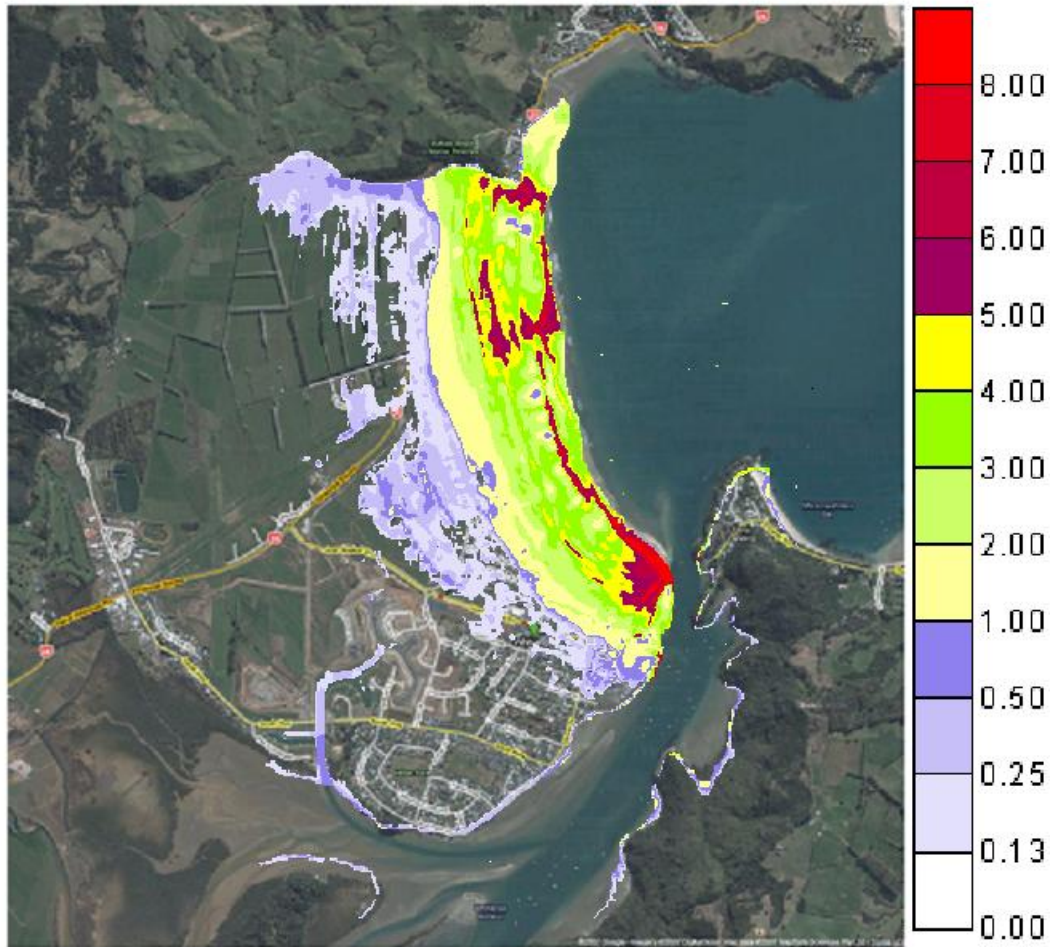


Figure 55. Maximum tsunami overland flow velocities (in metres/second) for Whitianga. This diagram shows that the highest flow velocities occur along the beach front, behind Taputapuatea Stream and in the area between Albert Street and Mill Streets near the Central Business District and wharf.

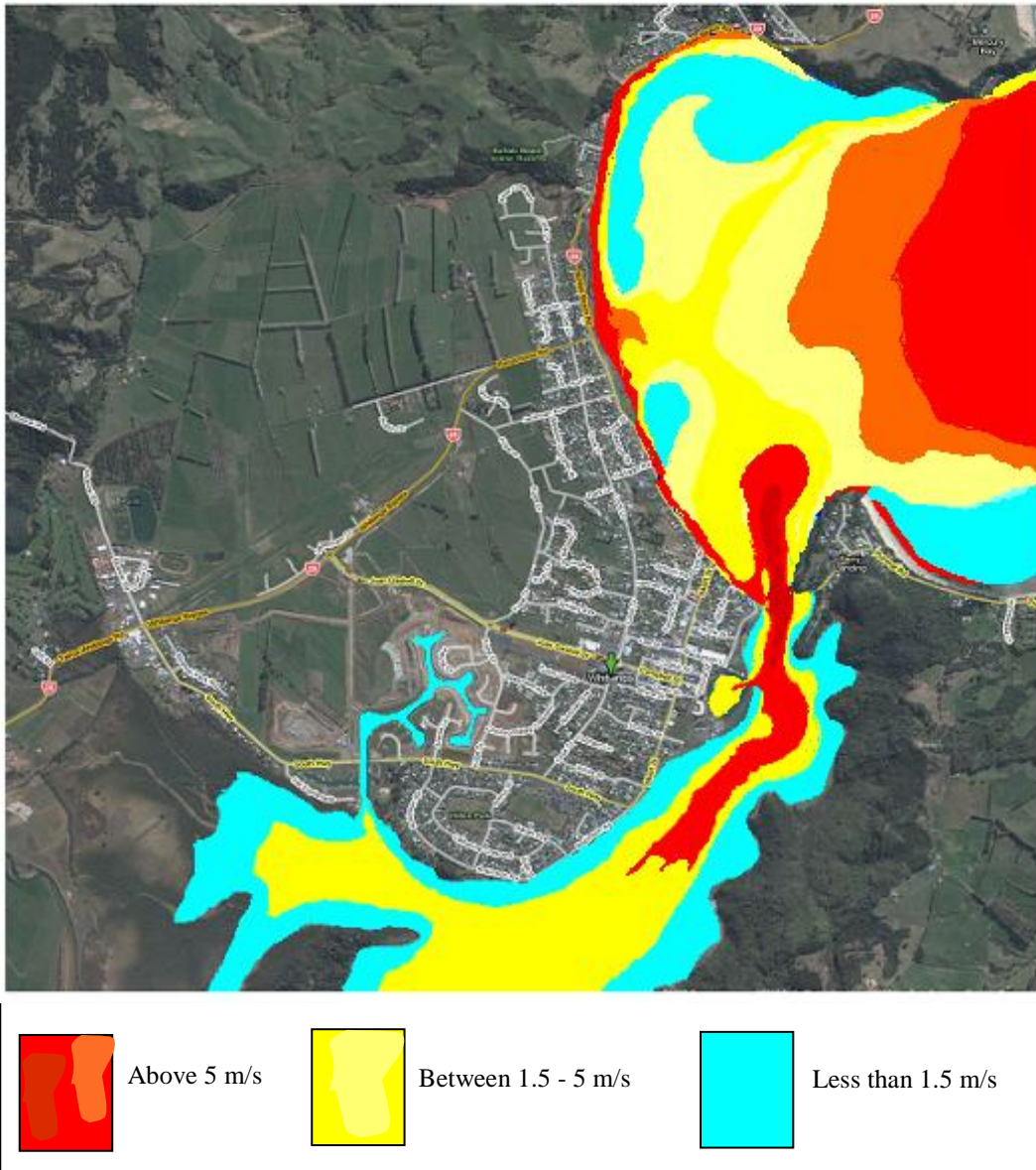


Figure 56. Maximum tsunami current speeds in Buffalo Bay and Whitianga Harbour (in metres/second). Current speeds are derived from modeling results based on both the Kermadec Trench and 1960 Chilean type scenarios.

Tsunami hazard zones

The hazard zones were defined by the combination of inundation depth and velocities (Figure 57) and are discussed below.

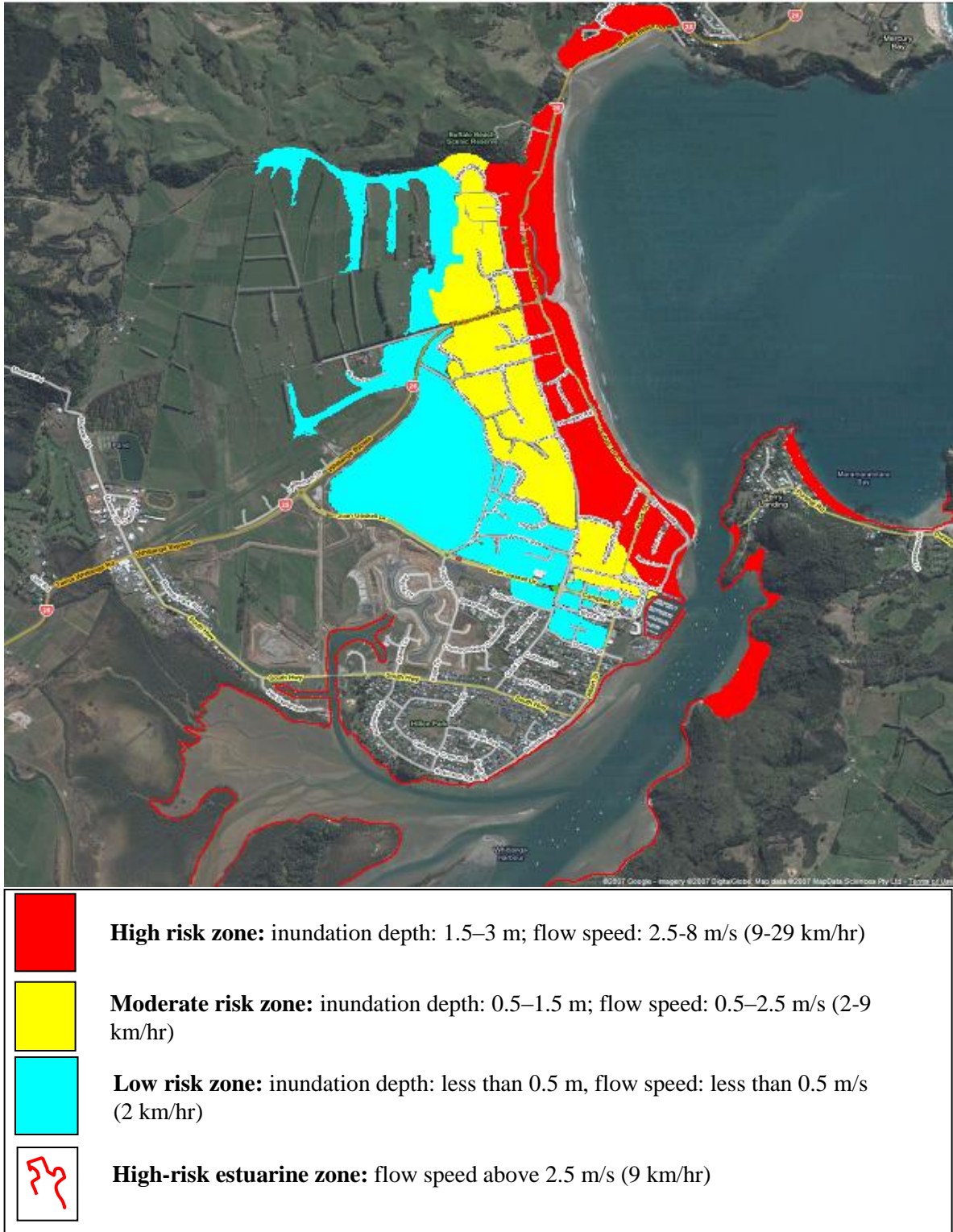


Figure 57. Whitianga tsunami hazard zones. The hazard zones are derived from modeling results based upon both the Kermadec Trench and 1960 Chilean type tsunami scenarios.

High risk zone

The high risk (red) is the zone where people and structures are most vulnerable to tsunami because:

- a. Flow depth is between 1.5 m and 3 m - the depth at which it is dangerous for humans; and
- b. Flow speed during inundation is between 2.5 m/s and 8 m/s - the current speed at which it is very difficult for people to stand and swim, and mainly beyond the limit for a building to resist heavy damage.

If the tsunami flow velocity is above 4 m/s, most wooden houses will suffer heavy damage, while buildings with a reinforced concrete structure will suffer if the flow speed exceeds 7 m/s (Shuto and Matsutomi, 1994).

Figure 57 indicates that most of the area from Cook Drive to the shoreline is assigned within this zone. An exception to the flow depth of 1.5m - 3m occurs within the sand dunes located on both sides of the Taputapuatea Stream along the shoreline - from Marlin St in the north to Halligan St in the south. The flow depth in this area is between 0.5 m and 1 m; however flow speeds are high - up to 8 m/s – so it is still considered high risk. The flow direction inland through the high risk zone remained in line with the direction of the incoming waves until the flow speed decreased to 2.5 m/s. At this stage, most of the flow follows the lower lying terrain, and is affected by land use features.

Moderate risk zone

The moderate risk zone was defined as areas where the flow depth is between 0.5 m and 2.5 m, and the flow speed is between 0.5m/s and 2.5m/s.

Both flow speeds and inundation depth decrease after the tsunami passes over Cook Drive, and hence inland from Cook Drive is assigned as moderate risk. Within this zone, the tsunami flow mainly follows the lower lying terrain, and is affected by land use features. This moderate risk zone extends from Cook Drive to Kupe Drive up to 550 m inland – as measured along Jackman Avenue. At the northern end, the extent of inundation from Cook Drive ranges from 200 m to 400 m inland, and in the south extends to Coghill Street near the marina.

Low risk zone

The low risk zone is defined as areas where the flow depth is less than 0.5 m, and the speed is less than 0.5 m/s. Within the low risk zone, tsunami flows are strongly controlled by topography and obstructions.

As tsunami inundation continues inland, the flows flood the low risk zone between Kupe Drive-Whitianga Bypass and Joan Gaskell Drive. To the north, flows inundate farm areas through the swales. In the south, flows continue up to Dundas Street. The area inland from the Whitianga Bypass, which is a continuation of the airfield, is not flooded, and would be ideal for a temporary evacuation site during a tsunami event.

High risk estuarine zone

The current speed distribution within the Whitianga Harbour and Buffalo Bay is shown in Figure 56. A strong current is generated at the harbour entrance and in the middle of Buffalo Bay, with velocities above 5 m/s. These velocities occur both during tsunami run-up and run-down due to the restricting geometry of the harbour entrance and Buffalo Bay. The current speed inside the harbour varies between 1.5 m/s and 5 m/s in the middle of the harbour, to less than 1.5 m/s along the edges. In the Whitianga Waterways canal system the current speed is between 1.5 m/s and 2.5 m/s. There is no inundation of Whitianga from the tsunami flow coming through the harbour. This is due to the size and geometry of the harbour, with a narrow entrance that restricts the flow, and large embayment upstream that disperses the tsunami.

Discussion

Summary of results

Modelling simulations show that Whitianga is vulnerable to tsunami from local and regional sources (Kermadec Trench), and from distant sources beyond the New Zealand continental shelf - such as South and North America. The Kermadec earthquake scenarios show that the initial tsunami wave penetrates Mercury Bay within 75-98 minutes after fault rupture. It takes a further 11-18 minutes for the first waves to arrive at the Whitianga foreshore.

Within a tsunami wave train, there are potentially 3-5 waves that will inundate the town. The inundating waves are typically later in the tsunami train as they are amplified by interactions with

reflections of earlier waves. The period between waves is 40–60 minutes. Therefore, there is enough time for residents to be evacuated to tsunami shelter sites.

Strong currents are generated within Buffalo Bay, Whitianga Harbour, and from overland flows. The flow speeds range from 1.5 m/s to 8 m/s for overland flows, and above 8 m/s within the entrance to Whitianga Harbour, and in the middle of Buffalo Bay.

In order to mitigate the risks from tsunami, in addition to the definition of hazard zones it is necessary to consider at least the following¹⁵:

- A tsunami warning system to indicate that people should be evacuated from high to low risk zones;
- A land-use management system for coastal areas that designates:
 - Usage restrictions;
 - Construction prohibitions;
 - Specific design criteria in tsunami-prone areas; and
 - Evacuation routes and shelter sites.
- A risk-based insurance system for coastal areas.

Evacuation routes and shelter sites

The primary and most effective strategy for saving lives immediately before tsunami waves arrive is the evacuation of people from the hazard zones, either through:

- a) Horizontal evacuation: moving people out of the hazard zones to areas of higher ground, or
- b) Vertical evacuation: moving people within hazard zones to higher elevations that are not subject to inundation, within or upon structures - such as upper floors in specific buildings (NTHMP 2001).

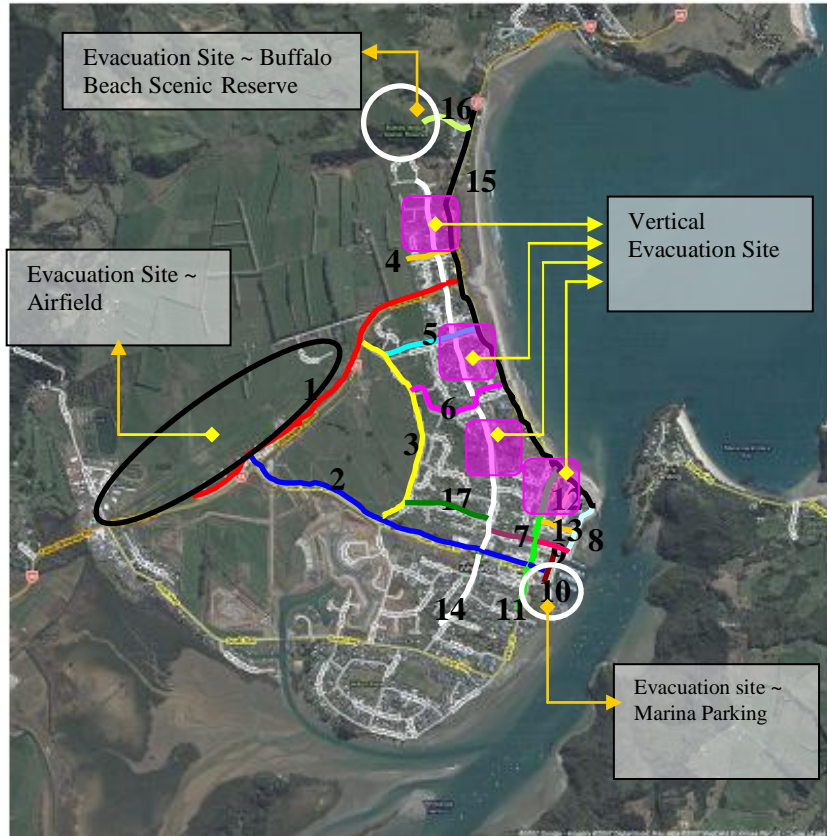
Based on the identified tsunami hazard zones and tsunami depths and flow velocities, possible evacuation routes and shelter sites for the high-risk zone, and vertical evacuation within the high-moderate risk zone are identified. Roads that run perpendicular to the coast can serve as important evacuation routes, since most of the topography inland is relatively high compared to the areas that are close to the shore. However, during an emergency situation, evacuation routes will not always be through normal roads, and any access route to an evacuation site will be beneficial.

¹⁵ Cox, 1979, NTHMP 2001

Most of the roads within the high risk zone that run perpendicular to the coast are connected to Cook Drive - the boundary of the high and moderate risk zones. The exceptions to this are Racecourse Road and Jackman Avenue, which extend further into the low risk zone.

Potential evacuation routes and sites can be seen in Figure 58, and Figure 59 shows these in relationship to the hazard zones.

Identifying suitable evacuation shelter sites, and how to access them is crucial in order to minimize the risks to life. As outlined above, there is likely to be enough time to evacuate most Whitianga residents, due to the lag time between a Kermadec Trench event and the first wave arrival at Whitianga.



No	Routes	Remarks
1	Racecourse Road – Whitianga Bypass	Airfield (Evacuation Site)
2	Campbell St – Joan Gaskell Dr	Airfield (Evacuation Site)
3	Kupe Dr	Airfield (Evacuation Site)
4	Marlin St	Airfield (Evacuation Site)
5	Jackman Ave	Airfield (Evacuation Site)
6	Halligan Rd – Park Ln – Meadow Dr	Airfield (Evacuation Site)
7	Lee St	Airfield – Marina (Evacuation Site)
8	Esplanades	Marina (Evacuation Site)
9	Blacksmith Ln	Marina (Evacuation Site)
10	Victoria St	Marina (Evacuation Site)
11	Albert St	Marina (Evacuation Site)
12	Mill Rd	Marina (Evacuation Site)
13	Monk St	Marina (Evacuation Site)
14	Cook Dr	Boundary - Connection
15	Buffalo Beach Rd	Boundary - Shore
16	Kawakawa Rd	Buffalo Beach Scenic Reserve

Figure 58. Potential tsunami evacuation routes and shelter sites

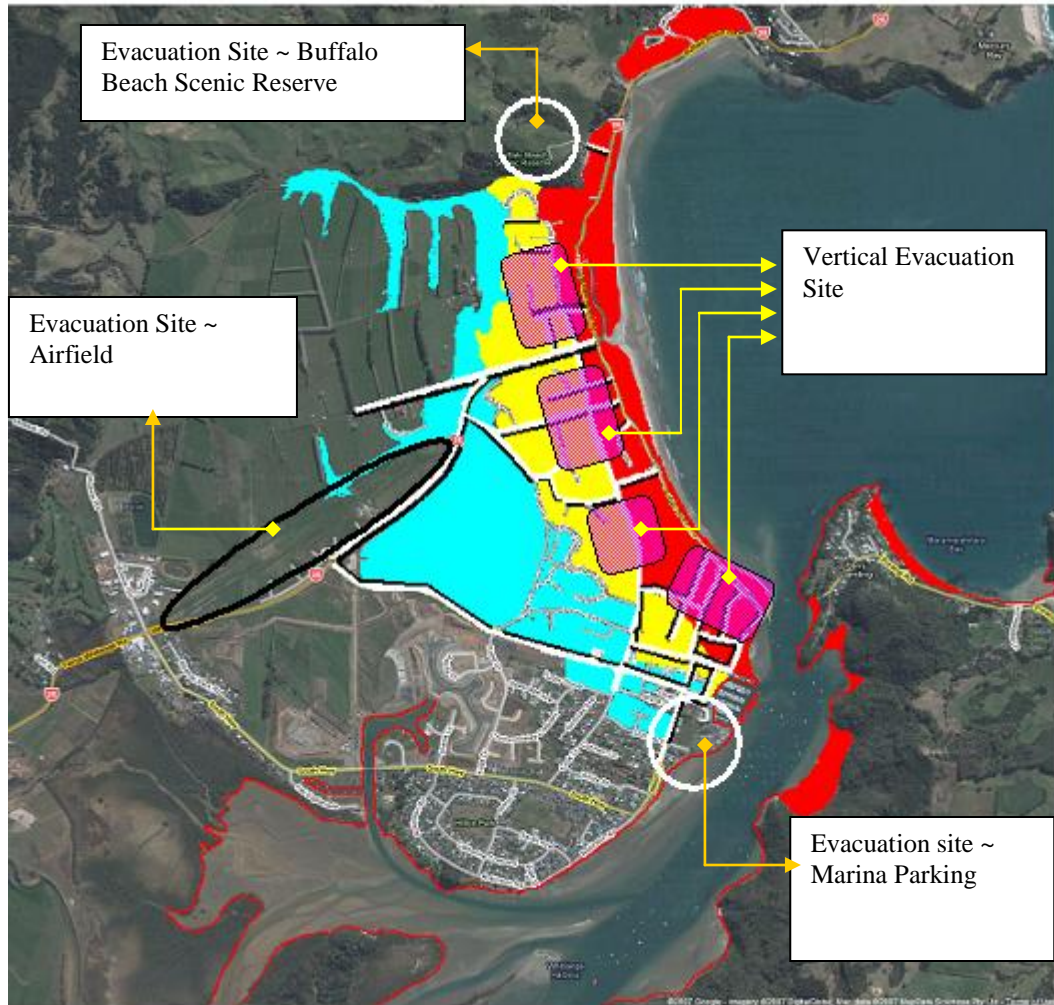


Figure 59. Potential evacuation routes and sites within Whitianga Township in relation to the tsunami hazard zones. Red is for high-risk, yellow for moderate risk, and cyan for low-risk zone.

The proposed evacuation routes and shelter sites identified that are safe in the various scenarios are as follows:

Buffalo Beach Scenic Reserve

At the north end of Buffalo Beach, the scenic reserve (white circle on Figures 58 and 59) becomes an ideal site for an evacuation site for people in this vicinity - within a perimeter of up to 1 km. This site is a hill about 56m above mean sea level, and can be reached within 10-20 minutes by foot through Kawakawa Road. An alternative pedestrian shortcut access could be designed to minimize the possibility of traffic jams during an emergency situation.

Airfield area (corner of Racecourse Road and Whitianga Bypass)

This site can be accessed directly from Racecourse Road (refer to the black ellipse region on Figures 58 and 59). This road is a vital evacuation route for the most vulnerable zones located around the Taputapuatea Stream mouth. It is important to have evacuation roads that give direct access to higher ground inland. Another road that has direct access to this site is Jackman Avenue - around 300 m south of Racecourse Road. Jackman Avenue is an important road that gives access from the shore to Kupe Road (the end of moderate risk zone), and to the potential evacuation site at the airfield.

Other roads that run perpendicular to the shore within this zone are Marlin Street, Surf Street and Halligan Road. These also allow further access inland, however, these roads end at the moderate risk zone. In the south, Joan Gaskell Drive and Campbell Street are also important for evacuation purposes to reach this site.

Marina parking area

This site is located at the edge of the marina (white circle on Figures 58 and 59) between Dundas Street and Bryce Street, and is a potential evacuation site for the marina area. Even though it is located near the Whitianga Harbour, the models show it does not become inundated for either of the scenarios. Access from Buffalo Beach is through Albert Street and Victoria Street.

Vertical evacuation

Vertical evacuation should be considered within the high and moderate risk zones, where the population is high. Potential vertical evacuation sites are marked on Figures 58 and 59 - indicated by the purple coloured blocks. Within these areas, vertical evacuation sites should be located within 15 minutes walking distance or 200 m of all residential structures to allow for children, elderly people or people carrying children to reach the sites. A combination of scientific input on inundation behaviour and local resident participation are important when deciding where the most suitable locations should be.

An inventory of existing buildings within the high-risk zone that can be used as vertical evacuation is important. However, if there are no suitable buildings that can be used, new buildings need to be designed to function as vertical evacuation sites, and have sufficient structural integrity to resist expected tsunami and earthquake forces. Such buildings should go

beyond the minimum life safety requirement of most standard building codes (NTHMP 2001). Vertical evacuation is particularly important for high population density areas with limited access to horizontal evacuation routes, and also where warning times may be insufficient.

Examples of vertical evacuation buildings within high population areas, and purpose-built vertical evacuation sites where there are no buildings that can be used for vertical evacuation, are illustrated in Figures 60 and 61.



Figure 60. Vertical evacuation sites using existing buildings. Buildings are located in the high-risk zone with a high population density, and have signage placed on the outside of the building (Source: Shuto, N., 2007).

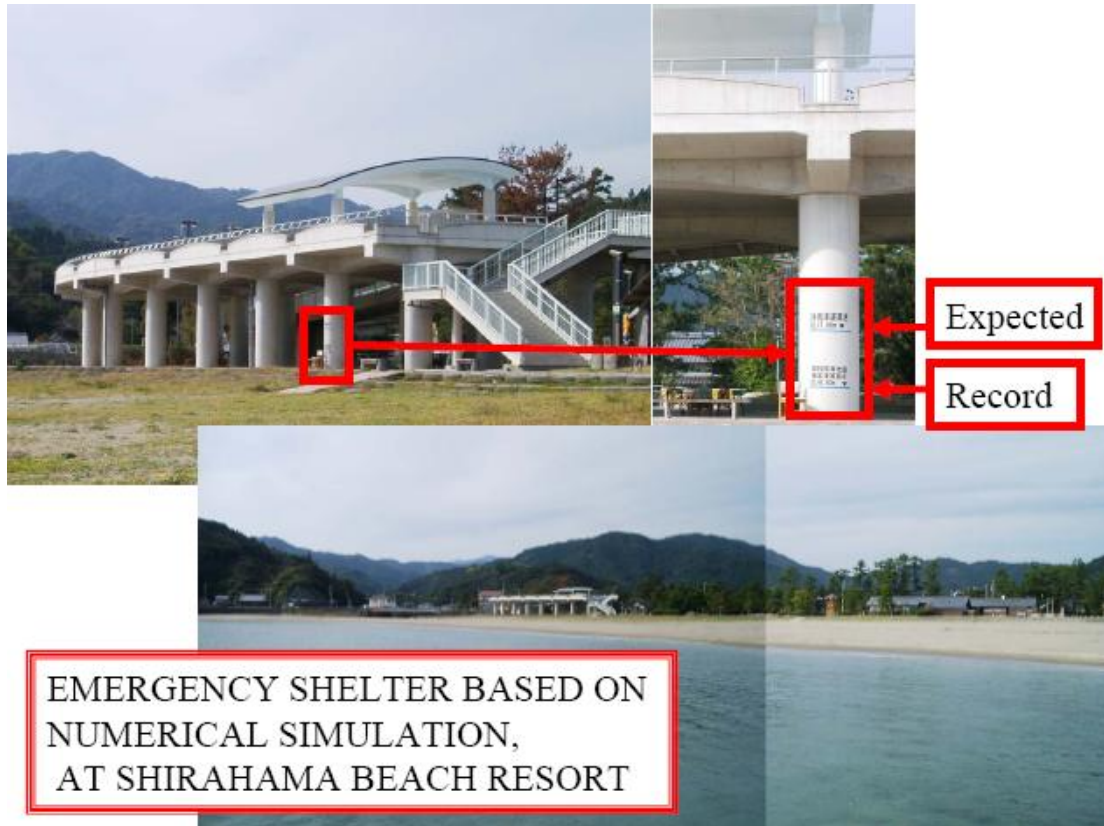


Figure 61. Purpose built vertical evacuation structure at Shirahama Beach resort, Japan. Anticipated tsunami inundation heights based on modeling and historical records are identified on the structure (Source: Shuto, N., 2007)

Overland flow velocities and the Building Code

Overland flow information derived from modelling with the ground-striking LIDAR data set provides useful information regarding configuration of new development that occurs in tsunami inundation areas. In addition, overland flow information helps to guide policies aimed at protecting existing development from future tsunami losses, through redevelopment, retrofit, and land reuse plans and projects. The overland velocity distribution information in Figure 56 can be used for this purpose.

Construction of buildings in areas with flow velocities above 2.5 m/s requires specific design criteria. According to Matsutomi and Shuto (1995), a wooden house will suffer heavy damage if flow speeds are above 4 m/s, while reinforced concrete buildings and/or concrete block buildings will suffer heavy damage in flows exceeding 7 m/s.

Evaluation of existing building within the high-risk zone to mitigate future human and economic losses, and application of a tsunami building code for new development areas within the high and moderate risk zones should be considered. The overland velocity distribution information in Figure 56 can also be used for this purpose.

Tsunami-resistant retrofits of existing buildings within the high risk zone along the waterfront would not only minimize structural losses, but also minimise the creation of floating debris that can damage nearby buildings. Most building codes primarily address new construction, and do not comprehensively address tsunami renovations and retrofitting (NTHMP 2001). Therefore, for any new developments within tsunami prone areas, building codes should include the tsunami hazard/risk context of building renovations, and apply tsunami policies to existing buildings.

Building designs to mitigate against tsunami waves must adequately consider the following issues (Hwang et al., 2005):

- **Duration of impact:** the impact either from waves, overland flows or debris on both ground-supported and elevated structures;
- **Localized scour:** scour that occurs around building foundations is a critical consideration due to the fact that most buildings collapse because of loss of either load bearing capacity or anchoring resistance around posts, piles, piers, columns, footings or walls; and
- **Tsunami loads:** if the tsunami acts as a rapidly rising tide, most damage is due to buoyant and hydrostatic forces. A bore-like wave will create a strong current, making its effect more damaging.

Some structural components such as grade beams and diagonal braces can be used to enhance the performance of piers and columns, in order to prevent the collapse of structures. Grade beams can be either wooden or concrete, and provide support in the horizontal plane parallel to the floors, to help keep structures from collapsing. Diagonal braces can add considerable support to piers and columns, are normally attached to the pile near the top, and are secured to the adjacent pile either near or on the ground surface.

Coastal defence structures

In reducing economic impacts, the usual response is to opt for structural mitigation measures, such as building seawalls or breakwaters, as illustrated in Figure 62. However, Horikawa and Shuto (1983) state that based on past experiences in Japan, it is dangerous to believe that the impacts of tsunami can be completely prevented by man-made structures, and it is incorrect to depend too much on the functioning of coastal defence structures, and this was clearly demonstrated during the 2011 Tohoku Tsunami. However, coastal defence structures can minimise possible impacts when they are properly designed, and involve a combination of “soft” (non-structural) and “hard” (engineering or structural) measures.

A combination of coastal sand dunes and forest is an option to protect the Whitianga waterfront. This can be done along the coast on both sides of the Taputapuatea Stream mouth. However, in order to prevent major impacts through the Taputapuatea Stream, a stop gate could be an option, as illustrated in Figure 63. In Japan, many coastal rivers have stop gate structures in place. A stop gate system could also be used to prevent strong currents entering the marina and the Whitianga Waterways. However, the gates are only effective if the barrier is higher than the tsunami.

After the 2004 South-east Asian tsunami, the effectiveness of coastal forest in reducing tsunami energy and impacts along parts of the Indonesian shoreline was recognized. The effectiveness of such coastal vegetation had been previously recognized by Shuto (1993), who noted the following positive aspects – vegetation can:

- Stop floating debris;
- Reduce water flow velocity and inundation height;
- Provide a life-saving function by catching people carried off by tsunami, and
- Collect wind-blown sands and raise dunes that act as a natural barrier against tsunami.



Figure 62. Tsunami coastal structure, Taro, Japan. Taro town in Japan has experienced several tsunami in the past that have devastated the town, and caused many deaths. The town is now growing fast, and to prevent damage from future tsunami hazards, coastal defense structures were built – including the 10m high tsunami wall constructed along the coast, and a dike along the river (Source: Shuto, N., 2007). These defenses failed during the 2011 Tohoku Tsunami resulting in the loss of most of the town.

However, Shuto (1993) also noted that some trees could be up-rooted by tsunami, and become destructive floating debris. Further research should be done on this matter, and careful design should be considered before implementing coastal forest as a mitigation measure.



Figure 63. Tsunami stop gate, Japan. The gate is constructed at a harbour entrance. The gate height is nearly 10m, the width is 40m, and the gate weighs over 400 tonnes. The gate will automatically close within 5 minutes when triggered by a seismograph signal (Source: Shuto, N., 2007).

Safety planning for ships and boats

Strong currents are generated inside and outside Whitianga Harbour by both scenarios - as seen in Figure 57. Strong currents are dangerous for ships and boats within Buffalo Bay as well as inside the harbour. Safety objectives for ships and boats are protection of the boat itself, and prevention of secondary damage caused by drifting vessels.

The amount of time required to evacuate ships and boats will depend on the tsunami source. For the 1960 Chilean-type event, this will be greater than 10 hours, while for the Kermadec Trench event, it is likely to be about 1 hour and 20 minutes from the event. Further work is needed on confirming evacuation guidelines for ships and boats within Buffalo Bay and Whitianga Harbour.

If the warning for arrival time is too short, it is dangerous to evacuate ships or boats to offshore waters. A combination of loose moorings and anchorages can reduce the risk of vessels drifting onto land. In addition, keeping the mooring and anchor cables loose can prevent boats from being damaged by the collision of the first wave, or strain from buoyancy, but this becomes difficult when currents become too strong. Constructing a stop gate at the mouth of the marina (Figure 63), or breakwater with a layout that alleviates strong currents may protect boats inside the marina.

Location of critical facilities

Some critical facilities in Whitianga, such as a rest home, are located within the high-risk tsunami zone. Therefore, their vulnerability during a tsunami is a community-wide concern that needs to be considered as part of tsunami risk management. Other critical facilities such as roads, fire station, and telecommunications, natural gas, water supply and electricity transmission facilities should be located outside the tsunami hazards zones.

If critical facilities are already within the high-risk zone, and they are impossible to relocate, renovation and/or retrofitting based on tsunami design criteria should be implemented, so that the facility will either be able to continue operation or be easily and rapidly repairable immediately after the event.

In the case of waterfront-dependent infrastructure, and where critical facilities cannot be newly designed or retrofitted to withstand tsunami forces, they should be considered expendable, and planning should be undertaken for evacuation, emergency response, recovery, and replacement facilities. It is important to remember that during a tsunami, an expendable building may turn into dangerous debris that can batter people and other infrastructure (NTHMP 2001).

Information and education programmes

Community preparedness is essential for preventing loss of life - as is an early warning system. There is a need for integration of life-long efforts to educate local communities about tsunami hazards and risks, and preparedness for tsunami events. Principle 7, and strategies 4 and 5 of the United States National Tsunami Hazards Mitigation Program (2001, p. 50) support this approach as follows:

Principle 7, Strategy 4: Implement Effective Information and Education Programs -

Communities can use brochures, single-page instructions, periodic warning system tests, electronic and print media information, signs, and emergency response exercises to maintain awareness and instill effective response behaviour. Some of this information will be directed towards specialized institutions, such as schools, hospitals, and convalescent-care facilities, and non-English speaking community members. Because of seasonal tourism in many coastal communities, some information is designed especially for tourists. Depending on the community's

needs, it is important that information and education efforts be routine, comprehensive, and tailored for special facilities and populations.

Principle 7, Strategy 5: Maintain the Program Over the Long Term

Tsunami are rare events, but their impacts on coastal communities can be devastating. It is a challenge to maintain emergency preparedness programs and procedures when the threat is perceived as remote. It is, therefore, important that vertical evacuation measures be integrated into community response plans and that they be reviewed and revised regularly. Since cooperation is essential, these reviews should include building owners and others involved in the program. Periodic simulations are a valuable learning exercise, and regular informational and instructional materials should be provided to those occupying potential tsunami damage areas.

As stated above, and from lessons learned from the 2004 Sumatra Tsunami, the biggest challenge for communities is to maintain an emergency preparedness programme that can be sustained from generation to generation. The return period for a major tsunami may be decades long, and in New Zealand, data on historical tsunami events is not long enough to predict large event return periods with any great degree of accuracy.

The ‘oral history’ that saved thousands of lives in remote Sumatran offshore islands in the Indian Ocean during the 2004 South-east Asian tsunami, and the recent (2007) event in the Solomon Islands shows the effectiveness of informal education material. In these cases, signs of an imminent tsunami are passed down from generation-to-generation as a part of their tradition. Unfortunately, this oral history tradition no longer exists in the cities, and this was demonstrated during the 2004 Sumatra Tsunami, where most of the casualties were in coastal cities. For urban communities, educational material should be in a form that fits in with their tradition or lifestyle, in order to be effective in building resilient coastal communities.

A series of video animations on various tsunami scenarios have been developed as education material in Japan and Hawaii. The educational material covers tsunami wave behaviour during generation, propagation and run up at regional, intermediate and local scales. In addition, tsunami hazards zones are well signposted, as illustrated in Figures 64 to 67. Similar signage could be considered for Whitianga.



Figure. 64. Examples of tsunami signage in the USA (NTHMP 2001).



Figure. 65. Tsunami signage within an identified hazard zone in Oregon, USA (source: Darienzo, 2003).



Figure. 66. Tsunami signage in Oregon, USA indicating the direction to the evacuation route (source: Darienzo, 2003).

Bibliography

- Atwater, B. F., Musumi-Rokkaku, S., Satake, K., Tsuji, Y., Ueda, K., and David, K.Y.(2005), The orphan tsunami of 1700, Japanese clues to a parent earthquake in North America, University of Washington Press. 133 p.
- Bell, R.G., Goff, J., Downes, G., Berryman, K., Walters, R.A., Chague-Goff, C., Barnes, P., Wright, I. (2004).Tsunami Hazard for the Bay of Plenty and Eastern Coromandel Peninsula: Stage 2. Environment Waikato Technical Report 2004/32. 70 p.
- Berryman, K.(compiler) (2005), Review of tsunami hazard and risk in New Zealand, Institute of Geological and Nuclear Sciences client report 2005/104. 140 p.
- Black , K.P. (2001), The 3DD Suite of Numerical Process Models, ASR Ltd., PO Box 67, Raglan, New Zealand. 90 p.
- Black , K.P. and Vincent, C.E.(2001), High-resolution field measurements and numerical modelling of intra-wave sediment suspension on plane beds under shoaling waves, Coastal Engineering, 42, p 173-197.
- Borrero, J.C., Bosserelle, C., Prasetya, G., and Black, K.P. (2007), Using 3DD to model tsunami inundation, Proceedings of the Australasian Coast and Port Conference. July 2007, Melbourne Australia
- Cox, D.K (1979), Local tsunamis in Hawaii- implications for hazard zoning. Hawaii Institute of Geophysics. University of Hawaii. 46 p.
- Goff, J., Walters, R., and Callaghan. (2006), Tsunami source study. Environment Waikato Technical Report 2006/49. 54 p.
- Horikawa, K and Shuto, N.(1983), Tsunami disaster and protection in Japan, in K.Iida and T.Iwasaki (eds). Tsunamis - Their Science and Engineering. Terra Scientific Publisher Co., Tokyo., p. 9 -22.
- Hwang, D., Francis, M., Choi, B.H., Singh, J.P., Stein, S., Borrero, J., Thio, H.K., Ratti, C., Bergado, D. (2005), Mitigating the risk from coastal hazards: strategies & concepts for recovery from the December 26, 2004 tsunami. Reinwald O'Connor & Playdon. 68p.
- Dariento, M. (2003), Tsunami sign placement guidelines, Oregon Emergency Management. 8 p.
- De Lange, W.P., and Moon, V.G. (2007), Tsunami washover deposits, Tawharanui, New Zealand, Sedimentary Geology, 16 p.
- De Lange, W.P, and Prasetya, G., Healy , T. (2001), Modelling of tsunamis generated by pyroclastic flows (ignimbrites), Natural Hazards, 24, p 251-266.
- De Lange, W.P., and Fraser, R.(1999), Overview of tsunami hazard in New Zealand, Tephra 17:3-9. Published annually by the Ministry for Civil Defence and Emergency Management.

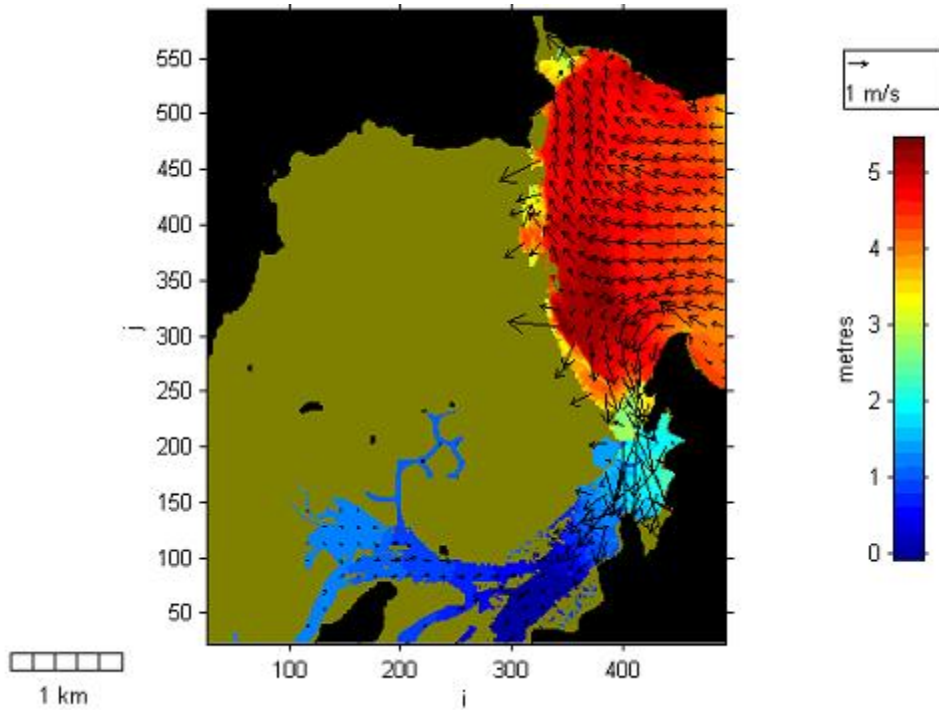
-
- ITDB/PAC (2004), Integrated Tsunami Database for the Pacific, Version 5.1 of June 2004. CD-ROM, Tsunami Laboratory, ICDMMG SD RAS, Novosibirsk, Russia.
- National Tsunami Hazard Mitigation Program (2001), Designing for tsunamis, Seven principles for planning and designing for tsunami hazards. NOAA, USGS, FEMA, Alaska, California, Hawaii, Oregon, and Washington. 60 p.
- Matsutomi, H., and Shuto, N.(1995), Tsunami inundation depth, current velocity and degree of damage to houses, in Smith, C.E., Bea, R.G., and Uwabe, T (comp). International Workshop on Wind and Earthquake Engineering for Offshore and Coastal Facilities: Proceedings, University of California, Berkeley, CA, January. 17-19, 1995, p 195-199.
- Manshina, L., and Smylie, E.(1971), The displacement fields of inclined faults, Bulletin of the Seismological Society of America, 61, p 1433-1440.
- Middleton, J.F., and Black,K.P.(1994), The low frequency circulation in and around Bass Strait: a numerical study, Continental. Shelf Research. 14, p. 1495–1521
- Okada, Y.(1985), Surface deformation due to shear and tensile faults in a half-space, Bulletin of the Seismological Society of America, 75, p 1135-1154.
- Okal, E., Borrero, J., Synolakis, C. (2006). Evaluation of Tsunami Risk from regional earthquake at Pisco, Peru. Bulletin of the Seismological Society of America. Vol.96. No.5. p. 1634-1648.
- Power, W., Downes, G., and Stirling, M. (2007), Estimation of tsunami hazard in New Zealand due to South American earthquakes, Pure and Applied Geophysics 164, p 547-564.
- Shuto, N.(1991), Numerical simulation of tsunamis – Its present and near future, Natural Hazard, 4, p 171-191.
- Shuto, N. (1993), Tsunami intensity and disaster, in S.Tinti (ed). Tsunami in the world, Advances in Natural and Technological Hazards Research, Kluwer Academic Publishers, Dordrecht, p 197 – 216.
- Shuto, N. (2007), Present practise of tsunami warning system and hazards mitigation programs in Japan. Proceeding of South China Sea Tsunami Workshop, December 5-7, 2007, Taiwan . 65 p.
- Synolakis, C.E., and Bernard, E. (2006). Tsunami science before and beyond Boxing Day 2004, Philosophical Transaction of The Royal Society A, Vol.364. No.1845. p.2231-2265.
- Walters, R.A., Goff, J., and Wang, K. (2006b). Tsunamigenic Sources in The Bay of Plenty, New Zealand. Science of Tsunami Hazards. Vol.24. No.5. Pages 339 -357.
- Wiegel., R.L. (2006), Letter to Prof. Harry Yeh, The National Science Foundation Tsunami Workshop 26-28 December 2006. Hilo. Hawaii. (pers.comm).

Zachariasen, J., Sieh, K., Taylor, F.W., Edwards, R.L., Hantoro, W.S. (1999), Submergence and uplift associated with the giant 1833 Sumatran subduction earthquake: Evidence from coral microatolls. *Journal of Geophysical Research* . Vol.104. p: 895-919.

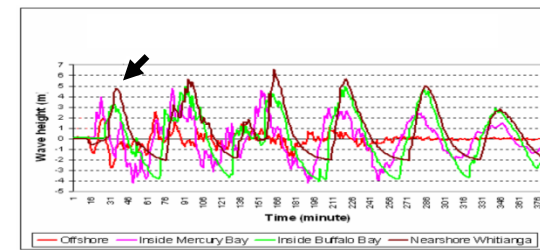
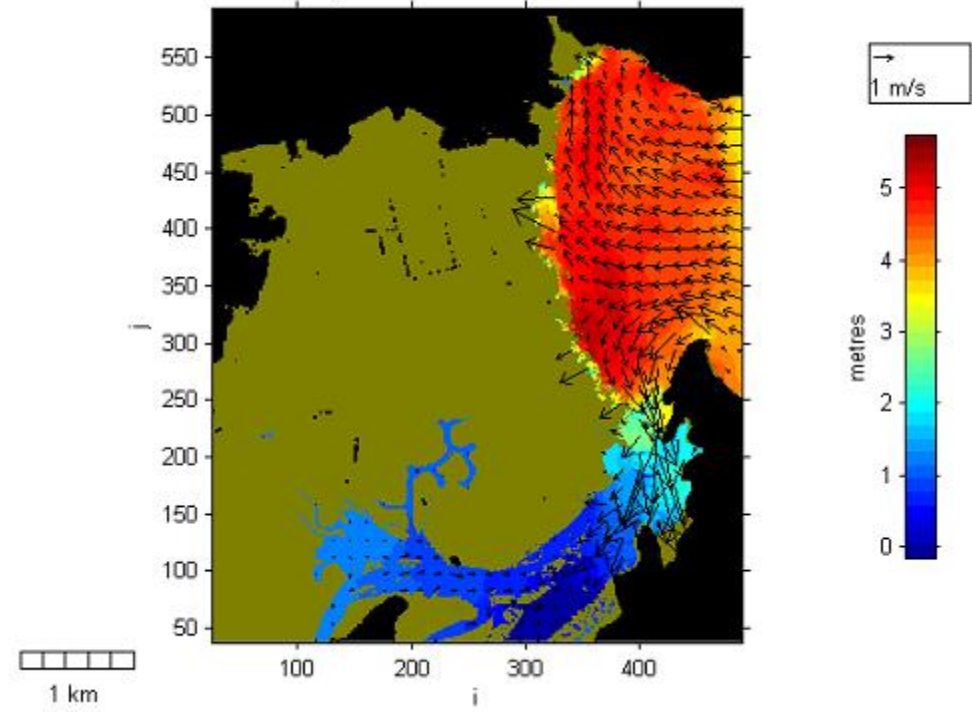
Appendix 1: Kermadec trench normal fault event scenario (Mw 9.0) inundation sequence and extent. Local model

First wave during run-up

Ground Striking Data

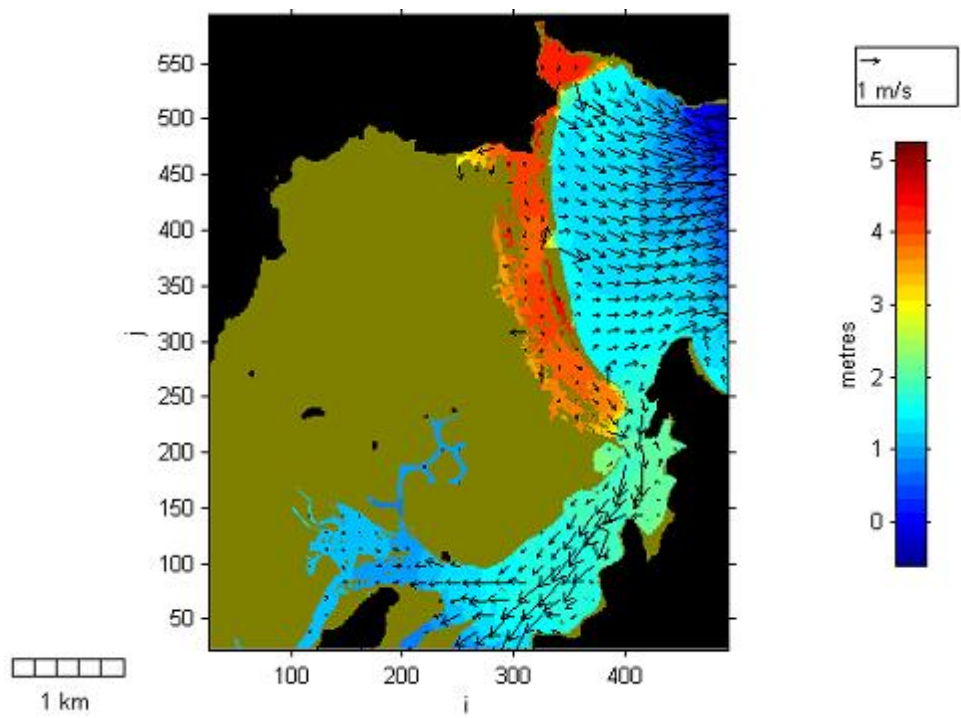


Non-Ground Striking Data

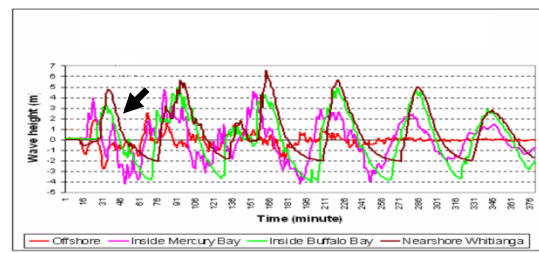
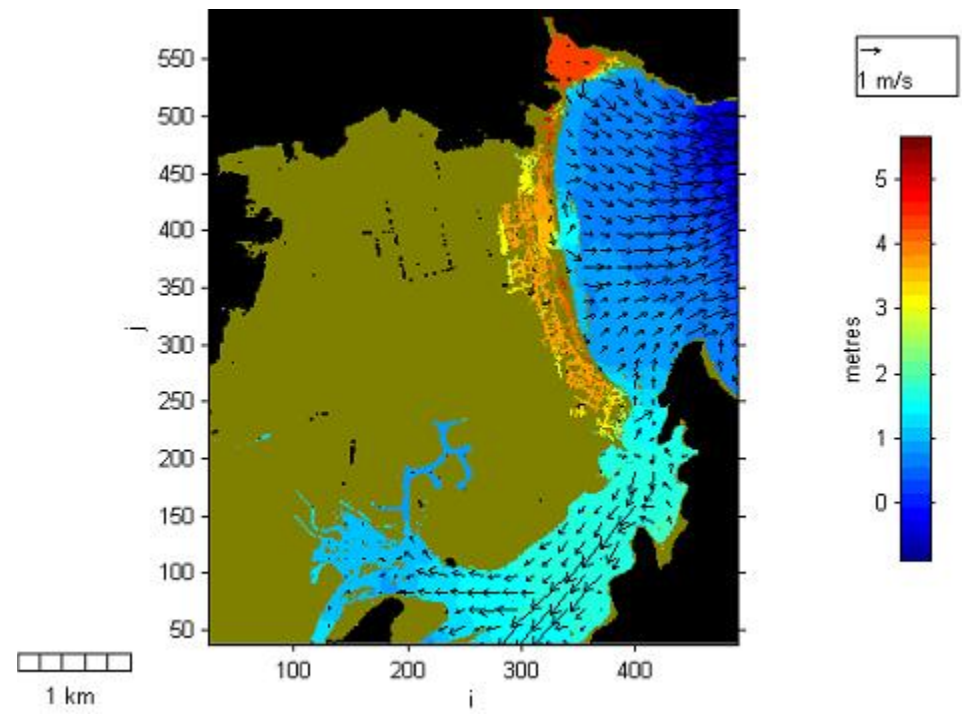


First wave during run-down

Ground Striking Data

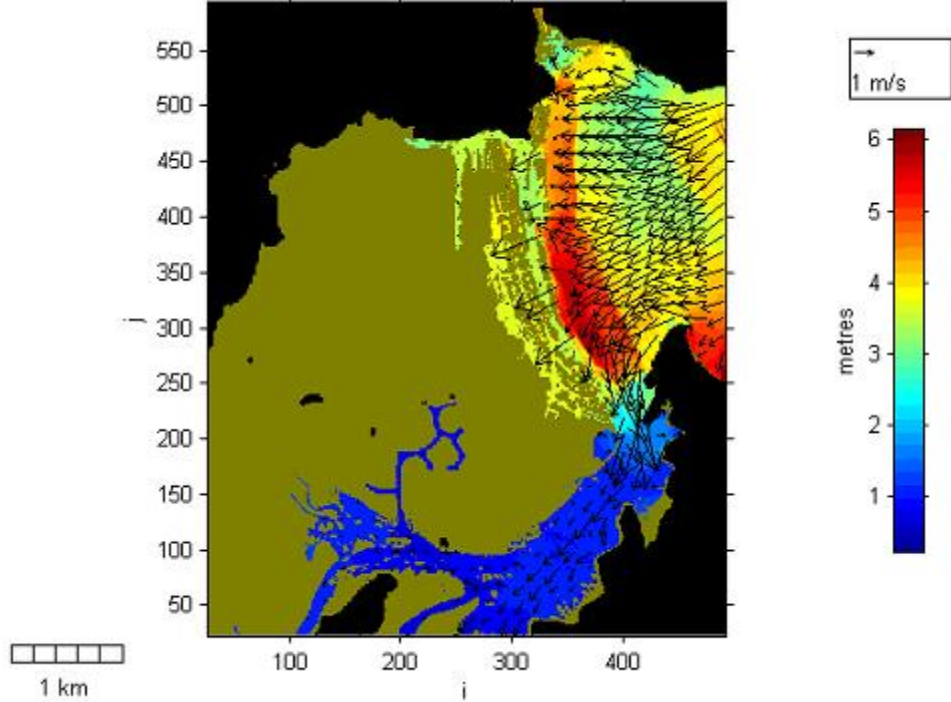


Non-Ground Striking Data

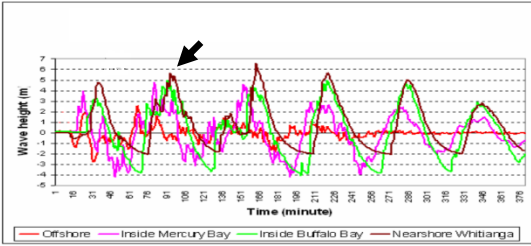
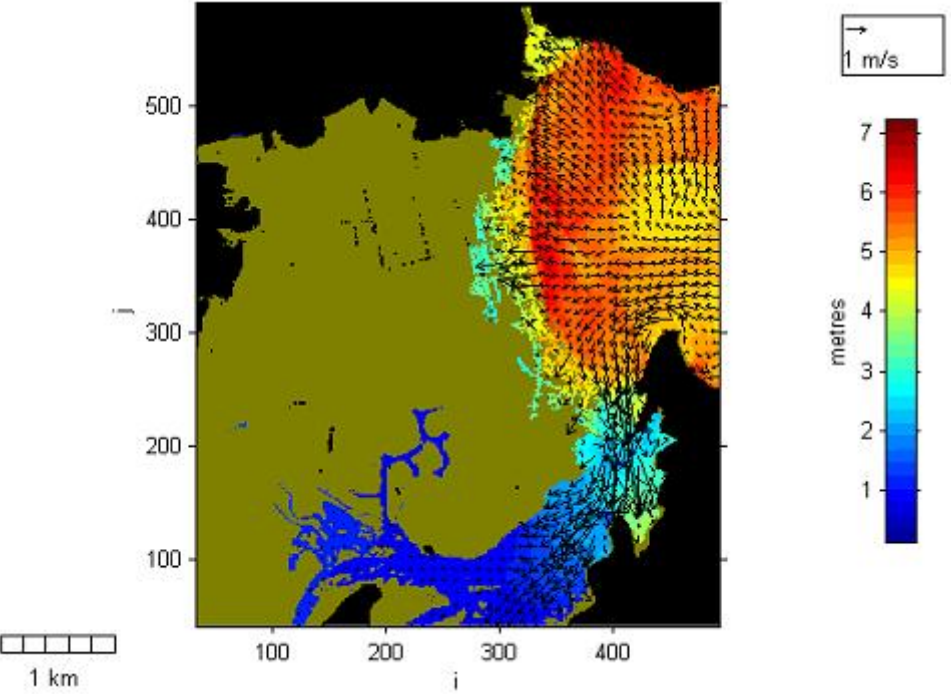


Second wave during run-up

Ground Striking Data

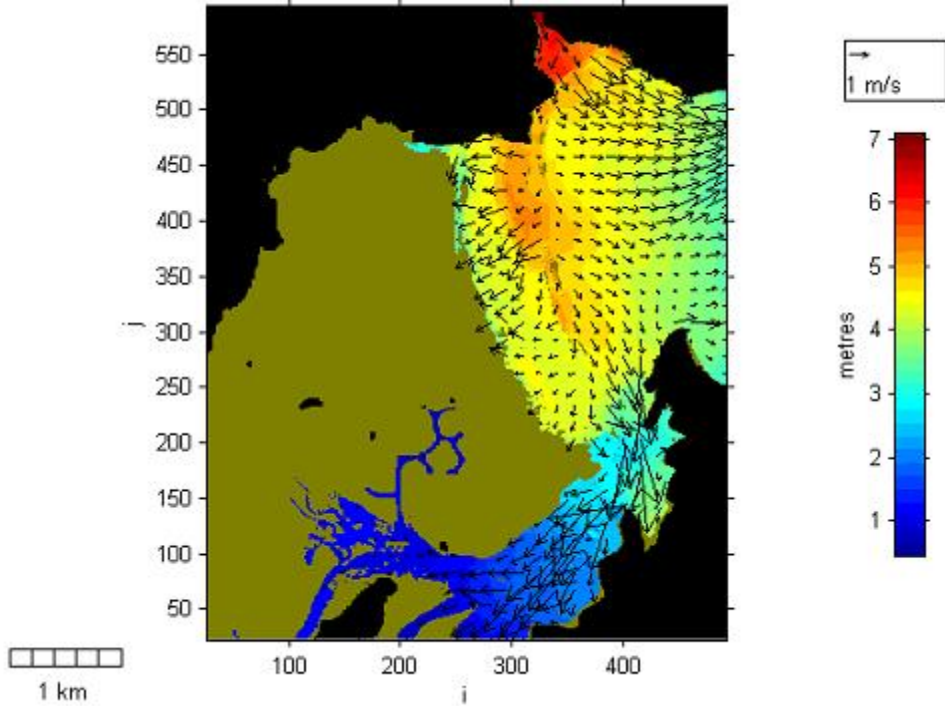


Non-Ground Striking Data

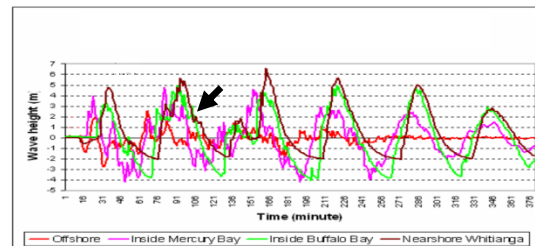
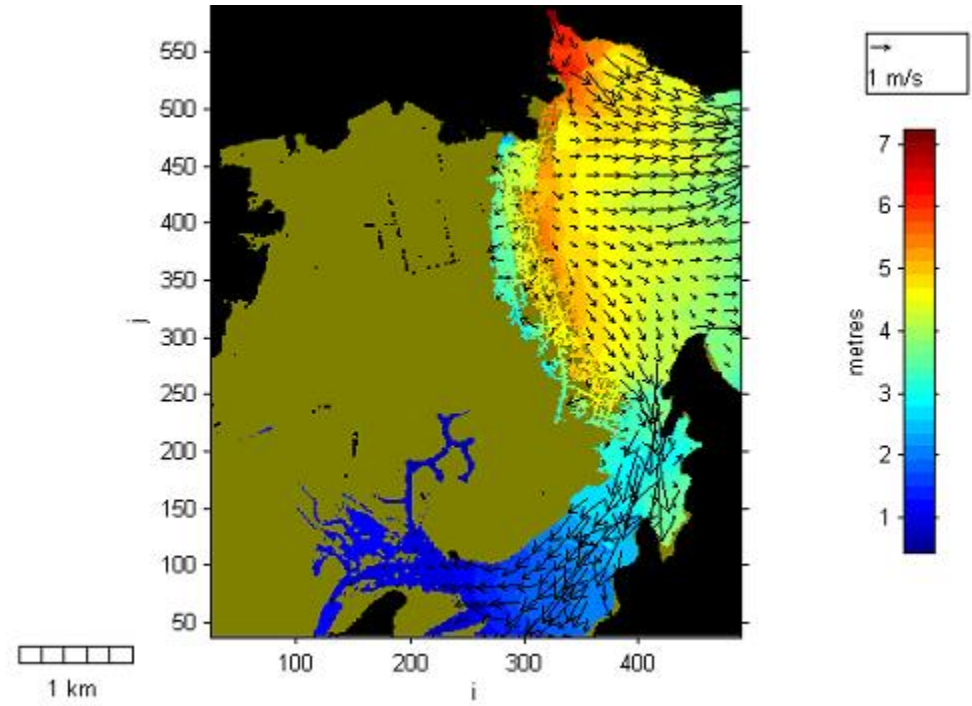


Second wave during run-down

Ground Striking Data

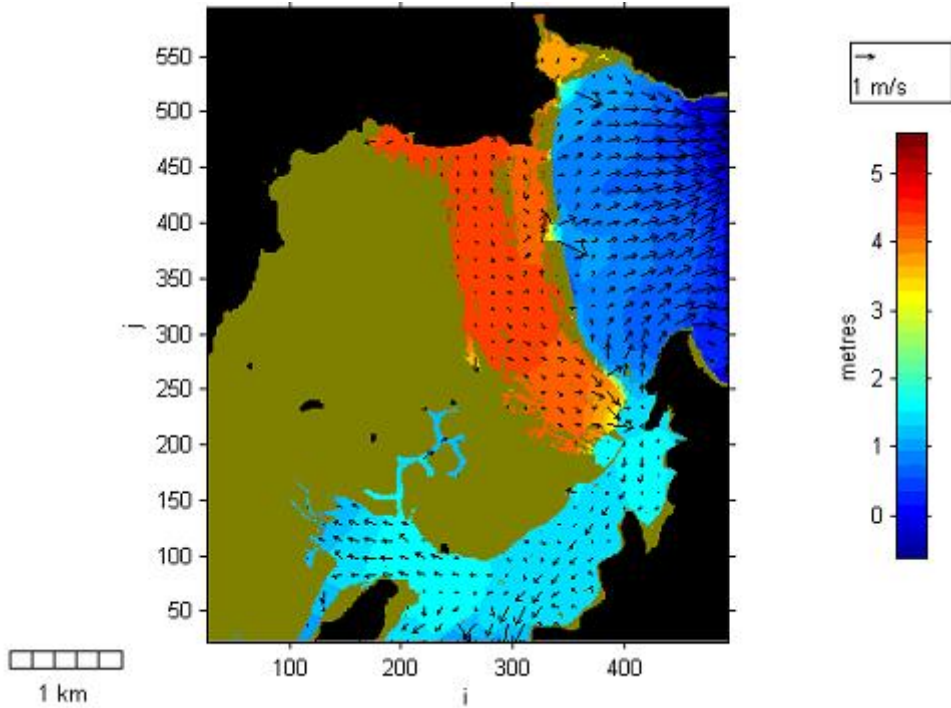


Non-Ground Striking Data

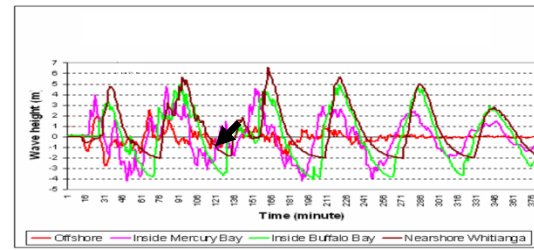
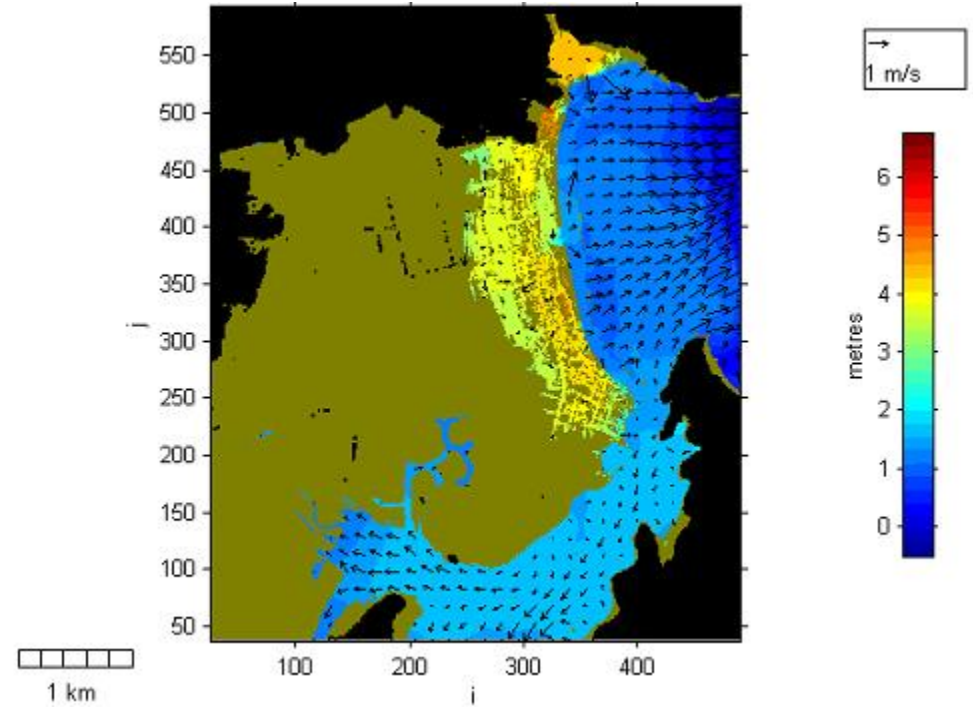


Second wave during run-down

Ground Striking Data

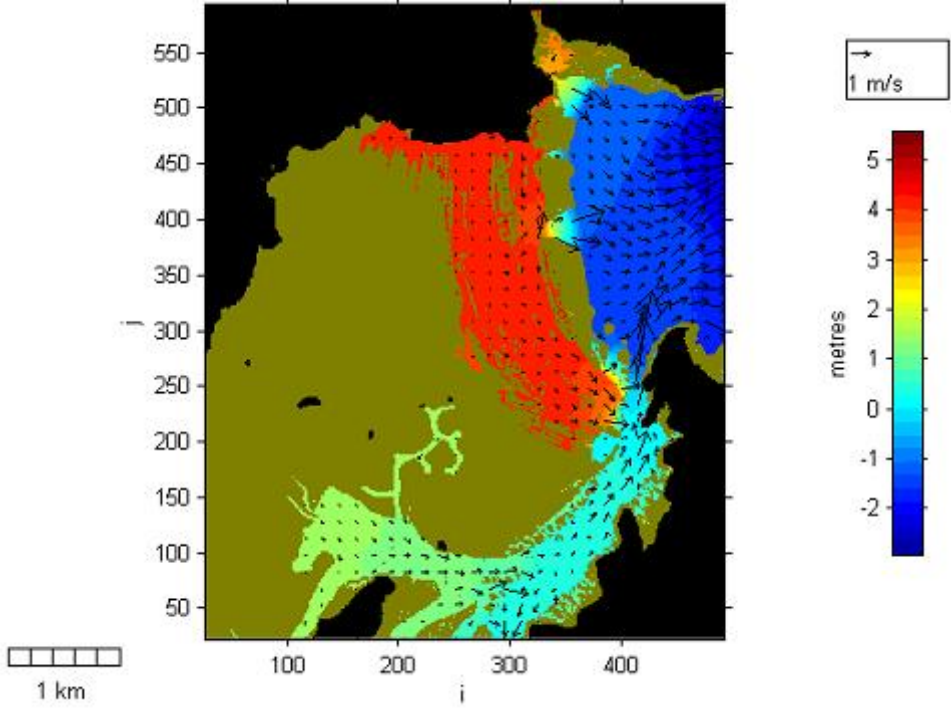


Non-Ground Striking Data

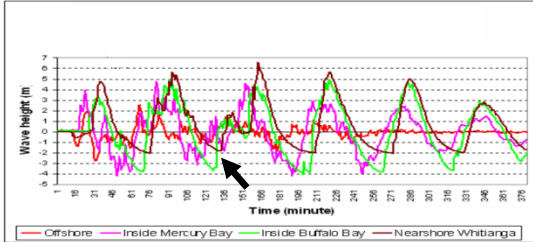
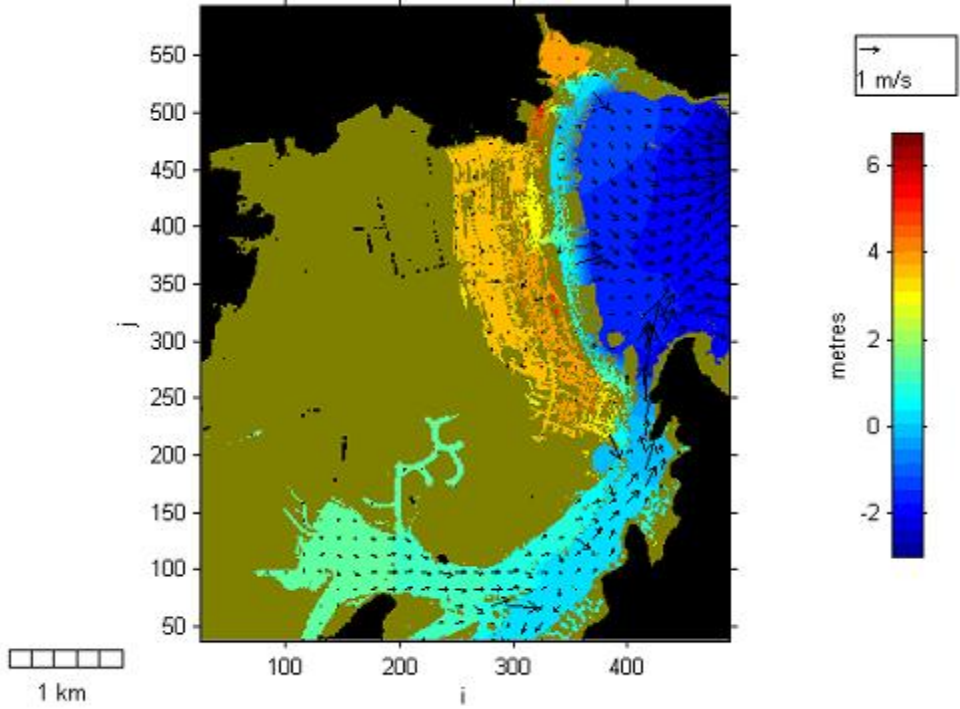


Second wave during run-down

Ground Striking Data

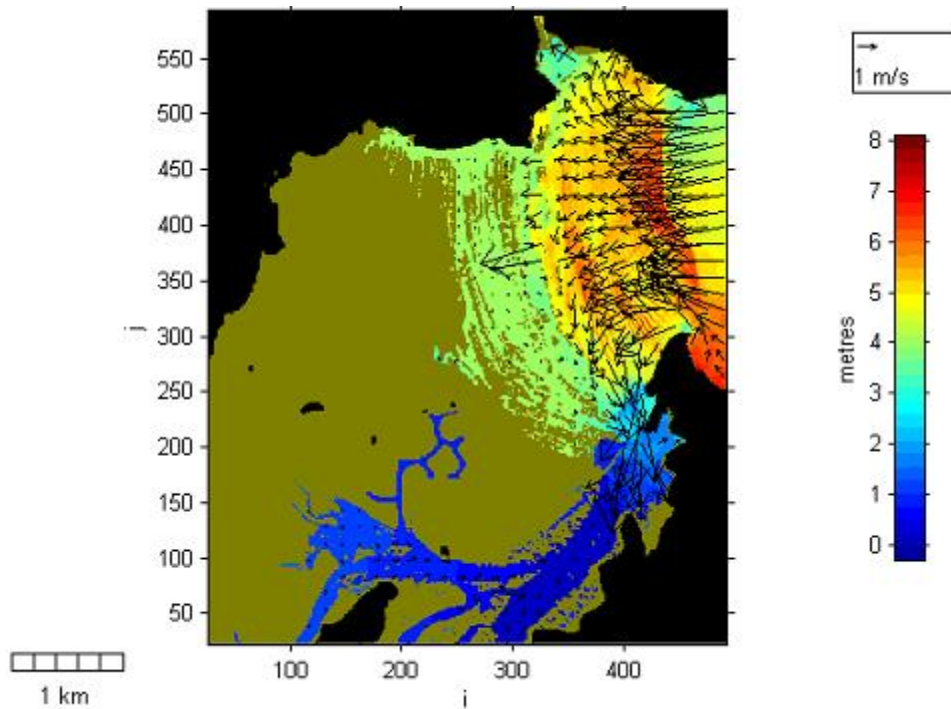


Non-Ground Striking Data

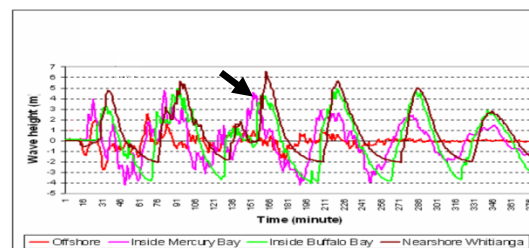
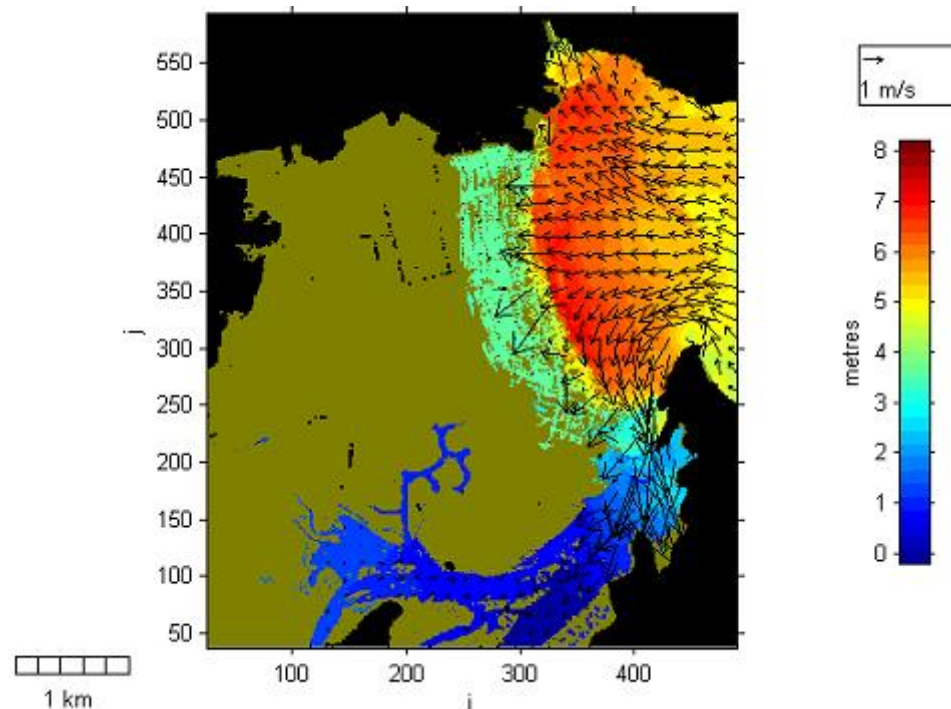


Third wave during run-up

Ground Striking Data

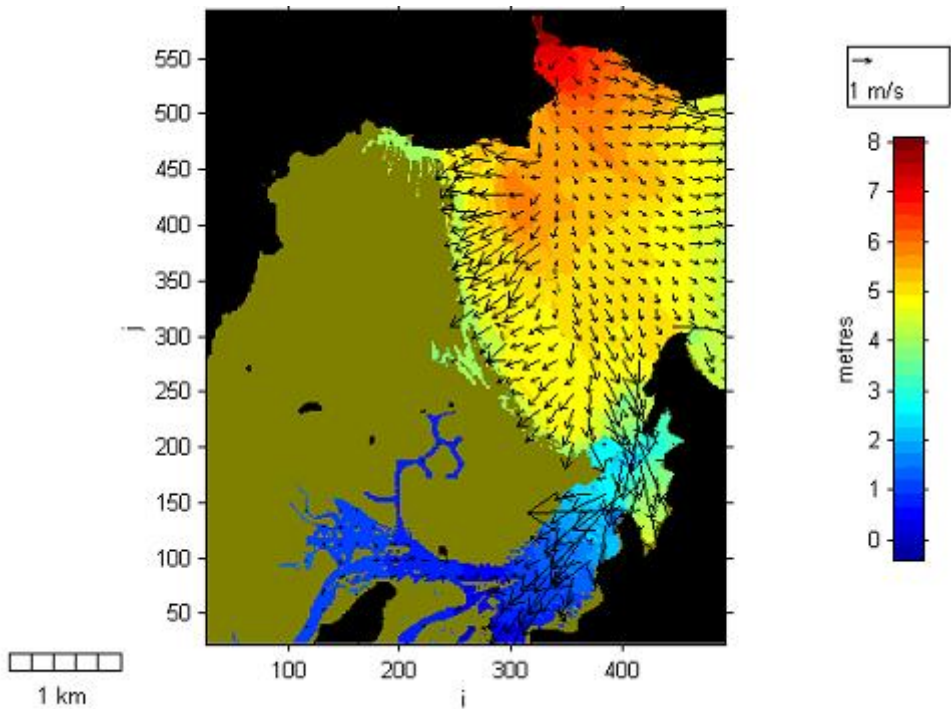


Non-Ground Striking Data

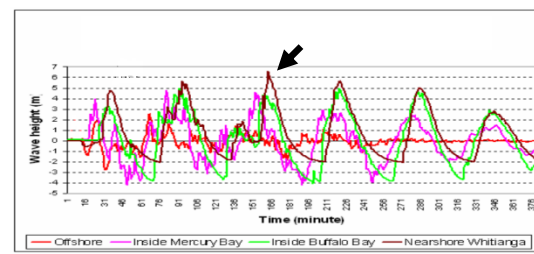
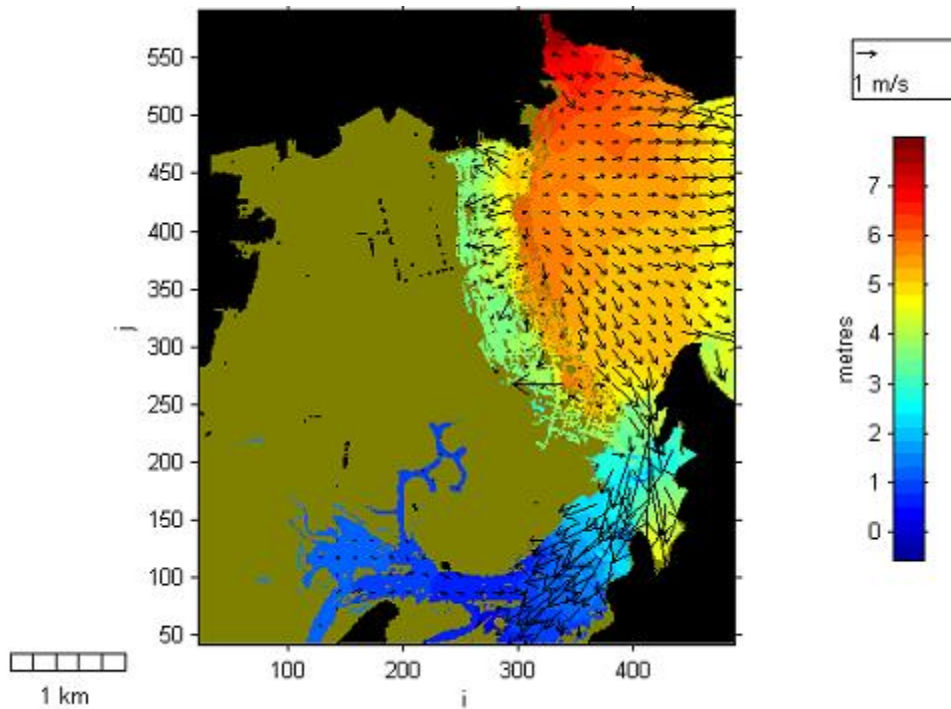


Third wave during run-up

Ground Striking Data

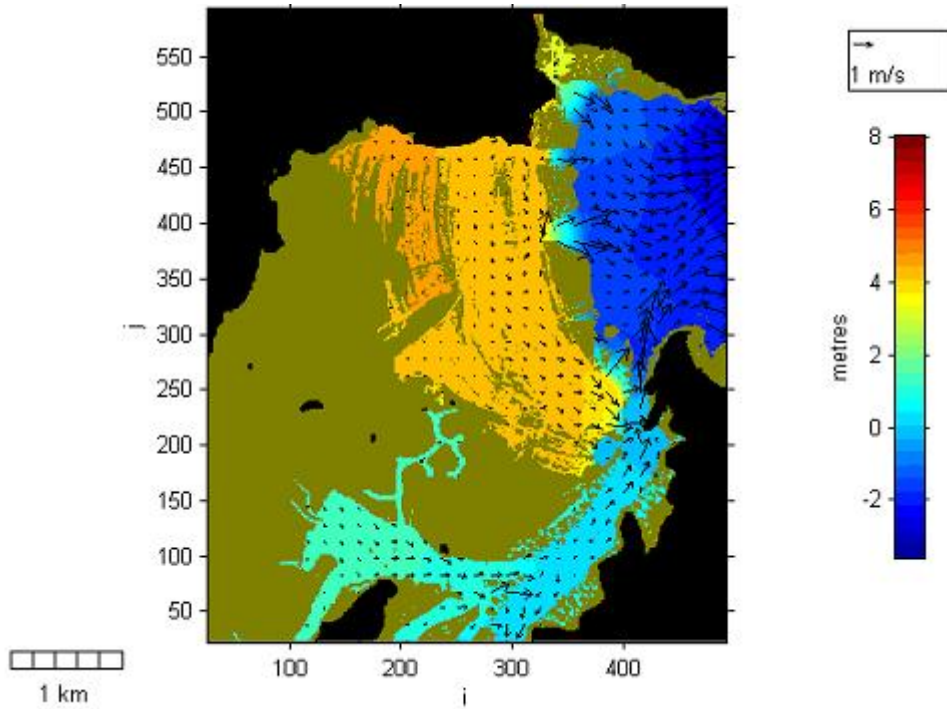


Non-Ground Striking Data

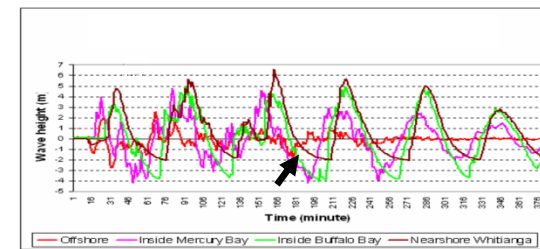
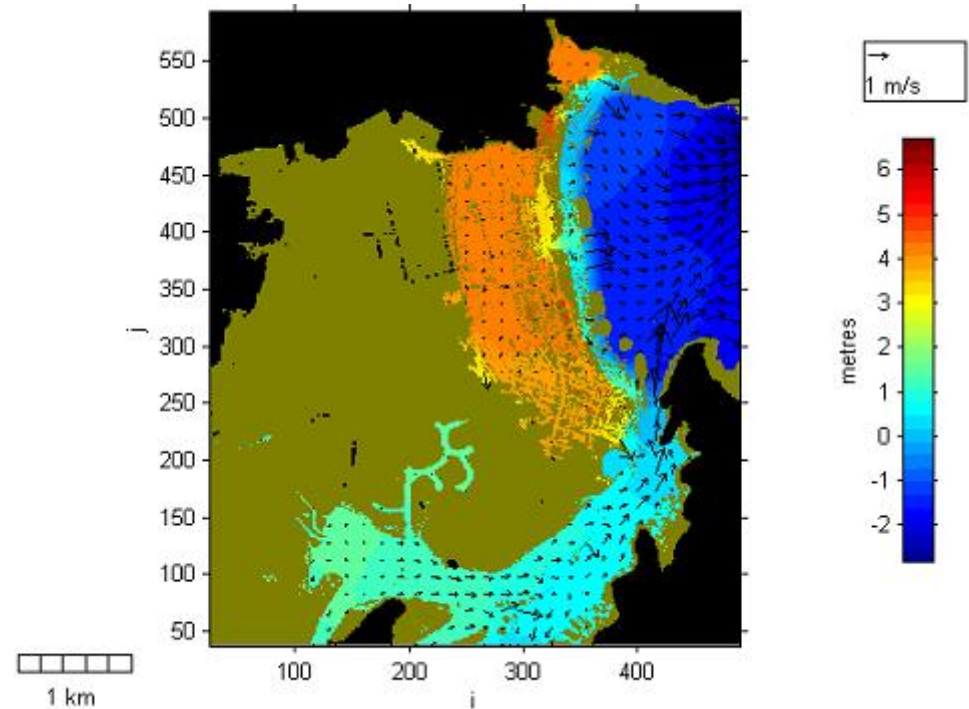


Third wave during run-down

Ground Striking Data

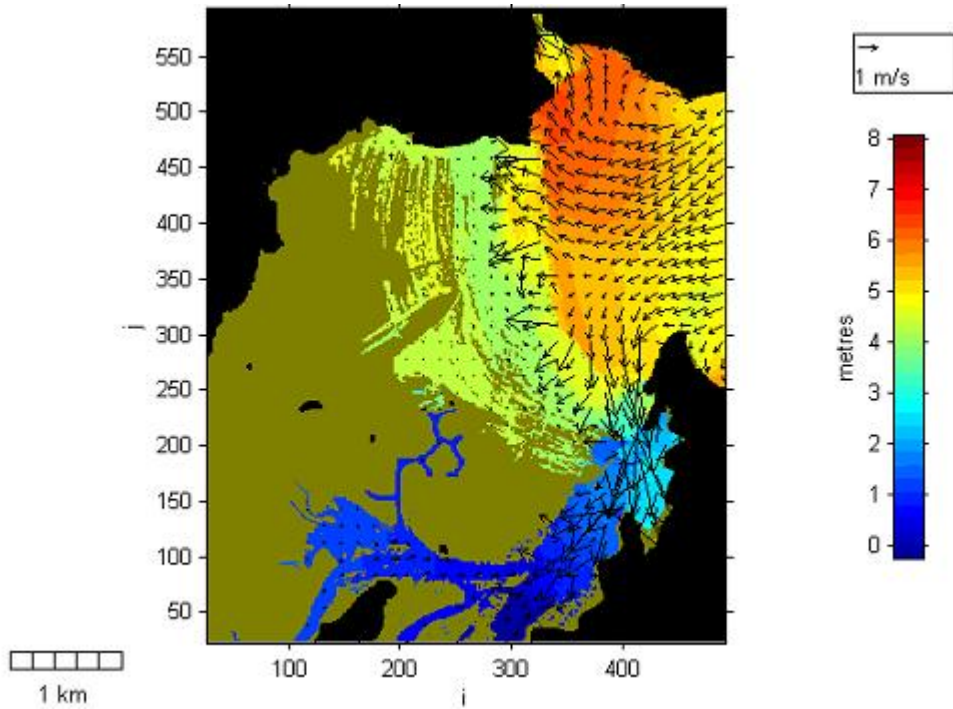


Non-Ground Striking Data

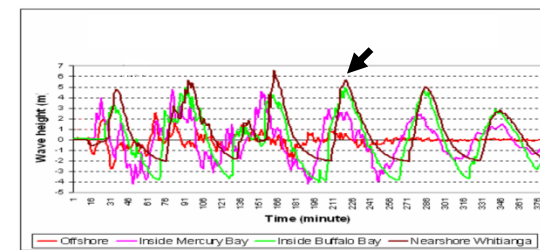
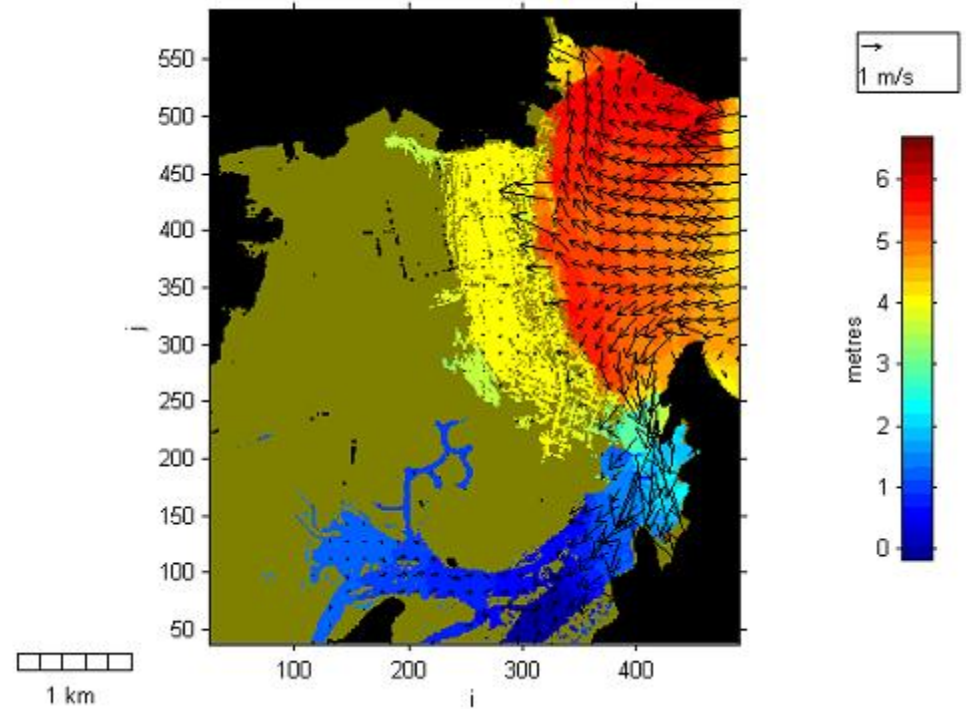


Fourth wave during run-up

Ground Striking Data

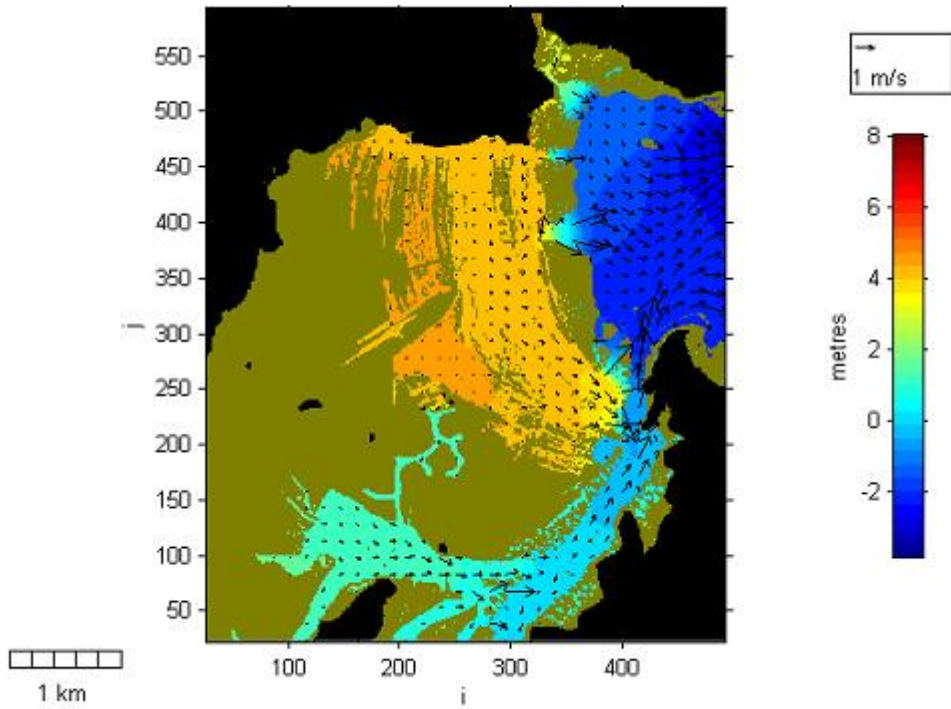


Non-Ground Striking Data

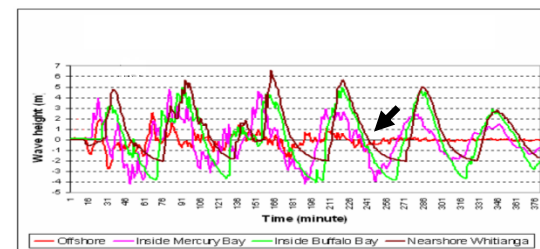
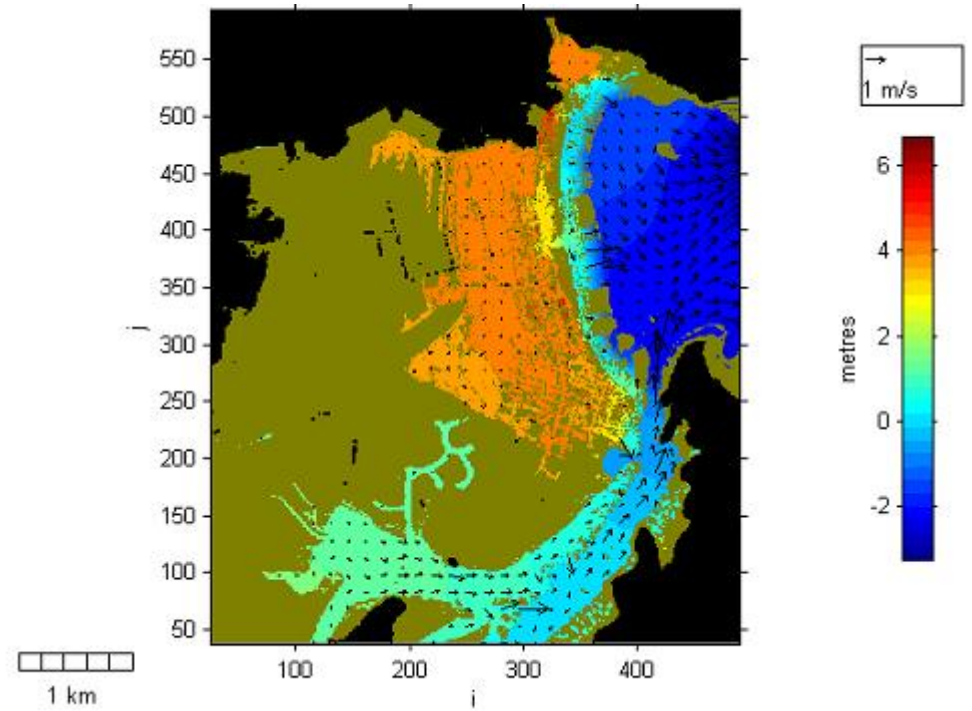


Fourth wave during run-down

Ground Striking Data

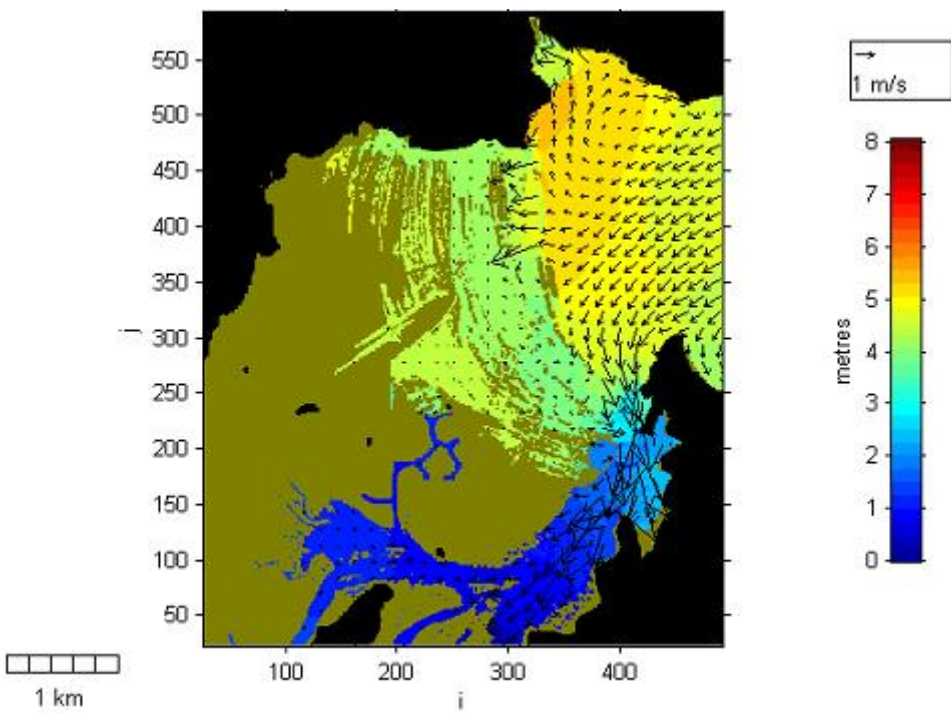


Non-Ground Striking Data

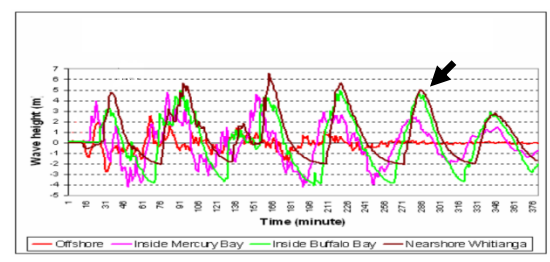
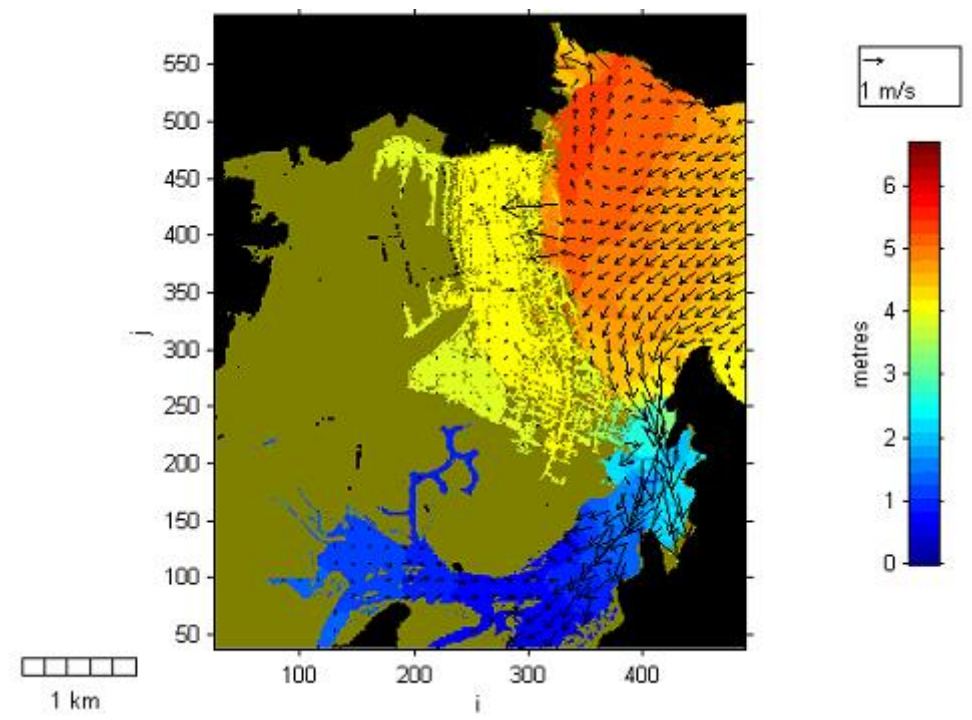


Fifth wave during run-up

Ground Striking Data

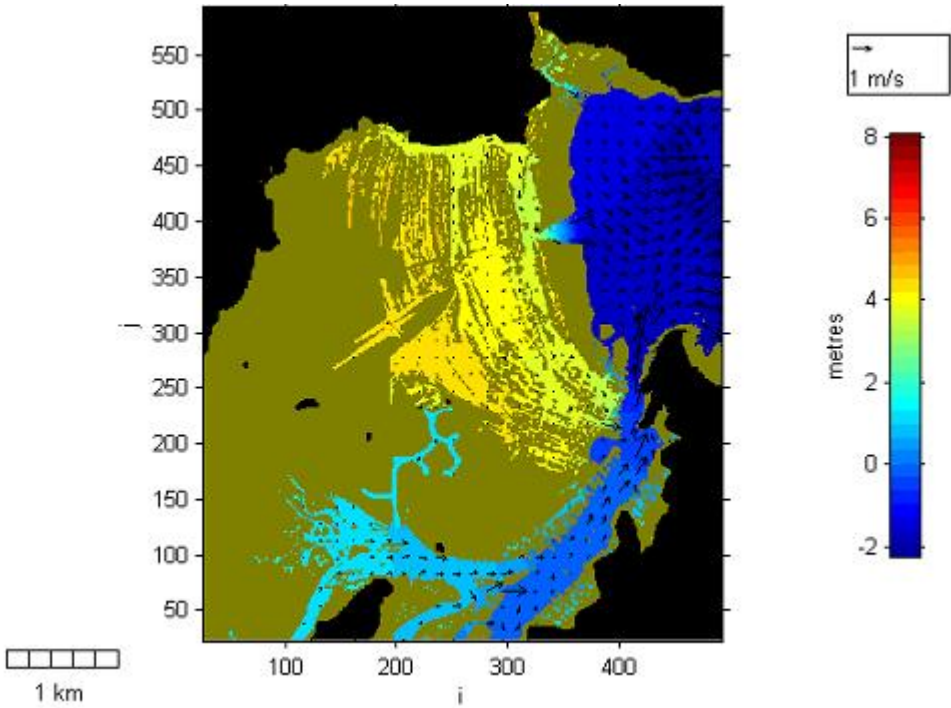


Non-Ground Striking Data

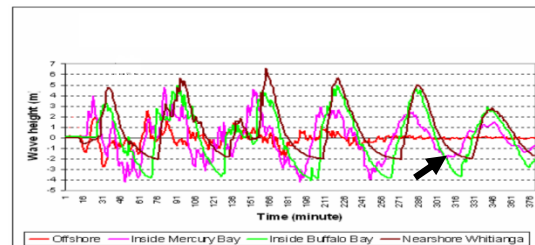
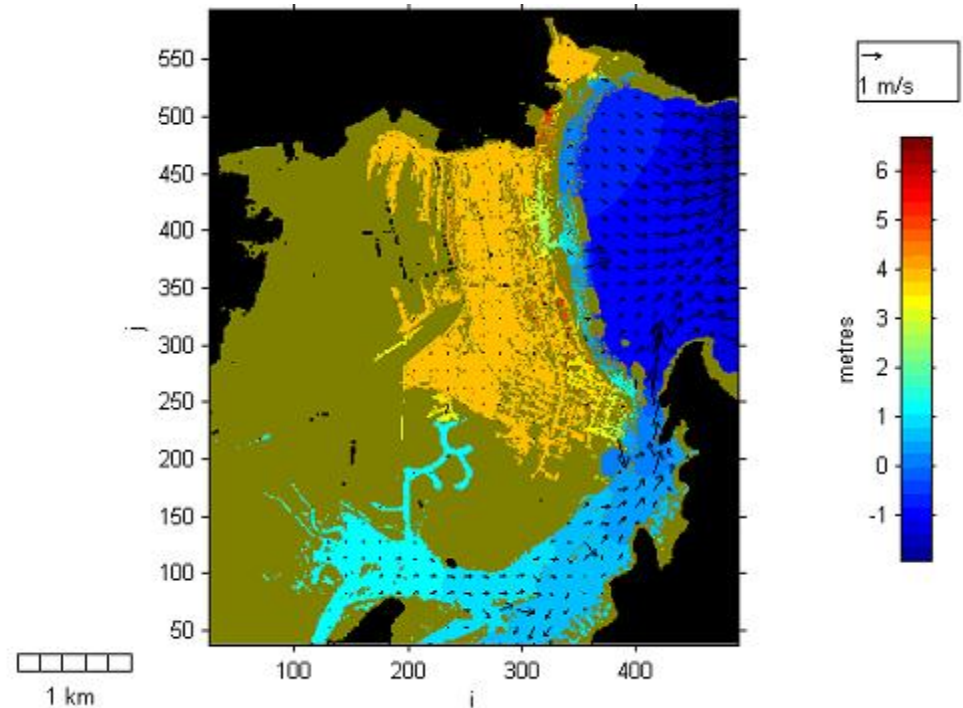


Fifth wave during run-down

Ground Striking Data

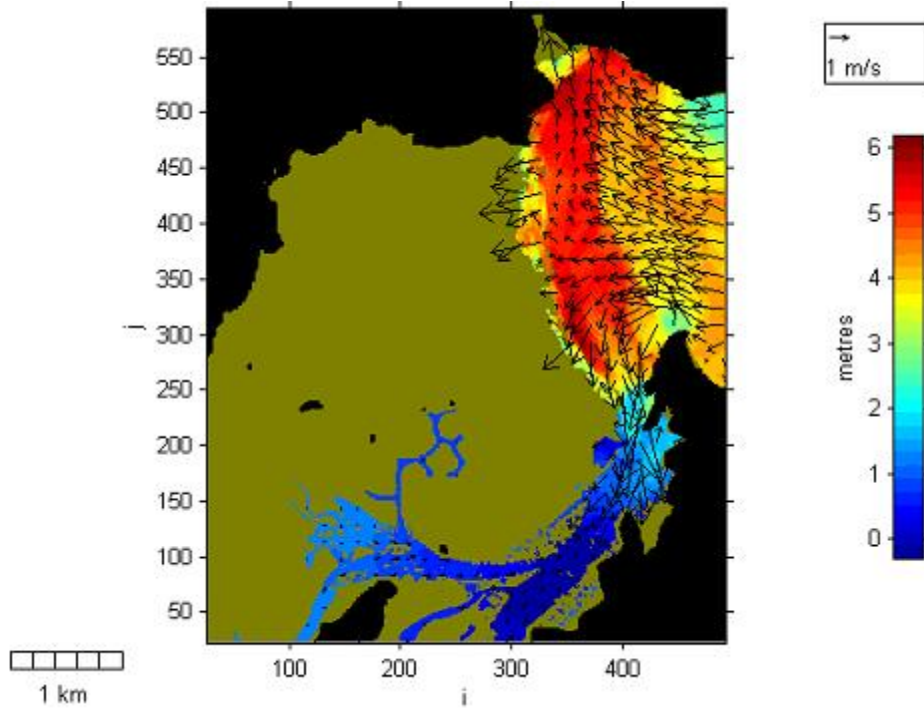


Non-Ground Striking Data

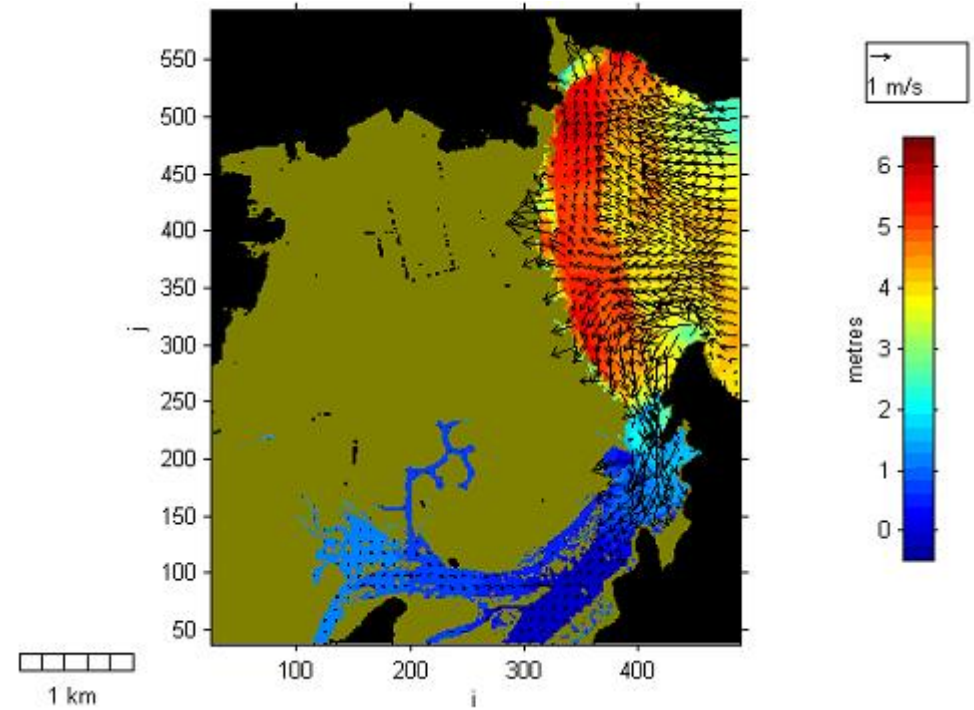


Appendix 2: 1960 Chilean-type scenario inundation sequence and extent. Local model

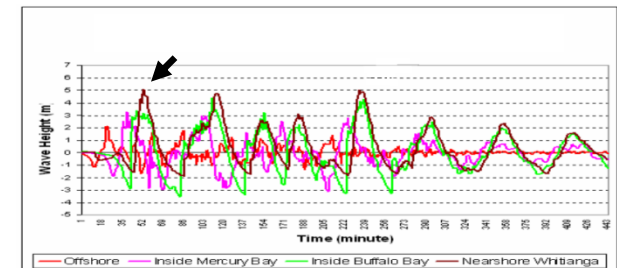
Ground Striking Data



Non-Ground Striking Data

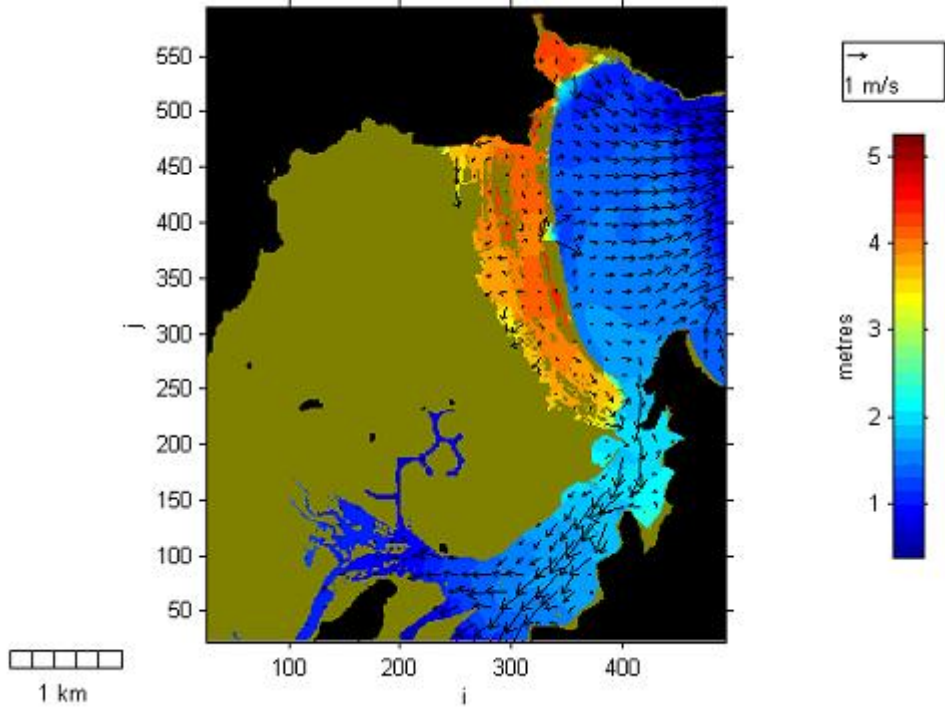


First wave during run-up

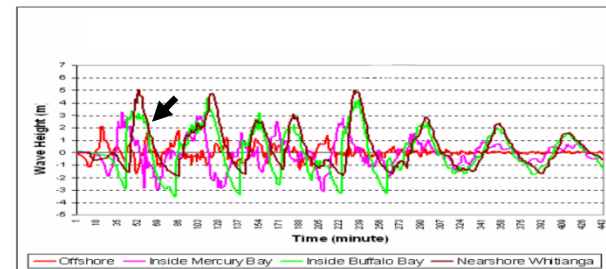
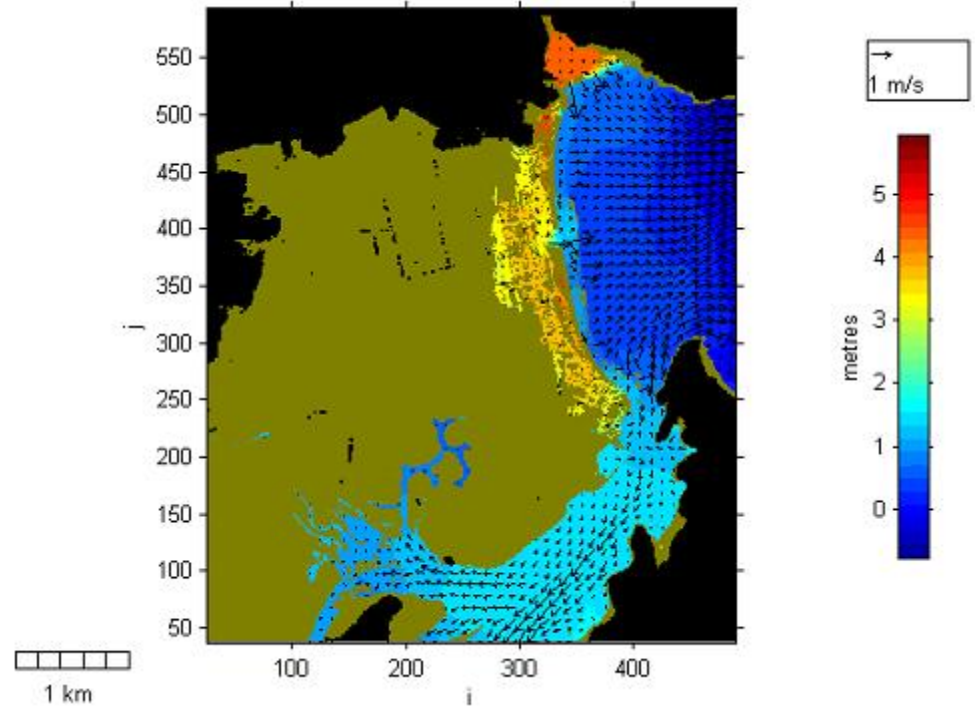


First wave during run-down

Ground Striking Data

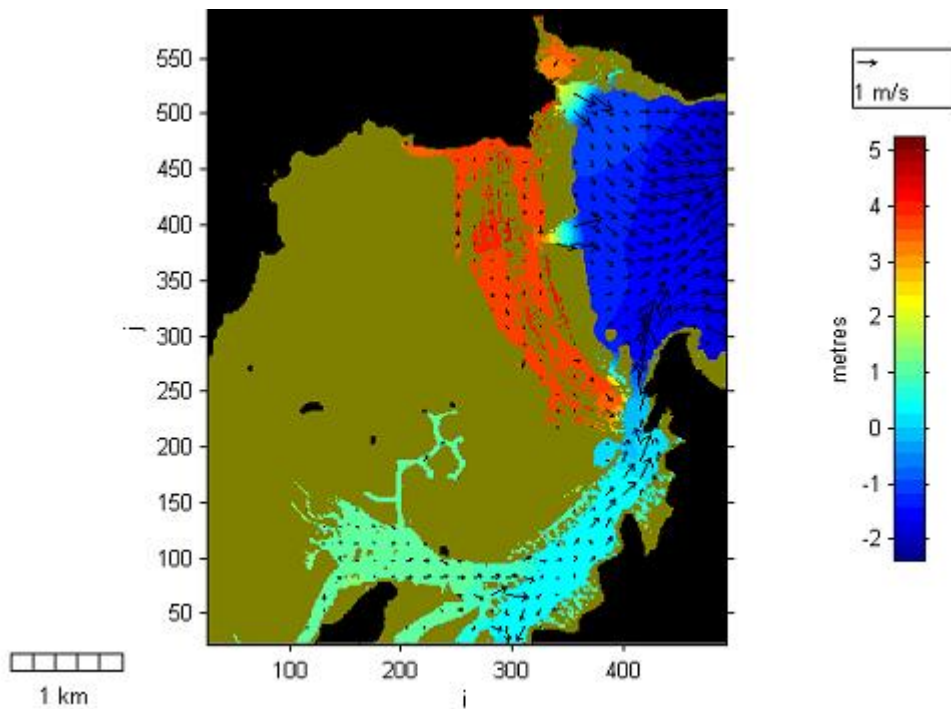


Non-Ground Striking Data

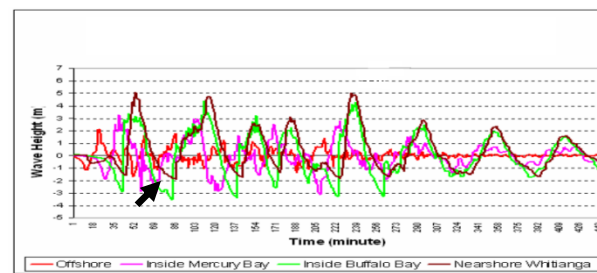
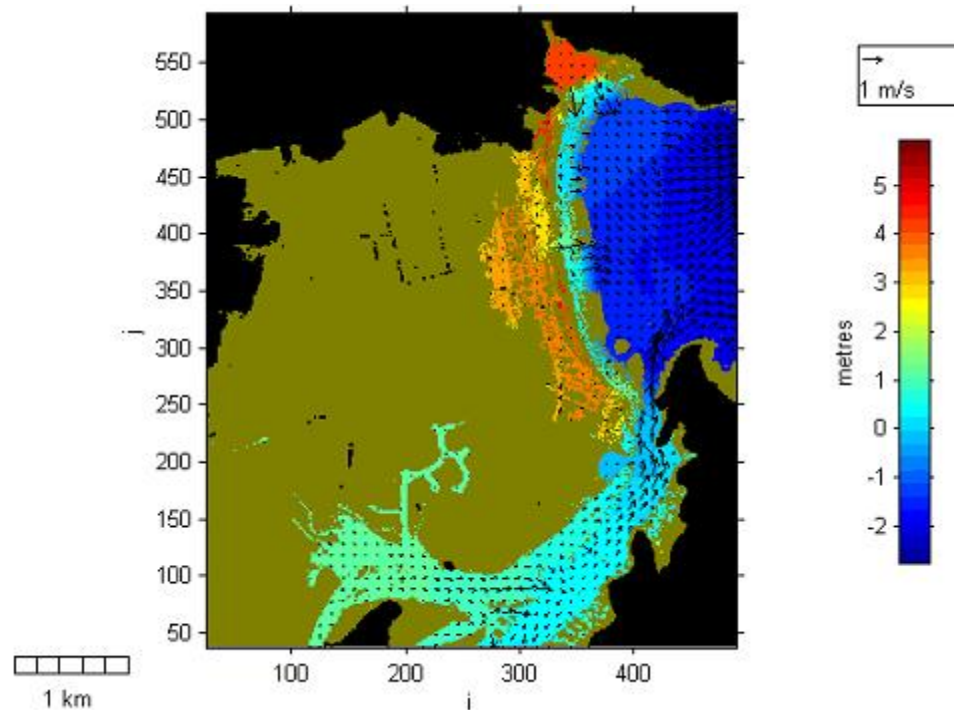


First wave during run-down

Ground Striking Data

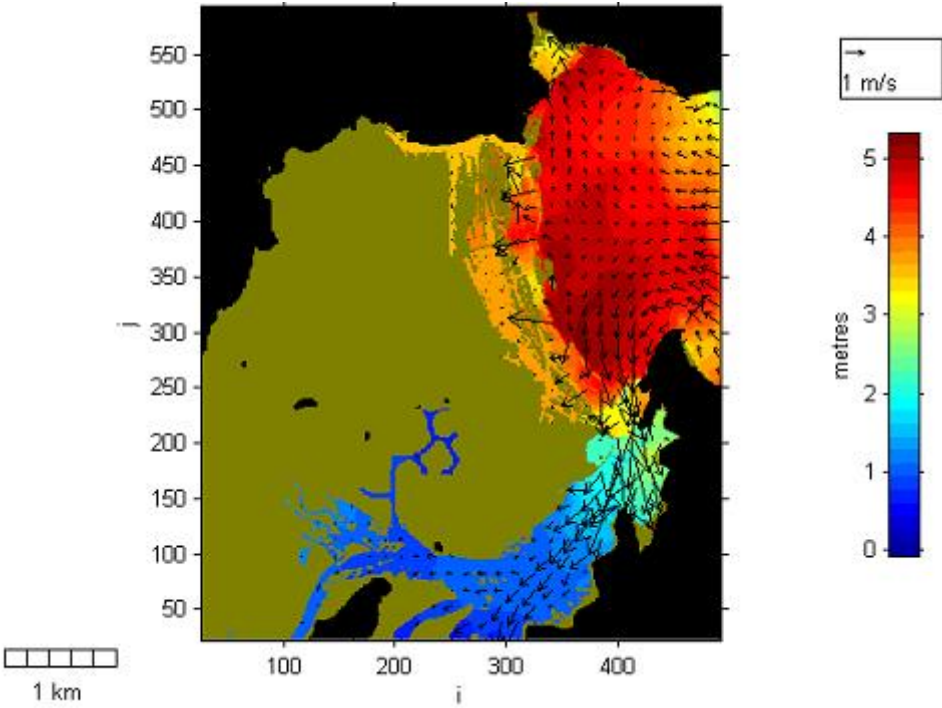


Non-Ground Striking Data

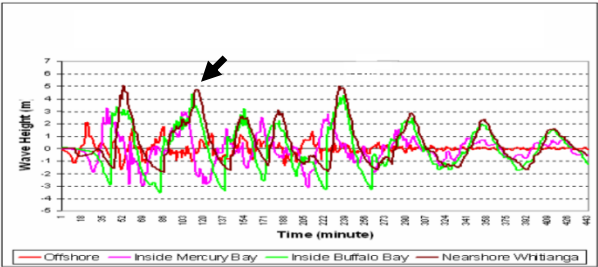
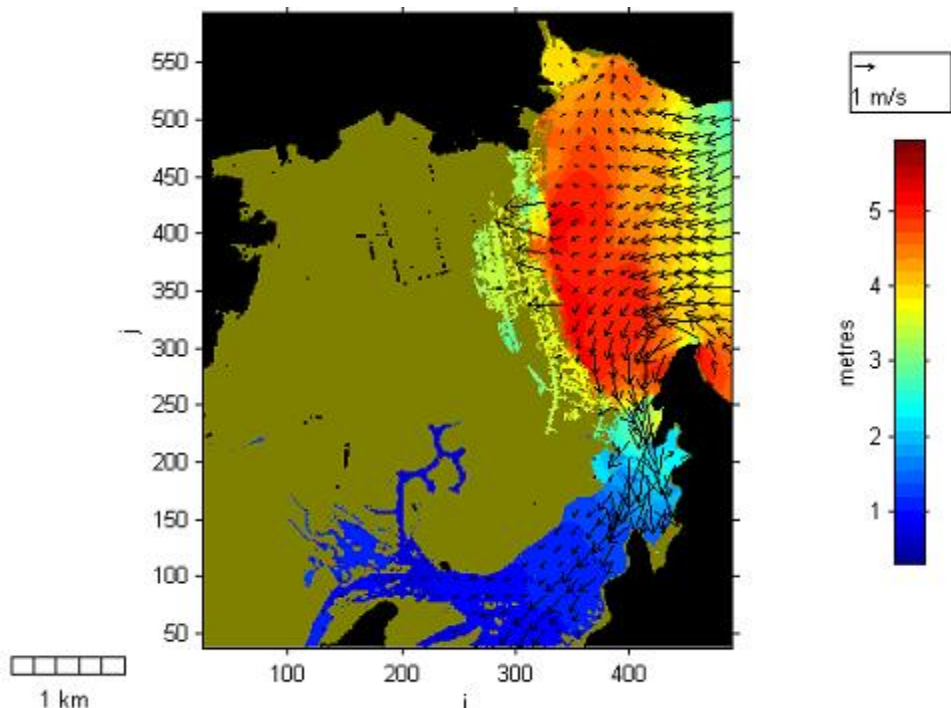


Second wave during run-up

Ground Striking Data

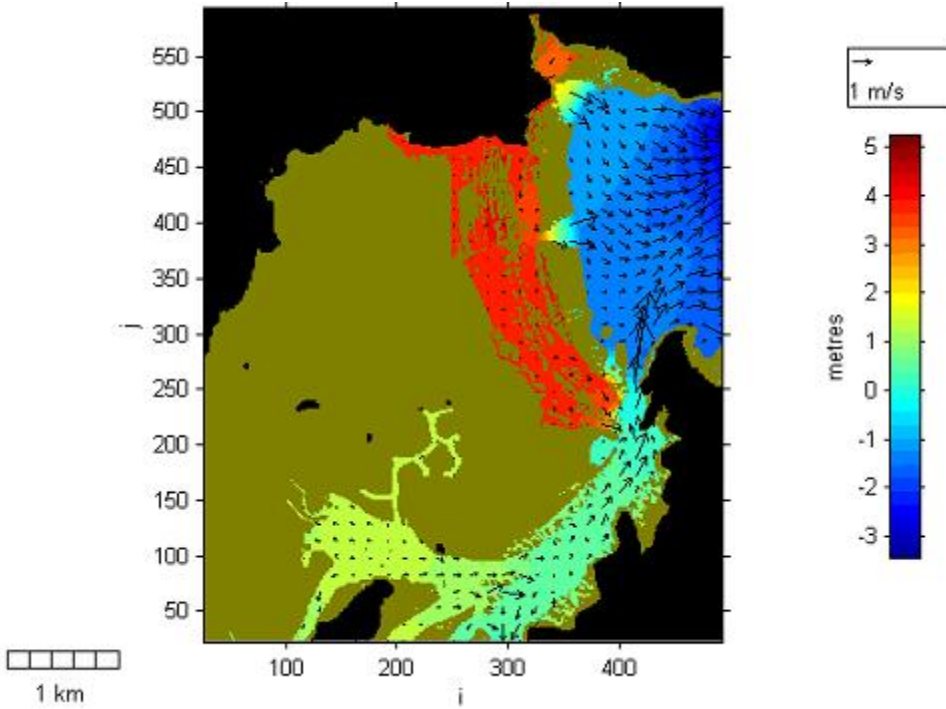


Non-Ground Striking Data

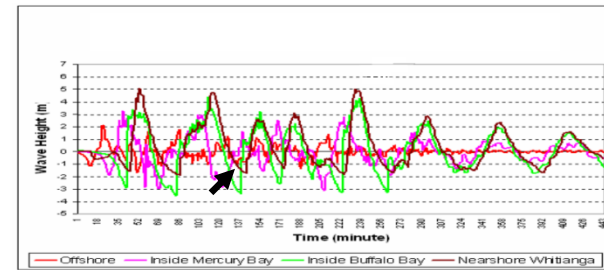
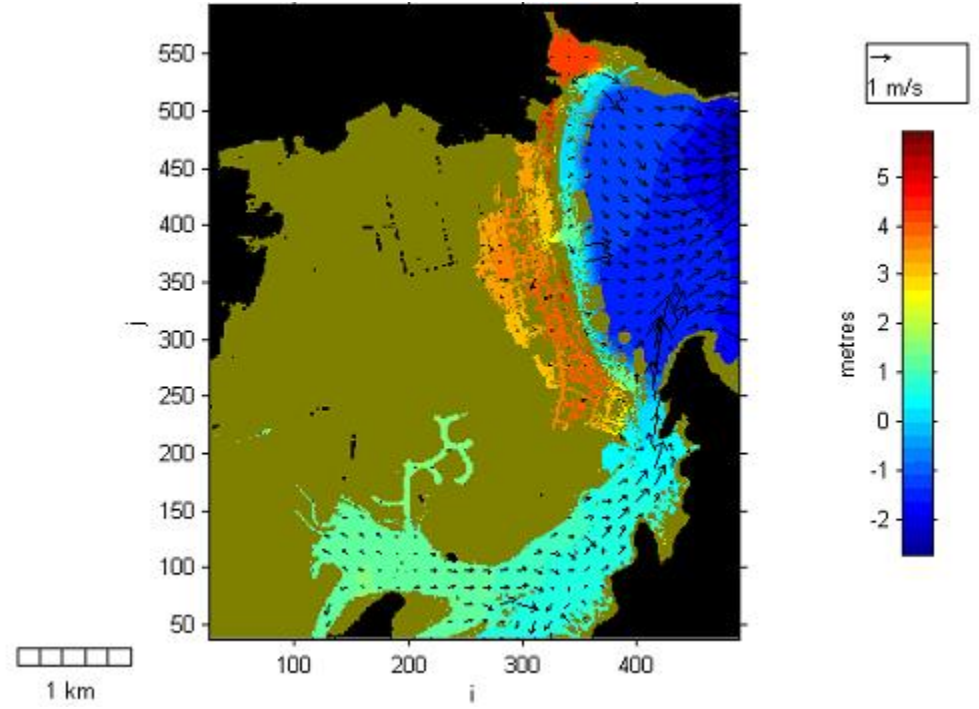


Second wave during run-down

Ground Striking Data

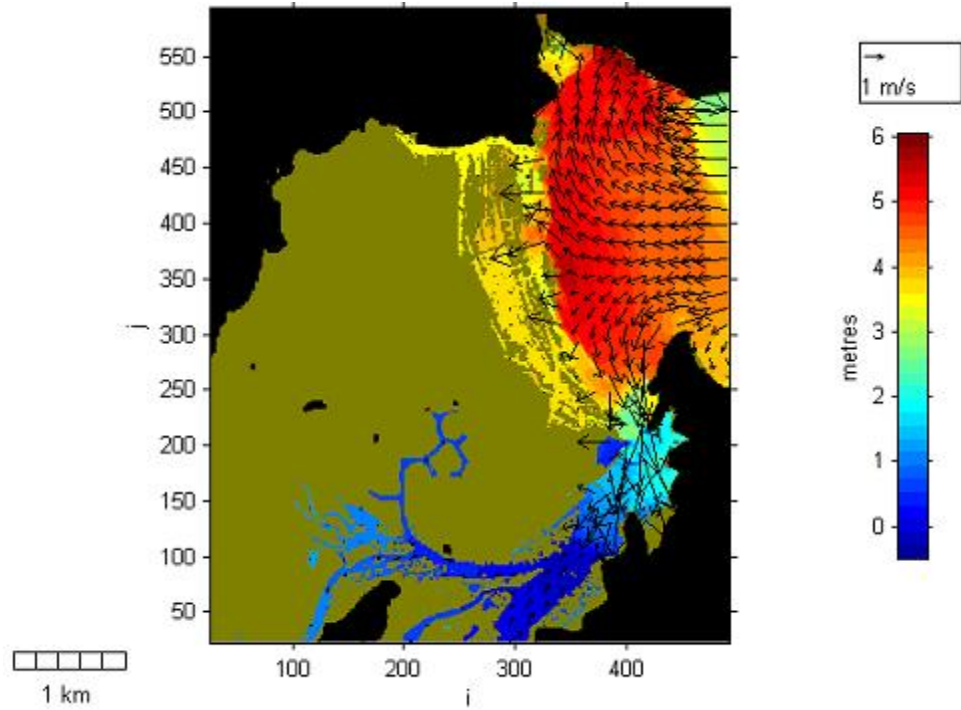


Non-Ground Striking Data

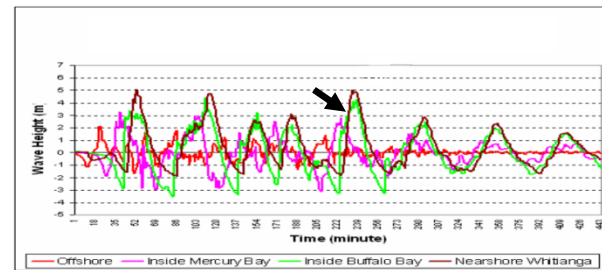
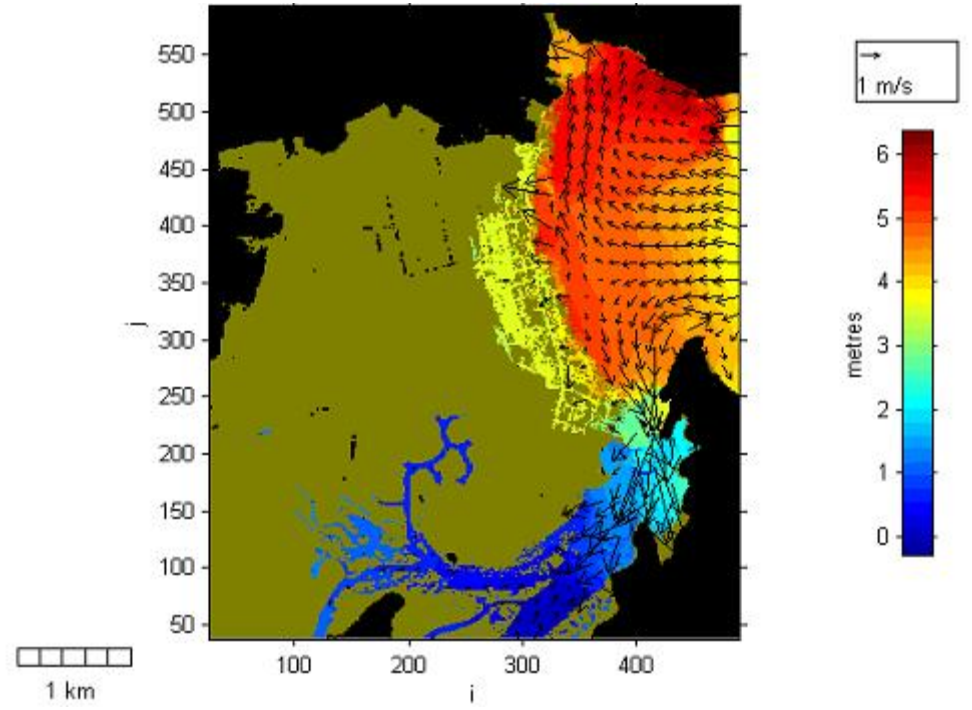


Fifth wave during run-up

Ground Striking Data

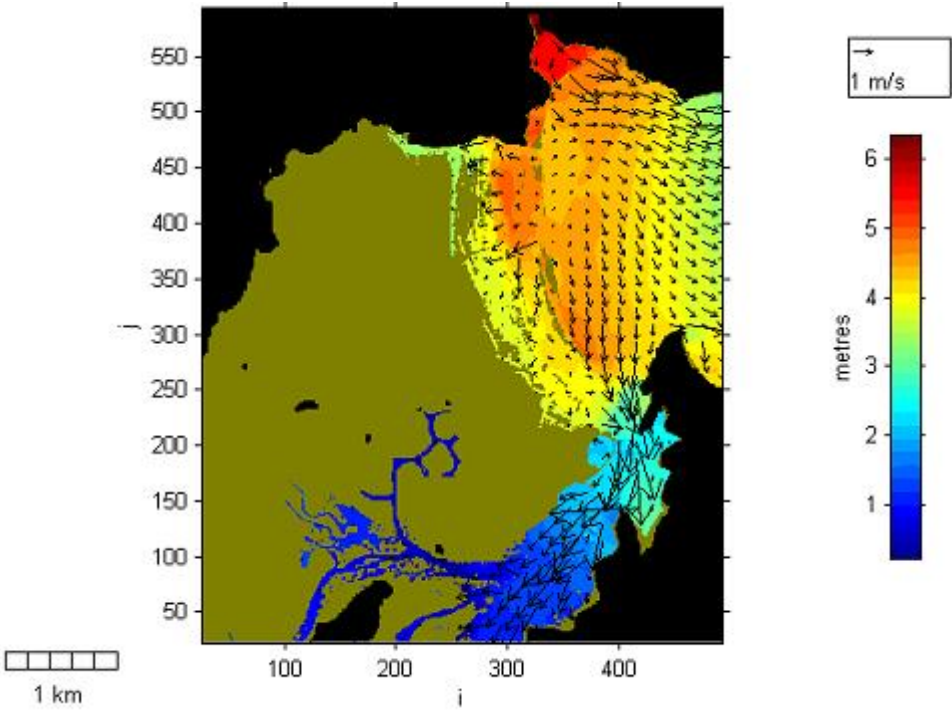


Non-Ground Striking Data

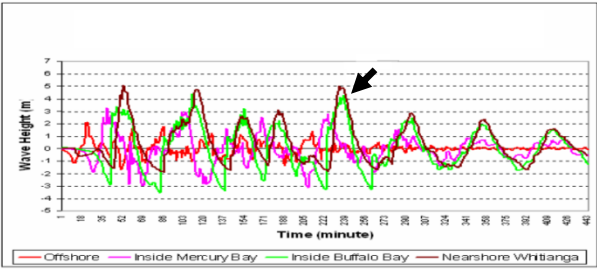
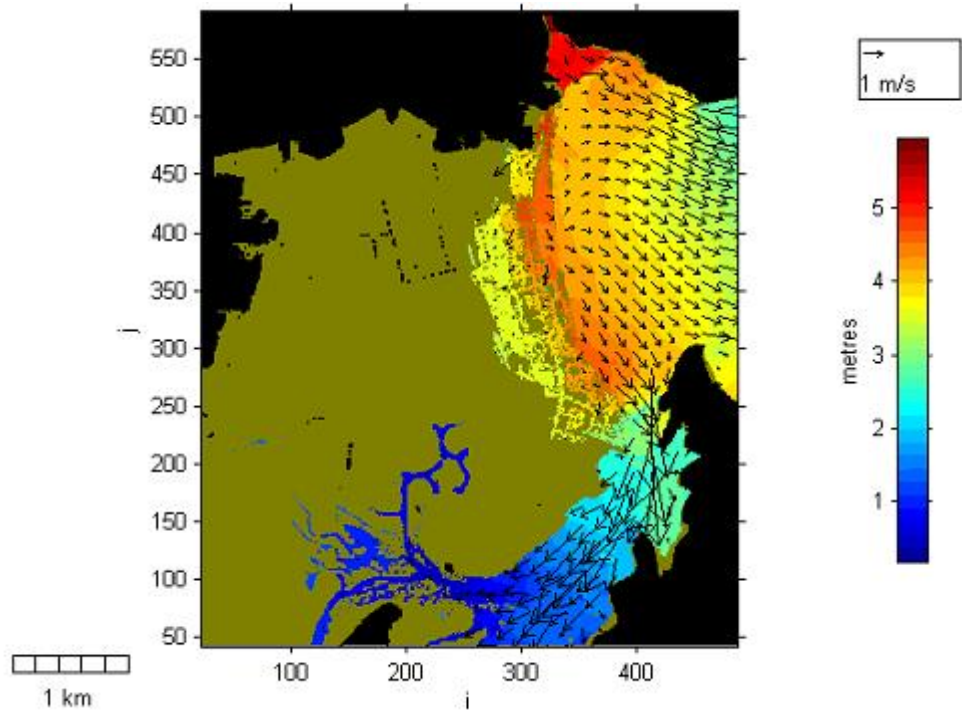


Fifth wave during run-up

Ground Striking Data

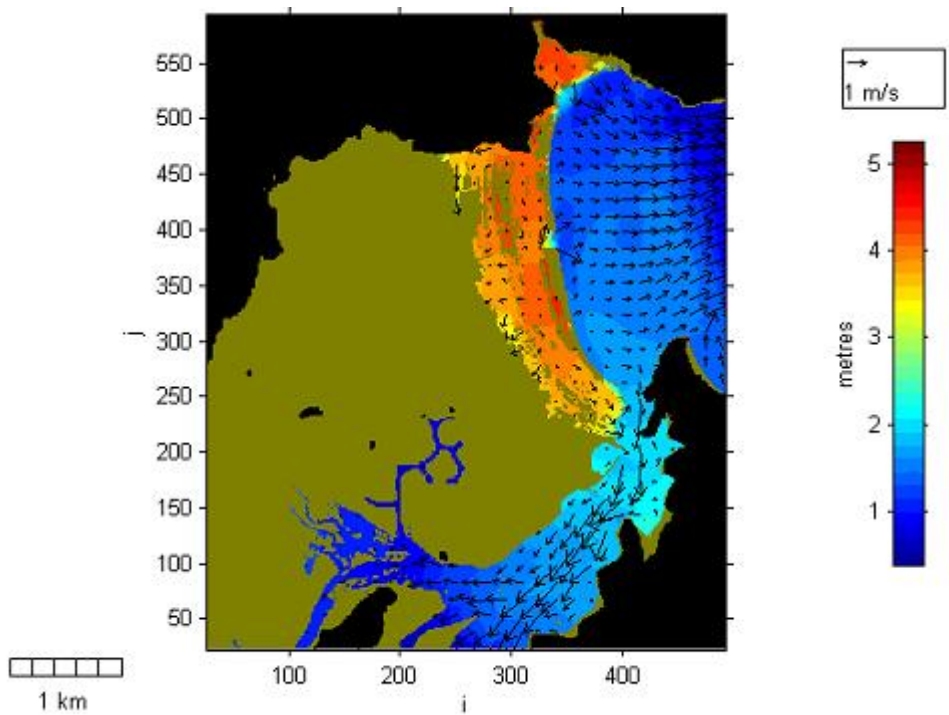


Non-Ground Striking Data

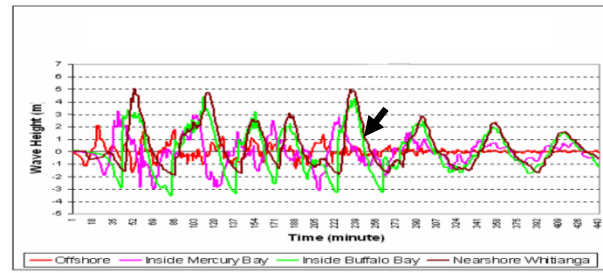
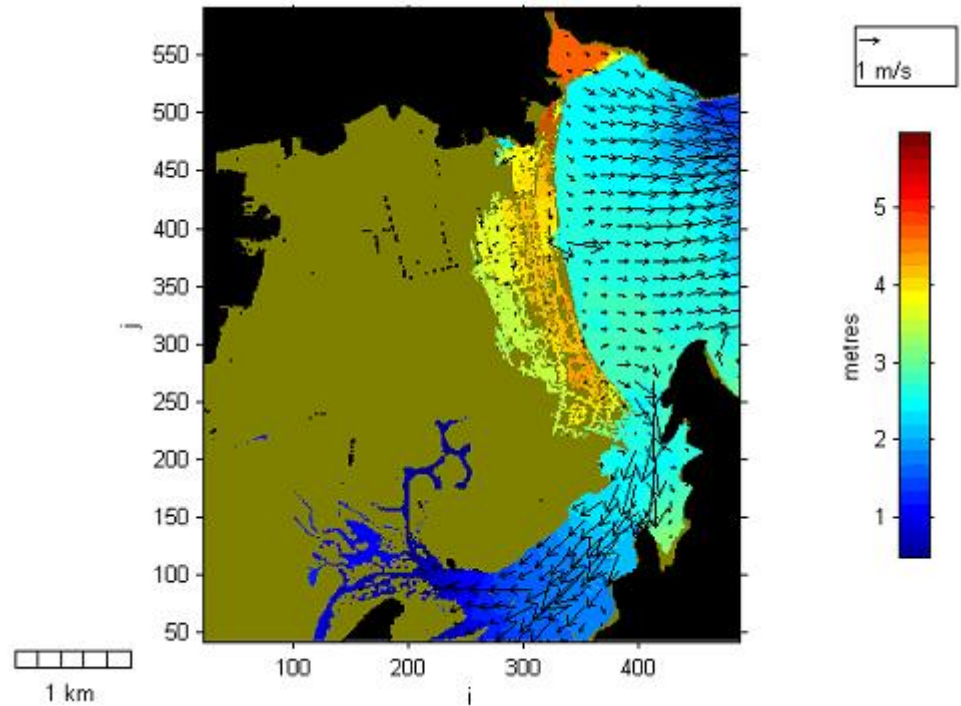


Fifth wave during run-down

Ground Striking Data

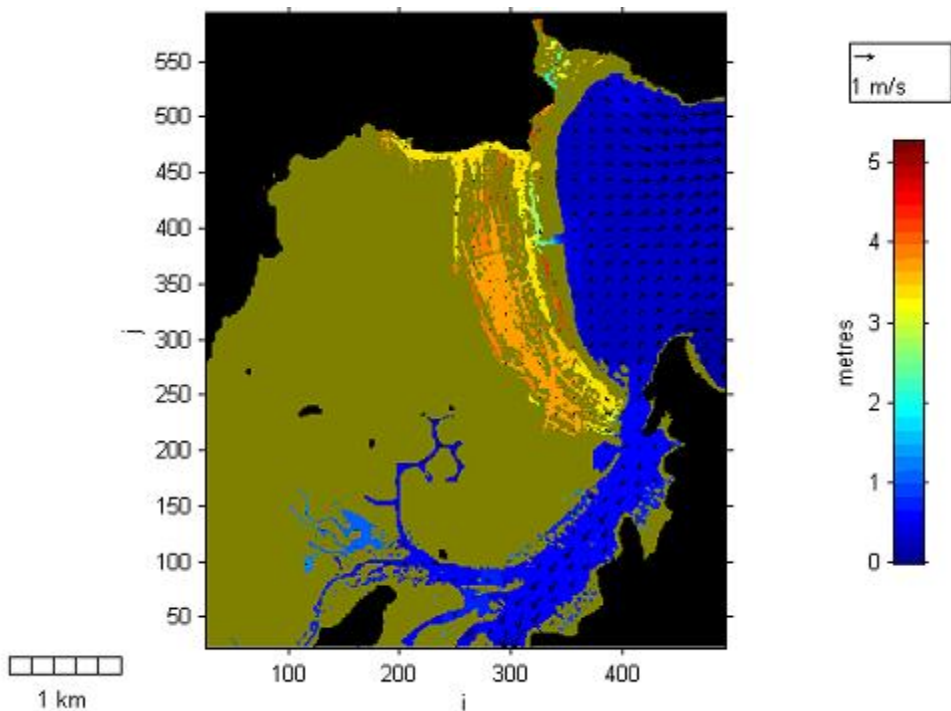


Non-Ground Striking Data

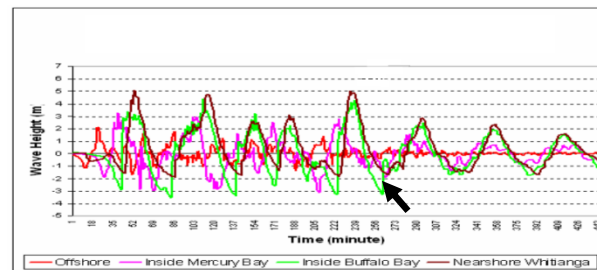
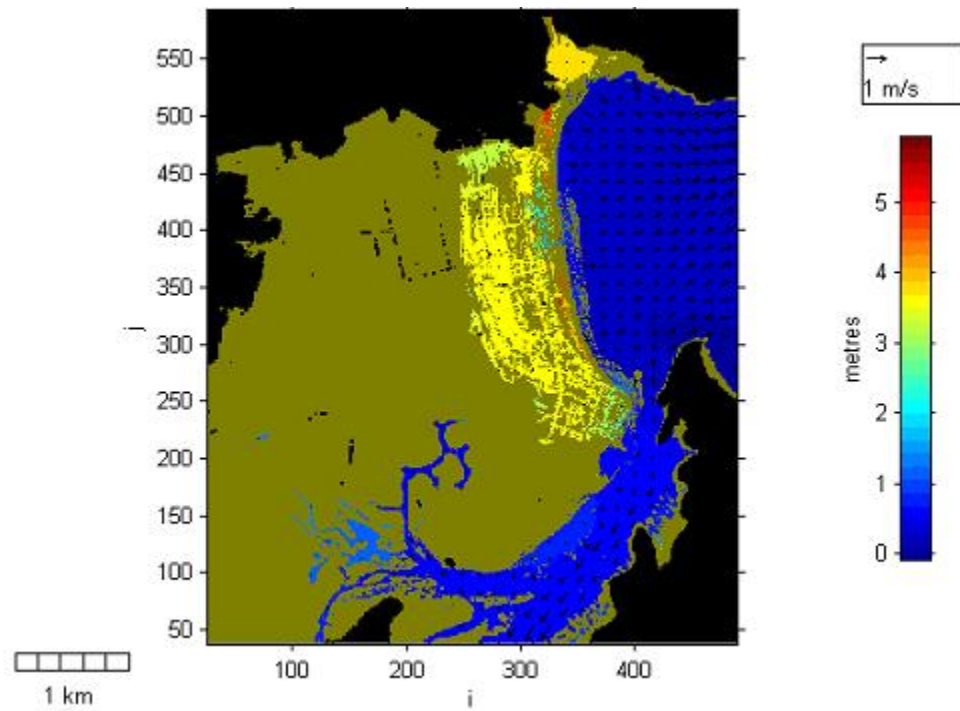


Fifth wave during run-down

Ground Striking Data



Non-Ground Striking Data



Appendix 3: animations of tsunami simulation results

Regional (wide area) model:

- Mt Healy eruption
- Kermadec trench scenarios:
 - Subduction thrust fault
 - Subduction normal fault
- 1960 Chilean type

Regional 50m model:

- Mt Healy eruption
- Kermadec trench scenarios:
 - Subduction thrust fault
 - Subduction normal fault
- 1960 Chilean type

5m/10m nested grid model

- The Kermadec Trench subduction normal fault – sea level, inundation depths and flow speeds
- 1960 Chilean type - sea level, inundation depths and flow speeds